

INVESTIGATION OF THE ROLE OF PROGRAMMED CELL DEATH 10  
(PDCD10) PROTEIN IN MULTIDRUG RESISTANCE

A THESIS SUBMITTED TO  
THE GRADUATE SCHOOL OF NATURAL AND APPLIED SCIENCES  
OF  
MIDDLE EAST TECHNICAL UNIVERSITY

BY

ÇAĞRI URFALI MAMATOĞLU

IN PARTIAL FULFILLMENT OF THE REQUIREMENTS  
FOR  
THE DEGREE OF DOCTOR OF PHILOSOPHY  
IN  
BIOLOGY

FEBRUARY 2018



Approval of the thesis:

**INVESTIGATION OF THE ROLE OF PROGRAMMED CELL  
DEATH 10 (PDCD10) PROTEIN IN MULTIDRUG RESISTANCE**

submitted by **ÇAĞRI URFALI MAMATOĞLU** in partial fulfillment of the requirements for the degree of **Philosophy of Doctorate in Biology Department, Middle East Technical University** by,

Prof. Dr. Gülbin DURAL Ünver

Dean, Graduate School of **Natural and Applied Sciences**

Prof. Dr. Orhan Adalı

Head of Department, **Biology**

Prof. Dr. Ufuk Gündüz

Supervisor, **Biology Dept., METU**

**Examining Committee Members:**

Assoc. Prof. Dr. Çağdaş Devrim SON

Biology Dept., METU

Prof. Dr. Ufuk Gündüz

Biology Dept., METU

Prof. Dr. Sreeparna Banerjee

Biology Dept., METU

Assoc. Prof. Dr. Özlem Darcansoy İşeri

Molecular Biology and Genetics Dept., Başkent University

Assoc. Prof. Dr. Bala Gür Dedeoğlu

Institute of Biotechnology, Ankara University

**Date:** 26/02/2018

**I hereby declare that all information in this document has been obtained and presented in accordance with academic rules and ethical conduct. I also declare that, as required by these rules and conduct, I have fully cited and referenced all material and results that are not original to this work.**

Name, Last name: Çađrı URFALI MAMATOĐLU

Signature :

## ABSTRACT

### INVESTIGATION OF THE ROLE OF PROGRAMMED CELL DEATH 10 (PDCD10) PROTEIN IN MULTIDRUG RESISTANCE

Urfalı Mamatoğlu, Çağrı

Ph.D., Department of Biology

Supervisor: Prof. Dr. Ufuk Gündüz

February 2018, 132 pages

Drug resistance, a major obstacle in chemotherapy, is the sum of several cellular alterations including resistance to induction of apoptosis. Apoptosis is a well-regulated cell death mechanism which is controlled by several signaling pathways and a vast number of proteins. Alterations in the proteins involved in the apoptotic regulation have been associated with drug resistance in cancer. Programmed Cell Death 10 (PDCD10) protein is a novel apoptotic regulator that is recently linked to the modulation of cellular proliferation and apoptosis. However, the role of PDCD10 in drug resistance has not been established. In this study, it was aimed to reveal the role of PDCD10 in drug resistance in different cancer cell lines.

Gene expression analyses showed that *PDCD10* expression was cell- and anti-cancer agent-specific. *PDCD10* expression was significantly

downregulated in doxorubicin- and docetaxel-resistant MCF7 cells while 2-fold upregulated in doxorubicin-resistant HeLa cells. On the other hand, *PDCD10* expression did not show any significant change in doxorubicin-resistant K562 cells, however, more than 2-fold downregulation was observed in imatinib-resistant K562 subline. siRNA-mediated downregulation of *PDCD10* expression in parental MCF7 cells resulted in an increase in docetaxel and doxorubicin resistance in these cells. whereas it caused resensitization in doxorubicin-resistant HeLa cells. Similarly, *PDCD10* overexpression in parental HeLa cells elevated the resistance to doxorubicin while it promoted chemosensitivity in doxorubicin-resistant MCF7 cells. The downregulation in *PDCD10* expression resulted in lower caspase 3/7 activity in MCF7 cells as the cells acquired resistance to etoposide-induced apoptosis. Consequently, the levels of apoptosis-related genes, *BCL-2*, *BAX*, *SURVIVIN* and *PUMA*, were altered.

The results suggest that *PDCD10* has a possible dual role in cancer drug resistance, both promoting and preventing the induction of apoptosis under different cellular conditions. *PDCD10* could be a novel target for reversal of drug resistance in cancer.

**Keywords:** Drug resistance, programmed cell death, apoptosis, *PDCD10*, cancer

## ÖZ

### **PROGRAMLI HÜCRE ÖLÜMÜ 10 (PDCD10) PROTEİNİNİN ÇOKLU İLAÇ DİRENÇLİLİĞİNDEKİ ROLÜNÜN İNCELENMESİ**

Urfalı Mamatoğlu, Çağrı

Doktora, Biyoloji Bölümü

Tez Yöneticisi: Prof. Dr. Ufuk Gündüz

Şubat 2018, 132 sayfa

Kemoterapide büyük bir sorun teşkil eden ilaç dirençliliği farklı hücresel sistemlerdeki değişimlerle gelişir. Bu sistemlerden biri de hücrelerin apoptoza dirençli hale gelmesidir. Apoptoz, farklı sinyal yolları ve proteinlerle regüle edilen bir tür programlı hücre ölümüdür. Apoptotik regülasyonda görev alan proteinlerin ifadelerinde oluşan değişimler daha önce kanserde ilaç dirençliliği ile ilişkilendirilmiştir. Yakın zamanda hücre ölümü ve apoptozla bağlantısı fark edilmiş “Programlı hücre ölümü 10 (Programmed Cell Death 10 - PDCD10)” proteini yeni keşfedilen bir regülatör proteindir. Ancak, PDCD10’un ilaç dirençliliğindeki rolü henüz bilinmemektedir. Bu tez çalışmasında, PDCD10’un farklı kanser hücrelerinde gelişen ilaç dirençliliğindeki görevi araştırılmıştır.

Gen ifade analizleri *PDCD10* gen ifadesinin hücre tipi ve hücrelerin direnç kazandığı anti-kanser ilaca bağlı olarak değişkenlik gösterdiğini ortaya koymuştur. *PDCD10* gen ifadesinin dosetaksel ve doksorubisine dirençli MCF7 hücrelerinde önemli ölçüde azaldığı, ancak doksorubisine dirençli HeLa hücrelerinde 2 kat arttığı belirlenmiştir. Öte yandan, *PDCD10* ifadesinin doksorubisine dirençli K562 hücrelerinde herhangi bir değişim göstermediği, ancak imatinibe dirençli K562 hücrelerinde 2 kat azaldığı görülmüştür. Parental MCF7 hücrelerinde *PDCD10* ifadesi siRNA kullanılarak susturulmuş ve gen ifadesindeki azalmanın MCF7 hücrelerini dosetaksel ve doksorubisine daha dirençli hale getirdiği gözlemlenmiştir. Öte yandan, azaltılan *PDCD10* ifadesi doksorubisine dirençli HeLa hücrelerinde ilaca karşı kemosenitizasyon sağlamıştır. Benzer şekilde, *PDCD10* ifadesinin artırıldığı HeLa hücrelerinde ilaç dirençliliğinde artış görülmüş ancak artan *PDCD10* ifadesi doksorubisine dirençli MCF7 hücrelerinde dirençliliğin geri çevrilmesine neden olmuştur. *PDCD10* ifadesi susturulan MCF7 hücrelerinde kazpaz 7 aktivitesinde düşüş görülmüş ve bu hücrelerin etoposid tarafından indüklenen apoptoza karşı direnç kazandığı belirlenmiştir. Buna bağlı olarak, apoptozla ilgisi bulunan *BCL-2*, *BAX*, *SURVIVIN* ve *PUMA* genlerinin ifadelerinde değişimler gözlemlenmiştir.

Bu tez çalışmasından elde edilen bulgular, *PDCD10* proteininin ilaç dirençliliğinde iki yönlü etkisi olduğunu, farklı hücrelerde hem apoptozu tetikleyebildiğini hem de inhibe edebildiğini göstermektedir. Kanserde ilaç dirençliliğini geri çevirmek için yapılan çalışmalarda *PDCD10* proteininin yeni bir hedef olabileceği öngörülmektedir.

**Anahtar kelimeler:** İlaç dirençliliği, programlı hücre ölümü, apoptoz, *PDCD10*, kanser

*To my beloved husband Güneş Mamatođlu  
and  
dearest brother ađatay Urfalı*

## ACKNOWLEDGMENTS

I would like to express my gratitude to my supervisor Prof. Dr. Ufuk Gündüz for her endless encouragement, guidance, and advice throughout this thesis study.

I am deeply grateful to Prof. Dr. Sreeparna Banerjee for her invaluable advice, precious comments, and guidance in the preparation of this thesis.

I owe my thanks to Assoc. Prof. Dr. Özlem Darcansoy İşeri for her comments and advice, not only for my thesis but also for my future career.

I am deeply thankful to Hasan Hüseyin Kazan, my partner-in-crime in the lab, for his invaluable help, fruitful discussions and scientific insights as well as his friendship and much-needed support in the form of “Hallederiz!”.

I am indebted to my more-than-labmates Ayça Nabioğlu, Maryam Parsian, Negar Taghavi and Esra Metin for their kind help, priceless friendship and moral support. Our lunch breaks are unforgettable. I am also thankful to all Lab206 members, current and former, for their friendship and support.

I owe my endless gratitude to my dearest friends Aktan Alpsoy and Murat Erdem for their technical help, invaluable suggestions, most precious friendship and endless encouragement.

I would like to extend my thanks to Merve Öyken, Esin Gülce Seza and Sinem Tunçer for their help and suggestions.

I would like to thank Assoc. Prof. Dr. Pelin Mutlu and METU Central Lab for their assistance in gene expression studies.

I would like to thank Prof. Dr. Dilek Keskin, Duygu Deniz Akolpoğlu, and Ali Deniz Dalgıç for their assistance in caspase assay measurements.

I am grateful to Esmâ and Erdem Guda, Uğurtan Demirtaş, and Alper Uyanık for their most precious friendship and support in much-needed time.

I would like to thank my long-time friends Bengü Okur Erdoğan and Elif Türkmen Çiftçi for their friendship and lunch-time bickerings that we all need. I cannot forget Deniz Şenyılmaz Tiebe who always makes me feel her support and love, even if she is away.

I would like to give my special thanks to my loving parents, Ayfer and Erol Urfalı, who raised me to the woman I am today, and Çağatay Urfalı, the “mighty emperor” and best brother one can have, for their everlasting love and endless support, not only in my education years but also in my entire life. This thesis would not be possible without them.

Last, but not least, I would like to express my deepest thanks to my beloved husband, Güneş Mamatoğlu, who has made his support, trust, and patience available in a number of ways at every stage of this thesis study. I cannot thank him enough for showing me my inner strength and teaching me that I could do anything, even when I am alone.

I greatly acknowledge TUBITAK-BİDEB for the 2211 Domestic Doctorate Scholarship Program.

## TABLE OF CONTENTS

ABSTRACT.....	v
ÖZ.....	vii
ACKNOWLEDGMENTS .....	x
TABLE OF CONTENTS.....	xii
LIST OF FIGURES .....	xv
LIST OF TABLES .....	xix
LIST OF ABBREVIATIONS .....	xx
CHAPTERS	
1 INTRODUCTION .....	1
1.1 Cancer.....	1
1.1.1 Breast Cancer .....	2
1.1.2 Cervical Cancer.....	4
1.1.3. Chronic Myeloid Leukemia .....	6
1.2 Cancer Treatments.....	9
1.3 Drug Resistance in Cancer .....	10
1.4 Apoptosis.....	12
1.5 Programmed Cell Death 10 (PDCD10).....	16
1.5.1 PDCD10 – Drug Resistance Relationship .....	21
1.6 Aim of the Study .....	22
2 MATERIALS AND METHODS.....	23
2.1 Materials.....	23
2.2 Cell Lines and Cell Culture .....	23
2.2.1 Subculturing .....	24
2.2.2 Cell Freezing and Thawing .....	24
2.2.3 Cell counting by Trypan Blue cell exclusion method.....	25
2.3 Gene Expression Analysis.....	26

2.3.1	Isolation of Total RNA .....	26
2.3.2	DNase Treatment and cDNA Synthesis.....	26
2.3.3	Quantitative Real Time Polymerase Chain Reaction (qRT-PCR) .....	27
2.3.4	Quantification of qRT-PCR .....	30
2.4	siRNA Mediated Silencing.....	31
2.4.1	<i>PDCD10</i> Knockdown in 6-Well Plates .....	31
2.4.2	<i>PDCD10</i> Knockdown in 96 Well Plates.....	31
2.5	Overexpression of <i>PDCD10</i> .....	32
2.5.1	Competent <i>E. coli</i> preparation .....	33
2.5.2	Transformation.....	33
2.5.3	Plasmid isolation.....	34
2.5.4	Insert preparation .....	34
2.5.5	Gel Extraction .....	36
2.5.6	Double digestion .....	36
2.5.7	DNA Clean Up.....	38
2.5.8	Ligation.....	39
2.5.9	Colony PCR .....	40
2.5.10	Transfection of cells with overexpression vector .....	41
2.5.11	Total Protein Isolation and Determination of Protein Concentration.....	42
2.5.12	Sodium dodecyl sulfate-Polyacrylamid Gel Electrophoresis (SDS-PAGE).....	42
2.5.13	Wet Transfer .....	43
2.5.14	Membrane Blocking.....	44
2.5.15	Western Blotting and Imaging .....	44
2.6	Cell Viability Assay .....	45
2.7	Intracellular Drug Accumulation Assay.....	46
2.8	Apoptosis Assay .....	46
2.9	Caspase 3/7 Activity Assay.....	47
2.10	Wound Healing Assay .....	47
2.11	Statistical Analysis .....	48
3	RESULTS AND DISCUSSION.....	49

3.1 Isolation of Total RNA from Parental and Drug-Resistant Cancer Cell Lines.....	50
3.2 Screening of parental and drug-resistant MCF7, HeLa and K562 cancer cells for <i>PDCD10</i> expression.....	51
3.3 Effect of <i>PDCD10</i> Expression on Drug Resistance .....	53
3.4 The Effect of <i>PDCD10</i> Expression on Intracellular Drug Accumulation .....	63
3.5 The Effect of <i>PDCD10</i> Expression on Apoptosis and Caspase Activity .....	66
3.6 The Effect of <i>PDCD10</i> Expression on Apoptosis-related Genes .....	72
3.7 The Effect of <i>PDCD10</i> Expression on Migration.....	84
3.8 <i>PDCD10</i> Expression in Breast Cancer Cells .....	88
4 CONCLUSIONS.....	91
5 FUTURE PROSPECTIVES .....	95
REFERENCES .....	97
APPENDICES	
A BUFFERS AND SOLUTIONS .....	117
B PDCD10 PROTEIN DETECTION BY WESTERN BLOT .....	121
C RESISTANCE INDICES .....	127
CURRICULUM VITAE.....	129

## LIST OF FIGURES

### FIGURES

<b>Figure 1.1</b> Healthy breast tissue and locations of lymph nodes.....	3
<b>Figure 1.2</b> Anatomy of female reproductive system.....	5
<b>Figure 1.3</b> HPV infection in cervical cancer.....	6
<b>Figure 1.4</b> Signal transduction pathways that are controlled by BCR-ABL tyrosine kinase. ....	7
<b>Figure 1.5</b> Action mechanism of imatinib. ....	8
<b>Figure 1.6</b> Development of drug resistance during anti-cancer agent treatment. ....	11
<b>Figure 1.7</b> Mechanisms of drug resistance in cancer. ....	12
<b>Figure 1.8</b> Extrinsic and intrinsic pathways of apoptosis. ....	13
<b>Figure 1.9</b> BCL-2 family proteins.....	14
<b>Figure 1.10</b> Proteins involving in different apoptotic pathways.....	15
<b>Figure 1.11</b> Structure of PDCD10.....	16
<b>Figure 1.12</b> Predicted interaction partners of PDCD10.....	18
<b>Figure 1.13</b> Epigenetic regulation of <i>PDCD10</i> promoter.....	20
<b>Figure 1.14</b> Post-translational modifications of PDCD10 protein.....	21
<b>Figure 2.1</b> PHAGE cTAP vector backbone. ....	32
<b>Figure 2.2</b> Primer sequences used in insert preparation.....	35
<b>Figure 2.3</b> Map of pcDNA3.1(-) vector. ....	37
<b>Figure 3.1</b> <i>PDCD10</i> expression in drug-resistant MCF7 sublines compared to parental MCF7 cells.....	49
<b>Figure 3.2</b> Total RNAs isolated from parental and drug-resistant MCF7, HeLa and K562 cells on 2% agarose gel. ....	50
<b>Figure 3.3</b> Expression of <i>PDCD10</i> in parental and drug-resistant a) MCF7, b) HeLa and c) K562 cells.....	51

<b>Figure 3.4</b> Expression of <i>PDCD10</i> in parental MCF7 cells after siRNA mediated <i>PDCD10</i> knockdown. ....	53
<b>Figure 3.5</b> The viability of parental MCF7 cells in increasing concentrations of docetaxel (DOC) after <i>PDCD10</i> knockdown. ....	54
<b>Figure 3.6</b> The viability of parental MCF7 cells in increasing concentrations of doxorubicin (DOX) after <i>PDCD10</i> knockdown. ....	55
<b>Figure 3.7</b> Expressions of <i>PDCD10</i> in MCF7/DOX cells after <i>PDCD10</i> overexpression. ....	58
<b>Figure 3.8</b> The viability of MCF7/DOX cells in increasing concentrations of doxorubicin (DOX) after <i>PDCD10</i> overexpression. ....	59
<b>Figure 3.9</b> Expression of <i>PDCD10</i> in HeLa cells after <i>PDCD10</i> overexpression. ....	60
<b>Figure 3.10</b> The viability of HeLa cells in increasing concentrations of doxorubicin (DOX) after <i>PDCD10</i> overexpression. ....	61
<b>Figure 3.11</b> Expression of <i>PDCD10</i> in HeLa/DOX cells after siRNA-mediated <i>PDCD10</i> knockdown. ....	62
<b>Figure 3.12</b> The viability of HeLa/DOX cells in increasing concentrations of doxorubicin (DOX) after siRNA-mediated <i>PDCD10</i> knockdown. ....	63
<b>Figure 3.13</b> Intracellular drug accumulation in a) parental MCF7 cells after <i>PDCD10</i> knockdown, b) MCF7/DOX cells after <i>PDCD10</i> overexpression, c) HeLa cells after <i>PDCD10</i> Overexpression and d) HeLa/DOX cells after <i>PDCD10</i> knockdown. ....	65
<b>Figure 3.14</b> Apoptotic activity in <i>PDCD10</i> -silenced MCF7 cells. ....	69
<b>Figure 3.15</b> Caspase 3/7 activity in <i>PDCD10</i> -silenced MCF7 cells. ....	71
<b>Figure 3.16</b> Expressions of a) <i>BCL-2</i> , b) <i>BAX</i> , c) <i>SURVIVIN</i> and d) <i>PUMA</i> genes in parental and drug-resistant MCF7 cells. ....	77
<b>Figure 3.17</b> Expressions of a) <i>BCL-2</i> , b) <i>BAX</i> , c) <i>SURVIVIN</i> and d) <i>PUMA</i> genes in <i>PDCD10</i> -silenced MCF7 cells. ....	79
<b>Figure 3.18</b> Expressions of a) <i>BCL-2</i> , b) <i>BAX</i> , c) <i>SURVIVIN</i> and d) <i>PUMA</i> genes in <i>PDCD10</i> -overexpressed MCF7/DOX cells. ....	80

<b>Figure 3.19</b> Expressions of a) <i>BCL-2</i> , b) <i>BAX</i> , c) <i>SURVIVIN</i> and d) <i>PUMA</i> genes in parental and drug-resistant HeLa cells. ....	81
<b>Figure 3.20</b> Expressions of a) <i>BCL-2</i> , b) <i>BAX</i> , c) <i>SURVIVIN</i> and d) <i>PUMA</i> genes in <i>PDCD10</i> -silenced HeLa/DOX cells. ....	82
<b>Figure 3.21</b> Expressions of a) <i>BCL-2</i> , b) <i>BAX</i> , c) <i>SURVIVIN</i> and d) <i>PUMA</i> genes in <i>PDCD10</i> -overexpressed HeLa cells. ....	83
<b>Figure 3.22</b> Migratory activity of <i>PDCD10</i> -silenced MCF7 cells at different time intervals. ....	84
<b>Figure 3.23</b> Migratory activity of <i>PDCD10</i> -overexpressed MCF7/DOX cells at different time intervals. ....	85
<b>Figure 3.24</b> Migratory activity of <i>PDCD10</i> -overexpressed HeLa cells at different time intervals. ....	86
<b>Figure 3.25</b> Migratory activity of <i>PDCD10</i> -silenced HeLa/DOX cells at different time intervals. ....	87
<b>Figure 3.26</b> <i>PDCD10</i> expression in T47D, MDA-MB-231 and SKBR3 breast cancer cells compared to MCF7 cell line. ....	89
<b>Figure B.1</b> <i>PDCD10</i> expression in doxorubicin-resistant HeLa, K562 and MCF7 cells. ....	121
<b>Figure B.2</b> <i>PDCD10</i> expression in parental and doxorubicin-resistant MCF7 cells. ....	122
<b>Figure B.3</b> Expression of <i>PDCD10</i> in MCF7/DOX cells after transfection with pcDNA_ <i>PDCD10</i> overexpression vector. A) <i>PDCD10</i> expression at mRNA level, B) <i>PDCD10</i> expression at protein level detected by anti- <i>PDCD10</i> antibody and C) <i>PDCD10</i> expression at protein level detected by anti-FLAG antibody. ....	123
<b>Figure B.4</b> <i>PDCD10</i> expression in Pepstatin A- and MG132-treated MCF7 and MCF7/DOX. ....	124
<b>Figure B.5</b> <i>PDCD10</i> expression after treatment with hydrogen peroxide in MCF7/DOX cells. A) <i>PDCD10</i> expression at mRNA level and B) <i>PDCD10</i> expression at protein level. ....	125

**Figure B.6** PDCD10 expression in parental and doxorubicin-resistant MCF7 cells on native PAGE. ....126

## LIST OF TABLES

### TABLES

<b>Table 2.1.</b> PCR ingredients and conditions for <i>PDCD10</i> expression. ....	28
<b>Table 2.2.</b> Primer sequences.....	29
<b>Table 2.3.</b> PCR ingredients and conditions for apoptosis-related genes.....	30
<b>Table 2.4.</b> PCR ingredients and conditions for insert amplification. ....	35
<b>Table 2.5.</b> Ingredients of digestion reaction. ....	38
<b>Table 2.6.</b> Ingredients of ligation reaction. ....	39
<b>Table 2.7.</b> Ingredients and conditions of colony PCR.....	40
<b>Table 2.8.</b> Ingredients and amounts stacking and separating gels. ....	44
<b>Table 3.1.</b> IC <sub>50</sub> values and resistance indices of <i>PDCD10</i> -silenced and <i>PDCD10</i> -overexpressed cells. ....	55
<b>Table C.1.</b> Resistance indices of <i>PDCD10</i> -silenced and <i>PDCD10</i> -overexpressed cells compared to MCF7 and HeLa cells. ....	127

## LIST OF ABBREVIATIONS

<b>APS</b>	Ammonium persulfate
<b>BCL-2</b>	B-cell lymphoma 2
<b>BAX</b>	Bcl-2 associated X protein
<b>BCR-ABL</b>	Break point cluster region-Abelson leukemia virus oncogene
<b>DOC</b>	Docetaxel
<b>DOX</b>	Doxorubicin
<b>DMSO</b>	Dimethyl sulfoxide
<b>ERK</b>	Extracellular signal-regulated kinase
<b>ETO</b>	Etoposide
<b>MAPK</b>	Mitogen activated protein kinase
<b>MST4</b>	Mammalian Ste-20 like protein kinase 4
<b>PAGE</b>	Polyacrylamide gel electrophoresis
<b>PBS</b>	Phosphate buffer saline
<b>PDCD10</b>	Programmed cell death 10
<b>PUMA</b>	p53 upregulated modifier of apoptosis
<b>Ph</b>	Philadelphia chromosome
<b>SDS</b>	Sodium dodecyl sulfate
<b>STK25</b>	Serine/threonine kinase 25
<b>TBS</b>	Tris buffer saline
<b>TBST</b>	Tris buffer saline-Tween 20

## **CHAPTER 1**

### **INTRODUCTION**

#### **1.1 Cancer**

Cancer is a pathological condition that is characterized by the presence of abnormal cells with limitless cell proliferation, invasive and metastatic ability. American Cancer Society expected approximately 2 million new cancer cases, excluding carcinoma in situ (noninvasive) cases, to be diagnosed only in the United States and more than half-million cancer-related deaths were expected in 2017 (American Cancer Society, 2017). After heart diseases, cancer was the second leading cause of mortality worldwide, with approximately 9 million cancer-related deaths in 2015 (World Health Organization, 2017).

Normal cells transform into malignant cells through a wide range of genetic alterations including oncogene activation and tumor suppressor inactivation, both of which promote cell proliferation (Boland and Goel, 2005). These alterations is the result of a number of factors such as mutations (point or frameshift) that result in gain or loss in protein function, chromosomal translocations, DNA instability, epigenetic changes, alterations in hormone levels, free radicals, reactive lipid and oxygen species generated by metabolic events, immune system activation/suppression, viral/bacterial/fungal

infections, radiation and smoking (Bertram, 2001; Rieger, 2004; American Cancer Society, 2017). Hanahan and Weinberg presented the common features of cancerous cells as six hallmarks of cancer, namely self-sufficiency in cell proliferation, activation of invasive and metastatic ability, insensitivity to growth suppressors, replicative immortality, sustained angiogenesis and evasion of cell death (Hanahan and Weinberg, 2000). Similarly, Bertram reported that carcinogenesis requires the activation or inactivation of major cellular pathways that result in the development of growth factor independence, insensitivity to growth inhibitory signals, resistance to cell death, the generation of an infinite proliferative and angiogenic potential (Bertram, 2001). However, recent studies revealed that cancer cells have deregulated cellular energy metabolism and can escape from immune destruction by modulating immune system (Hanahan and Weinberg, 2011).

Different organizations reported that breast, colorectum, endometrial, lung and cervical cancers are the most commonly diagnosed cancer types in women worldwide while prostate, lung, colorectum, stomach, and liver cancers are the most frequently seen cancers in men with high mortality rates. Lymphomas, nervous system tumors and leukemias constitute the majority of childhood cancers (American Cancer Society, 2017; National Cancer Institute, 2017).

### **1.1.1 Breast Cancer**

Breast cancer, the most prevalent cancer type in women, is one of the leading causes of cancer-associated deaths. 2% of annual breast cancer cases are seen in men (American Cancer Society, 2017).

Breast cancer generally starts in lobules, ducts or fatty and fibrous connective tissue ([www.breastcancer.org/symptoms/understand\\_bc/what\\_is\\_bc](http://www.breastcancer.org/symptoms/understand_bc/what_is_bc)). After

malignant transformation, cancerous cells firstly invade nearby healthy cells and underarm lymph nodes, then enter blood or lymphatic circulation to metastize to distant tissues. Secondary tumors developed due to breast cancer metastasis are mostly observed in lungs and bones (Keen and Lennan, 2011).

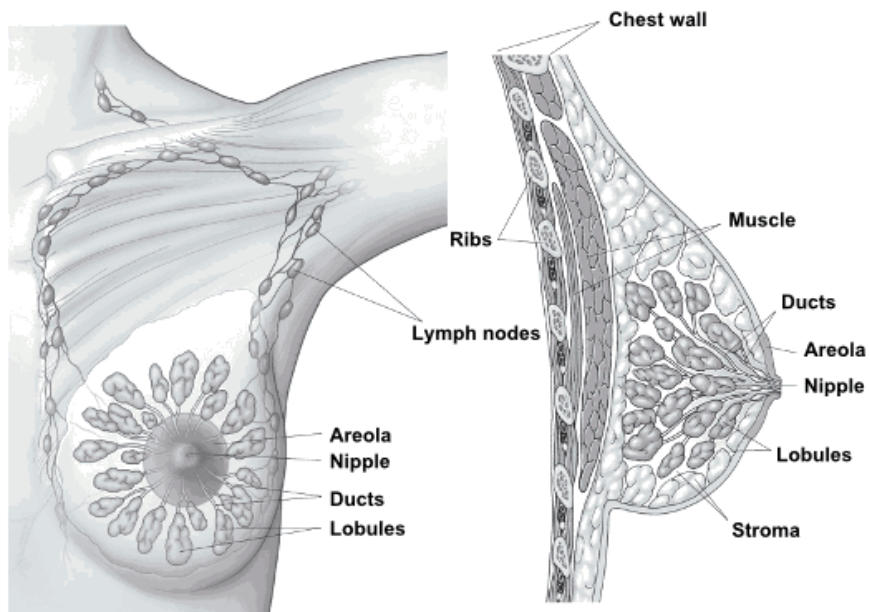


**Figure 1.1** Healthy breast tissue and locations of lymph nodes (American Cancer Society, 2017)

Several reasons of breast cancer includes age, unhealthy diet, high body-mass index, tobacco and alcohol use, longer menstruation history, extended oral contraceptive or hormone use and giving birth at old ages (Tyczynski et al, 2002; American Cancer Society, 2017). Even though majority of breast cancer cases are sporadic, familial background and genetic tendency have an impact on the development of breast cancer. Various studies showed that women with inherited *BRCA1* and *BRCA2* mutations have a higher risk to develop breast cancer compared to the ones without mutations (Serova et. al, 1997; Foulkes et. al, 2003; King et. al, 2003). Although they are less common, the mutations in *ATM* and *CHEK2* are also associated with hereditary breast cancer (Ahmed and Rahman, 2006; Apostolou and Papatiririou, 2017).

### **1.1.2 Cervical Cancer**

Cervical cancer starts in the lining of cervix, the channel that connects the uterus with vagina. The healthy ectocervix (the lower part of the cervix) is composed of squamous cells whereas the upper portion of the cervical canal, endocervix, composed of another columnar cells. The transformation zone or T-zone, the place endo- and exocervix meets, is the location at which most cervical cancer cases start.

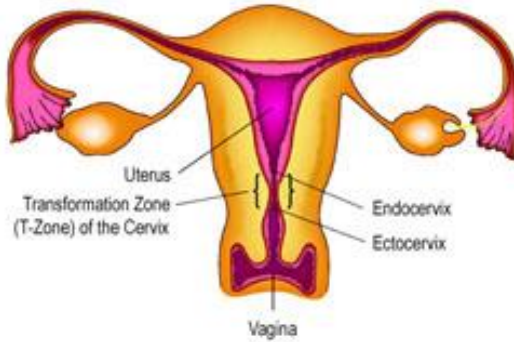


**Figure 1.2** Anatomy of female reproductive system (National Cervical Cancer Coalition, 2017)

Among several cervical cancer types, squamous cell cancers take up the most common cancer type with 80-90% occurrence rate. The remaining cases are adenocarcinomas which start in mucus-producing glands of endocervix. Rarely, cervical cancers representing both squamous and adenocarcinoma features can be seen and these cancers are called as adenosquamous carcinomas (American Cancer Society, 2017; National Cervical Cancer Coalition, 2017).

Human papillomavirus (HPV) infection is the leading cause of cervical carcinogenesis. Two high-risk HPV types (HPV-16 and HPV-18) are found to be related to more than 70% of cervical cancer cases. Viral E6 and E7 oncoproteins cause inactivation of tumor suppressors in infected tissues and promote malignant transformation and cancer proliferation (Yim and Park, 2005; Tomaic, 2016)

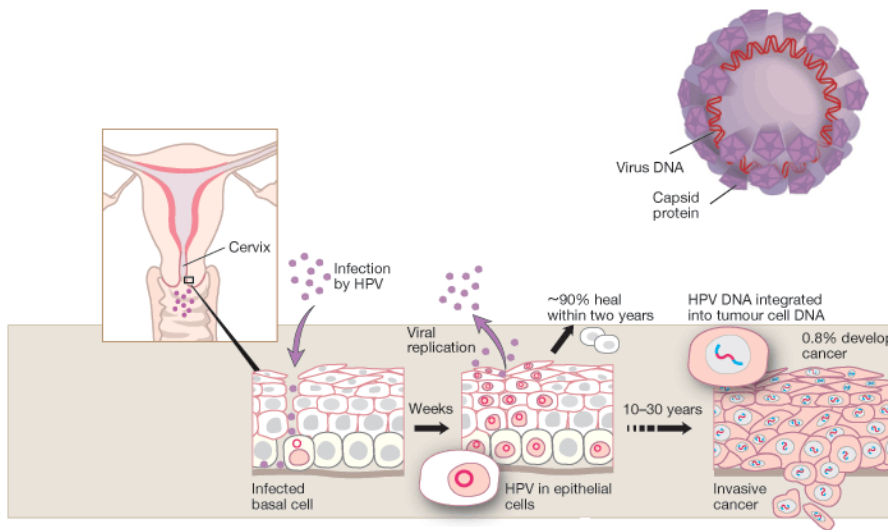


**Figure 1.3** HPV infection in cervical cancer

### 1.1.3. Chronic Myeloid Leukemia

Chronic myeloid leukemia (chronic myelogenous leukemia ; CML) is a clonal myeloproliferative disorder which comprises of 15% of adult leukemias (Jahagirdar et al, 2001; Kantarijan et al, 2010). CML starts in blood-forming cells of the bone marrow. In chronic phase of CML, myeloid precursors proliferate without control and expand bone marrow stem cell progeny. The accumulation of these abnormal cells in blood and extramedullary tissues promotes the disease by turning the relatively benign chronic phase into an intermediate accelerated phase, then potentially fatal blast crisis phase (Drummond and Holyoake, 2001; Jahagirdar et al, 2001; Radich, 2007; Danisz and Blasiak, 2013; Trela et al, 2014; American Cancer Society, 2017).

Chronic myeloid leukemia is generally characterized by the presence of a genetic abnormality which is caused by a translocation between long arms of chromosomes 9 and 22. This translocation (t(9:22)) generates a shortened chromosome called as Philadelphia (Ph) chromosome for which 95% of CML

and 15% of ALL (acute lymphoblastic leukemia) patients are positive (Jahagirdar et al, 2001, Krystal, 2001). Philadelphia chromosome is associated with the fusion of *BCR* (Breakpoint Cluster Region) and *ABL* (Abelson Leukemia Virus Oncogene) genes which creates a constitutively active tyrosine kinase. Several studies revealed that the BCR-ABL tyrosine kinase activity alone is essential for the transformation of normal bone marrow cells into CML since BCR-ABL tyrosine kinase regulates the activity of various important cell signaling pathways including ERK, PI3K/AKT, Jak-STAT and Src (Drummond and Holyoake, 2001; Jahagirdar et al, 2001, Danisz & Blasiak, 2013). Moreover, the actin binding domain at 3' end of BCR-ABL links the constitutively active tyrosine kinase to cellular adhesion and motility (Drummond and Holyoake, 2001).

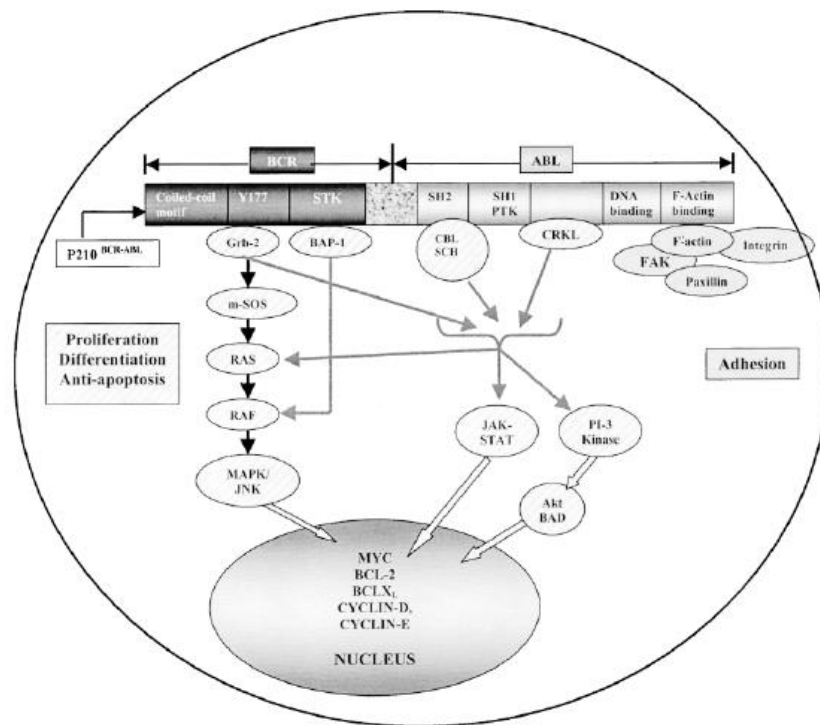


**Figure 1.4** Signal transduction pathways that are controlled by BCR-ABL tyrosine kinase (Jahagirdar et al, 2001)

For CML treatment, the standard therapy is to target the tyrosine kinase activity of BCR-ABL by using tyrosine kinase inhibitors (TKIs). Even though majority of the CML patients in chronic phase (80%) exhibit high survival rates after TKI therapy, this rate of survival decreases to 50% in accelerated phase and 20% in blast crisis phase (Radich, 2007).

Imatinib (STI571), a first generation TKI, is frequently used for CML treatment. It competitively binds to ATP-binding domain of Abl, stabilizes inactive form of BCR-ABL which is not phosphorylated in ATP-binding domain and prevents autophosphorylation and phosphorylation of other cellular substrates (Krystal, 2001; Trela et al, 2014).

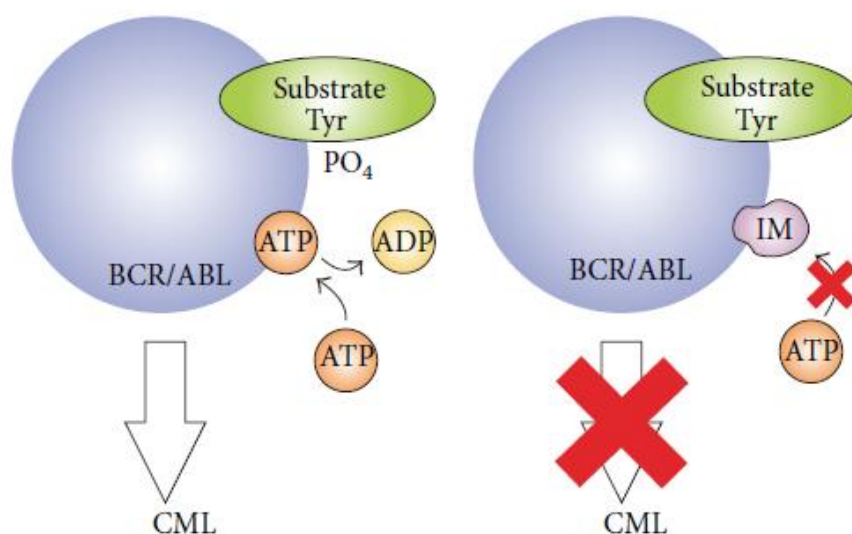


**Figure 1.5** The action mechanism of imatinib (Trela et al, 2014)

## 1.2 Cancer Treatments

Cancer treatment usually consists of combinations of several therapies including surgery, radiation therapy and chemotherapy. The treatment type is determined depending on cancer type, the location and size of tumor, stage of cancer, hormone responsiveness, metastasis to axillary lymph nodes as well as gender, age and patient preference (American Cancer Society, 2017).

Surgery is the first line of treatment for most of solid tumors (NIH Consensus Development Conference Statement, 2000). However, depending on the size, location and stage of tumor, surgery could be coupled with other treatment types. In radiation therapy (radiotherapy), high-energy beams are applied before surgery in order to shrink tumor size or after surgery to eliminate remaining cancerous cells.

Radiotherapy is used to disrupt cancer cells by damaging DNA structure or producing free radicals which lead extensive DNA damage inside the cell (American Cancer Society, 2017).

Chemotherapy is the application of anti-cancer agents to disrupt the cancer cells and to reduce relapse risk. Anthracycline antibiotics (doxorubicin, idarubicin, epirubicin), taxols (docetaxel, paclitaxel) and mitoxantrone are the most frequently used anti-cancer agents in breast cancer treatment while TKIs are more favorable in chronic myeloid leukemia (O'Shaughnessy, 2005; Glück, 2005). Bisphosphonates are used, coupled with the conventional chemotherapy, to increase the efficiency, and prevent invasion and metastasis in advanced bone and breast cancer cases (Maricic, 2006). Chemotherapy can be applied orally or intravenously in regular intervals, and the time period

between two doses is determined depending on the stage and/or location of the tumor. Beside conventional chemotherapy, adjuvant and neoadjuvant therapies are used to maximize the efficiency of chemotherapy. Neoadjuvant chemotherapy is used to shrink tumor size before surgery while adjuvant chemotherapy is applied after surgery to eliminate remaining cancer cells in order to increase the disease-free survival period (American Cancer Society, 2017).

In addition to these, hormone therapy (the use of selective hormone receptor modulators, SERMs), and targeted therapy (the use of monoclonal antibodies) can be used to treat cancer in combination with other treatment strategies.

### **1.3 Drug Resistance in Cancer**

Drug resistance in cancer is the sum of the cellular mechanisms that tumor cells are used to eliminate cytotoxic effects of anti-cancer agents (Simon and Schindler, 1994). The drug-resistant phenotype could be intrinsically present in tumor cells or they can acquire simultaneous resistance to various functionally and structurally distinct anti-cancer agents (Krishna and Mayer, 2000; Ejendal and Hrycyna, 2002). Longley and Johnston reported that drug resistance is the major reason of ineffectiveness of cancer treatment in nearly 90% of cancer cases (Longley and Johnston, 2005).

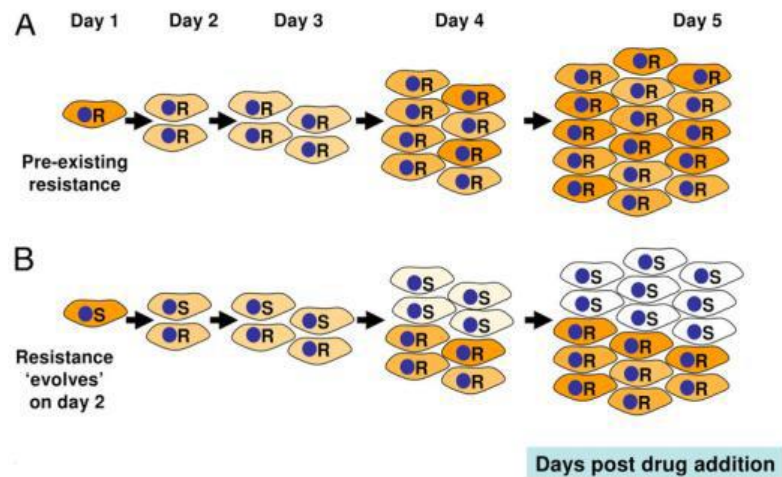


**Figure 1.6** Development of drug resistance during anti-cancer agent treatment (Robinson et al, 2011)

Most solid tumors are heterogeneous in terms of cellular composition, consisting of both drug-responsive and –resistant cells. Anti-cancer agents can efficiently eliminate drug-responsive cells, however, the drug-resistant cells can still remain alive and proliferate, forming drug-resistant tumors and leading to failure in treatment.

Drug resistance could be acquired through several cellular mechanisms. These mechanisms include decreased intake of anti-cancer agents through alterations in structure of cellular membrane, increased efflux of drugs by ATP-binding cassette (ABC) family transporter proteins, suppressed apoptosis, overactivation of proliferative pathways, activation of cellular detoxifying (P450 and/or glutathione-S-transferase based) systems, activation of DNA repair mechanisms and altered target protein structure and location (Longley and Johnston, 2005; Holohan et al 2013; Housman et al 2014).

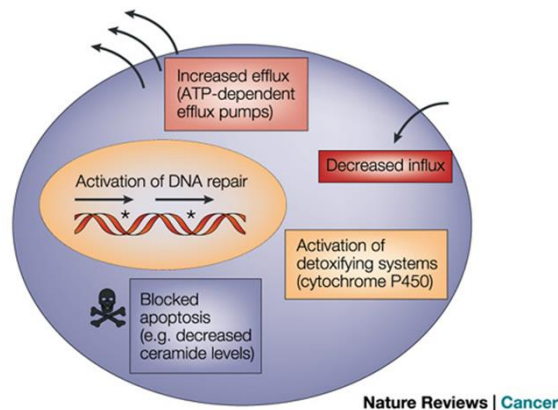


**Figure 1.7** Mechanisms of drug resistance in cancer (Gottesman et al, 2002)

## 1.4 Apoptosis

Apoptosis is a type of programmed cell death which is essential in immunity, development and homeostasis in adult tissues (Salvesen and Duckett, 2002). The apoptotic process can be morphologically distinguished from non-programmed cell deaths. In apoptotic cells, the nuclei, cytoplasm and mitochondria shrink and this shrinkage causes the cellular content entrapped in apoptotic bodies that are surrounded by plasma membrane. However, plasma membrane is disrupted so that phosphatidylserine molecules, which normally reside in the cytoplasmic side of the cellular membrane, get exposed at the outside of the membrane. Phosphatidylserine residues are recognized by phagocytic cells and upon recognition, apoptotic bodies are engulfed by phagocytes and degraded within their lysosomes without generating any inflammatory response (Kerr et.al, 1994; Salvesen and Duckett, 2002; Czabotar et. al, 2014).

There are two major pathways leading to apoptosis that involve the action of cysteine aspartyl-specific proteases (caspases). The first pathway, also called as extrinsic pathway, is initiated by ligand binding to death receptors, such as

Fas receptor (FasR), located on the cell membrane. The ligand binding causes the recruitment of different proteins which, in turn, will form the death-inducing signaling complex (DISC). DISC complex triggers activation of caspase 8, which further induce caspase 3. The activation of caspase 3, also called executioner or effector caspase, results in the cellular changes that define apoptosis. However, the intrinsic pathway, also known as the mitochondrial pathway, is stimulated by cellular stress, which triggers the translocation of pro-apoptotic proteins, including Bax and other pro-apoptotic members of BCL-2 family, to the mitochondrial membrane. This translocation, which induces the the formation of apoptosome complex by causing the oligomerization of the pro-apoptotic Apaf-1 factor, causes the cytochrome c release into the cytoplasm. The apoptosome complex activates caspase 9, which later activates caspase 3 (Salvesen and Duckett, 2002).

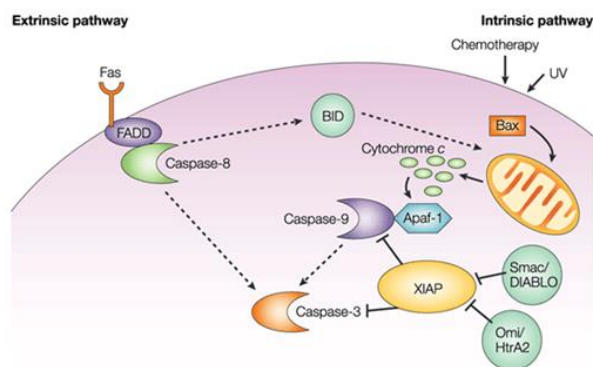


**Figure 1.8** Extrinsic and intrinsic pathways of apoptosis (Salvesen and Duckett, 2002)

Apoptosis is a highly complex cellular event that is regulated by several proteins. One of the important regulators of apoptosis is the BCL-2 protein family. *BCL-2* proto-oncogene was first identified in human B-cell lymphomas at the chromosomal breakpoint of t(14;18). BCL-2 family

comprises of both pro- and anti-apoptotic proteins whose ratio determines the fate of cells when the cell receives a death signal (Oltvai et.al, 1993). BCL-2 family proteins possess four different conserved BCL-2 homology (BH1-4) domains. These domains have  $\alpha$ -helical segments which are vital for responses to death signals. Depending on sequence homology in BH domains, Bcl-2 protein family can be categorized under three subgroups: BH3-only proteins (BAD, Noxa and PUMA) which display sequence homology only within the BH3 domain and promote apoptosis, anti-apoptotic proteins (BCL-2, BCL-w and BCL-xL) and pro-apoptotic effectors (BAX and BAK). BCL-2 family proteins can form both homo- and heterodimers, suggesting the structure of the multimer, as well as the ratio of the proteins within the cell, is important to determine the protein function (Gross et. al, 1999; Czabotar et.al, 2014).

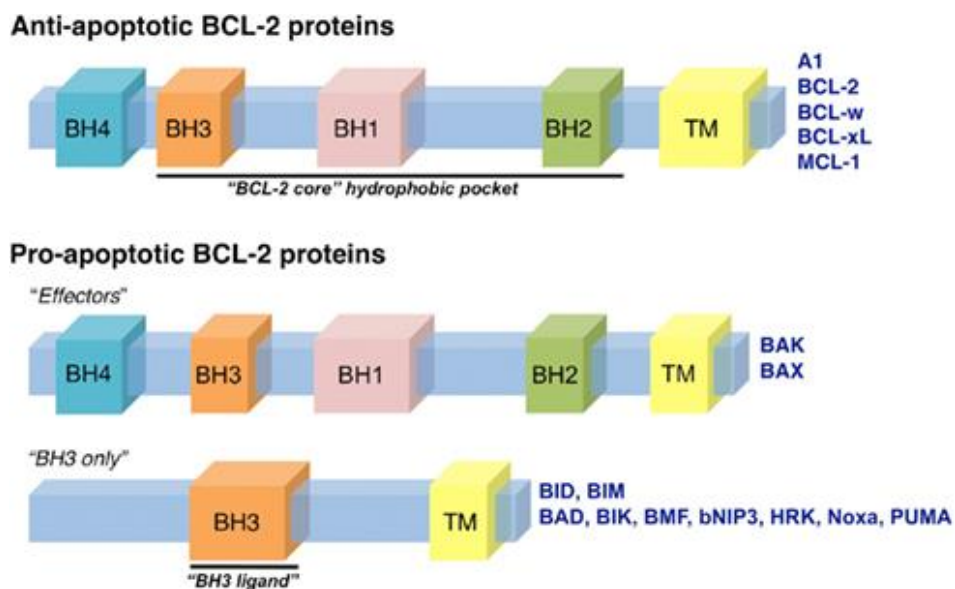


**Figure 1.9** BCL-2 family proteins (Anvekar et al, 2011)

Members of BCL-2 protein family modulate apoptosis by forming and regulating the activity of the membrane channels. Previous studies revealed that BCL-2, BAX and BCL-xL can initiate the formation of ion channels on mitochondrial membrane. It was suggested that upon receiving a signal, pro-apoptotic members of BCL-2 protein family translocate to mitochondria to control cytochrome c release. Moreover, overexpression of BAX or BAK was shown to lead altered mitochondrial membrane potential, ROS production and release of cytochrome c that activates downstream caspases. However, the elevated expression levels of BCL-xL and/or BCL-2 itself can counter these effects (Gross et al., 1999).

Apart from BCL-2 family proteins, p53, several kinases, transcription factors and proto-oncogenes involve in the regulation of apoptotic process. All of these proteins and pathways involving in regulation of apoptosis make it a highly complex cellular event.

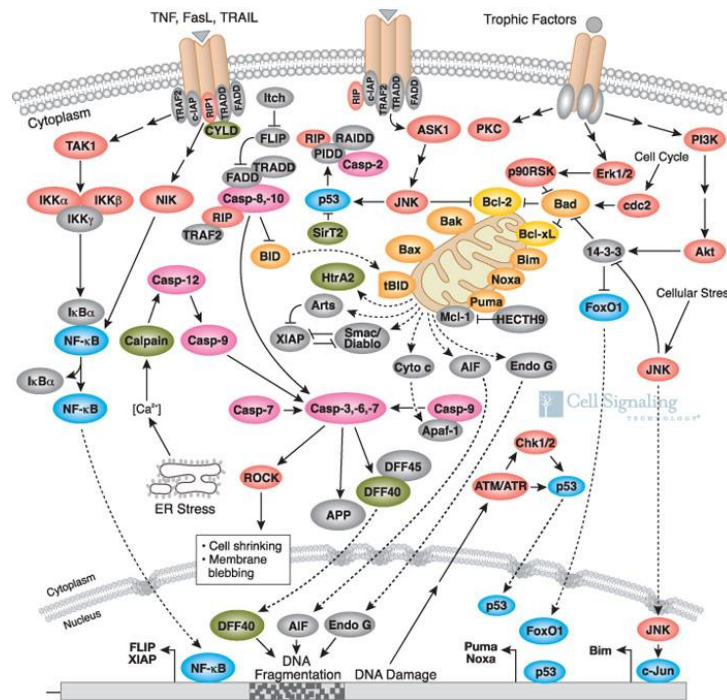


**Figure 1.10** Proteins involving in different apoptotic pathways (retrieved from Cell Signaling Technology, USA)

### 1.5 Programmed Cell Death 10 (PDCD10)

Programmed cell death 10 (PDCD10) gene, also known as TFAR15 (TF-1 cell apoptosis-related gene 15) or CCM3 (cerebral cavernous malformations 3), was initially cloned from a TF-1 myeloid cell line after inducing apoptosis by granulocyte macrophage colony-stimulating factor (GM-CSF) deprivation (Wang et. al, 1999). *PDCD10* is a 50-kb gene and mapped to chromosomal region 3q26.1. Until now, three alternative PDCD10 transcripts encoding the same protein have been identified. These alternative transcripts only differ in their 5' untranslated regions. The coding portion of the gene encodes a small protein (212 amino acids) that is highly conserved from nematodes to humans. Sequence analysis suggested that PDCD10 protein did not contain a

localization signal, a transmembrane domain or any identified functional domain.

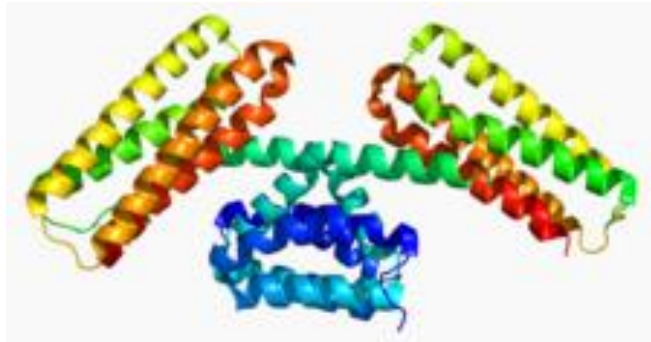


**Figure 1.11** Structure of PDCD10

It was found that PDCD10 interacts with several proteins, forming multiple signaling complexes including VEGFR2. Apart from the signaling pathways, PDCD10 involves in cell proliferation, apoptosis, Golgi assembly and cell migration.

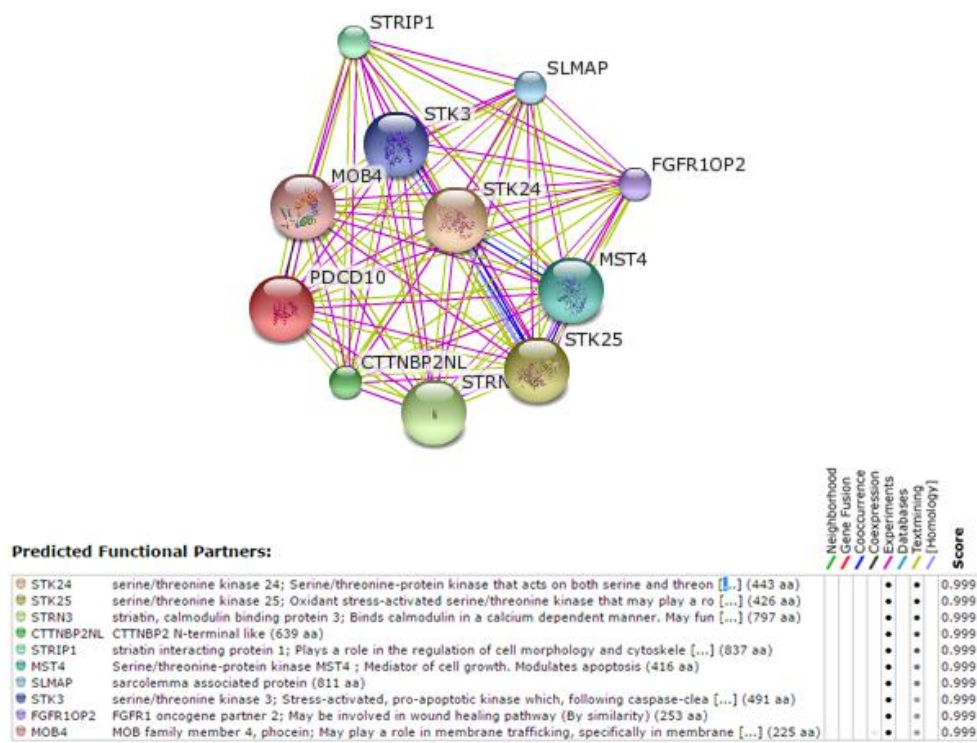


**Figure 1.12** Predicted interaction partners of PDCD10

It was found that PDCD10 is upregulated in pancreatic adenocarcinomas, metastatic colon cancer and laryngeal cell carcinoma cells (Aguire et al, 2004; Huerta et al, 2003; Chen et al, 2001). Similarly, recombinant PDCD10 was shown to inhibit apoptosis in fibroblast cells that were treated with apoptosis inducers (Wang et al, 1999, Wu et al, 2002). These data imply that PDCD10 can have an anti-apoptotic function. On the other hand, it was also shown that, under oxidative stress, PDCD10 stimulates apoptosis in HeLa cell line (Zhang et al, 2012). The different functions of PDCD10 under different cellular conditions could be associated with the interaction partner of PDCD10. It was shown that PDCD10 was co-localized with MST4 (Mst3 and SOK1 related kinase) in HEK293 human embryonic kidney, HeLa human cervical cancer and PC-3 human prostate cancer cell lines (Ma et al, 2007) MST4 (STK26) is a serine-threonine kinase which has vital roles in the regulation of mitogen activated protein kinase (MAPK) signaling pathway

during cellular functions (Dan et al, 2002). Lin et al demonstrated that MST4 regulates cellular proliferation through modulation of the activity of Ras/Raf independent ERK pathway (Lin et al, 2001). It was found that MST4 expression is correlated with tumorigenicity in prostate cancer samples and the overexpression of MST4 induces anchorage-independent growth and tumorigenesis (Sung et al, 2003). It was shown that endogenous or overexpression of PDCD10 increased MST4 kinase activity. In addition, co-expression of PDCD10 and MST promoted cellular proliferation by inducing phosphorylation of ERK. Similarly, silencing of PDCD10 decreased the P-ERK levels as well as increased the apoptotic cell number. These studies suggest that PDCD10 exerts its function through the interaction with MST4. This interaction results in an increase in the p-ERK levels, thus activating the ERK pathway (Ma et al, 2007). ERK pathway is one of the most predominant modulators of cellular proliferation and it involves in the regulation of pathogenesis, progression and oncogenic behavior of different cancers. The stimulation of ERK pathway by MST4-PDCD10 complex indicates that PDCD10 acts as an anti-apoptotic protein and the expression of PDCD10 favors survival and promotes cell growth. On the other hand, the same group showed that PDCD10 also co-localized with STK25 (Ste-20 related serine-threonine kinase 25) in cytoplasm in HEK293, HeLa and COS-7 cell lines. The expression levels of PDCD10 and STK25 were upregulated when cells were exposed to hydrogen peroxide, generating oxidative stress in the cells. It was demonstrated that increased STK25 expression under oxidative stress induced apoptosis and co-expression of STK25 and PDCD10 accelerated the cell death. PDCD10 expression was found to enhance STK25 activity, which, in turn, increases amounts of active caspase 3 and PARP in the cell, stimulating apoptosis (Zhang et al, 2012). The effect of PDCD10 on apoptosis seems to be controlled by its interaction partner which dictates the fate of the cell under different cellular conditions.

Although the exact interaction is not clear between PDCD10 and MST4 or PDCD10 and STK25, recent sequence analyses show that PDCD10 has a protein kinase binding domain at N-terminus, indicating that PDCD10 can directly interact with MST4 and STK25.

Eukaryotic promoter database (EPD) search for PDCD10 promoter site revealed that trimethylation occurs on H3K4 (H3K4me3) in K562 cells. H3K4me3 is associated with transcriptional activity which is further confirmed by the presence of PolII in promoter site. It was also shown that protease inhibitor *SERPINI1*, whose downregulation is found to be important in tumorigenesis in brain, and *PDCD10* genes are adjacently located on chromosome 3 (chromosomal region of 3q26), only separated by a short sequence (851 bp). A GC-rich 175-bp bidirectional promoter is located inside this intergenic region. This bidirectional promoter is vital for the transcriptional activity of both *SERPINI1* and *PDCD10* genes. This bidirectional gene pair is found to be controlled by an oncogenic transcription factor, c-Myc (Chen et al, 2009).

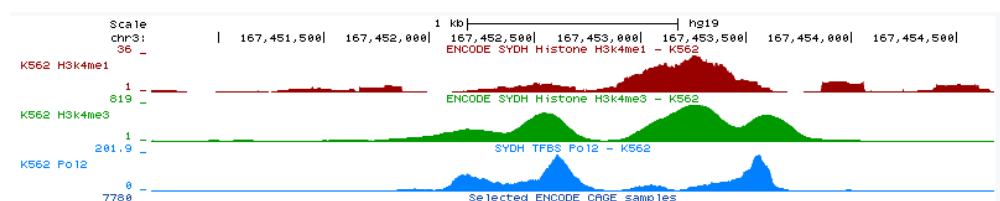


**Figure 1.13** Epigenetic regulation of *PDCD10* promoter

PDCD10 protein has three phosphorylation sites; two of which at N-terminus are responsible for protein kinase binding. Two lysine ubiquitination sites involve in the regulation of proteasome mediated degradation of PDCD10.



**Figure 1.14** Post-translational modifications of PDCD10 protein

### 1.5.1 PDCD10 – Drug Resistance Relationship

Up to now, the involvement of PDCD10 in multidrug resistance has not been examined in detail. Huerta et al showed that PDCD10 expression was upregulated in SW620 and SW480 metastatic colon cancer cells which were reported as resistant to cisplatin-induced apoptosis after 4h treatment (Huerta et al, 2003). However, in a recent study, Zhang et al reported that miR-425-5p overexpression modulated drug resistance in colon cancer cells by downregulation of *PDCD10* (Zhang et al, 2016). Similarly, our research group previously reported in a microarray based study that PDCD10 was remarkably downregulated (up to 130-fold) in several drug-resistant MCF7 sublines, implying that the downregulation of PDCD10 expression may provide selective advantage to drug-resistant MCF7 sublines (Kars, 2008; İşeri, 2009; Kars et al, 2011).

## 1.6 Aim of the Study

The main goal of this study is to establish the link between the function of *PDCD10* and multidrug resistance as well as to provide an insight to the differential functions of *PDCD10* in apoptosis. The objectives of this study are listed below:

- Determination of *PDCD10* expression levels in different drug-sensitive and –resistant cancer cells
- Determination of the effect of *PDCD10* expression changes on drug resistance status in different cancer cells
- Investigation of the effect of *PDCD10* expression changes on apoptosis and caspase 3/7 activity
- Examination of the *PDCD10* expression changes on expression levels of apoptosis-related genes
- Determination of the *PDCD10* expression changes on migratory, invasive and metastatic ability of cancer cells

## CHAPTER 2

### MATERIALS AND METHODS

#### 2.1 Materials

Doxorubicin was obtained from Saba, Turkey. Docetaxel was provided by Gulhane Medical School, Ankara, Turkey. Zoledronic acid was obtained from Novartis Pharma AG, Switzerland. Imatinib (Sigma-Aldrich, USA) was kindly provided by Asst. Prof. Dr. Ender Yıldırım, Çankaya University, Turkey.

#### 2.2 Cell Lines and Cell Culture

Doxorubicin-, docetaxel- and zoledronic acid resistant MCF7 breast adenocarcinoma, doxorubicin-resistant HeLa cervical cancer and doxorubicin- and imatinib-resistant K562 cells were previously developed from their corresponding drug-sensitive parental cell lines in our laboratory by step-by-step selection of cells in increasing drug concentrations (Baran et al, 2007; Kars, 2008; İşeri, 2009). All drug-sensitive and –resistant cells were maintained in RPMI 1640 medium supplemented with 10% (v/v) heat-inactivated filter-sterilized FBS and 0.2% (v/v) gentamycin. Drug-resistant cells were treated with proper concentrations of corresponding anti-cancer agents to maintain drug-resistant phenotype. Before experimentation, cell

viability analysis was performed for each drug-resistant subline to confirm resistance status.

### **2.2.1 Subculturing**

Cells should be regularly subcultured to provide them sufficient nutrient and oxygen as well as to eliminate waste products. Subculturing also prevents contact inhibition, an event cultured cells cease dividing when they reach the boundaries of cell culture flask. To subculture monolayer cells, the medium in which cells were growing was removed and the cells were washed with 5 ml PBS. Then, the cells were treated with 1 ml trypsin-EDTA solution (Biological Industries, Israel) for 5 min at 37°C. 3 ml of 10% FBS containing medium (full medium) was added in the cell culture flasks to stop the activity of trypsin and cells were homogenized by pipetting. The desired amount of cell suspension was transferred into new culture flasks and volume was completed to 10 ml with full medium. To subculture suspension cells, the desired amount of medium was taken from the cell culture flask into a 15 ml Falcon tube and centrifuged for 5 min at 1000 rpm. After discarding the supernatant, the cell pellet was dissolved in 5 ml PBS. After centrifugation for 5min at 1000 rpm, the supernatant was poured off, and the pellet was dissolved in 4 ml full medium. Then, the cells were transferred to a cell culture flask. 6 ml full medium was added to complete the volume to 10 ml.

### **2.2.2 Cell Freezing and Thawing**

To store cultured cells for a long time period, the cells should be cryogenically frozen. To that end, the cells were harvested, transferred to 15 ml Falcon tubes and centrifuged for 5 min at 1000 rpm. The supernatant was removed, the cell pellet was resuspended in 5 ml PBS and centrifuged at 1000

rpm for 5 min. After removal of the supernatant, the cell pellet was dissolved in 1 ml FBS: DMSO (with a ratio of 9:1) mixture and immediately transferred to -80°C in cryovials for overnight incubation. For long-term storage, the cryovials should be kept in liquid nitrogen tanks. Before experimentation, frozen cell stocks were incubated in water bath at 37°C until thawing. Cell suspensions were immediately taken into 15 ml Falcon tubes, mixed with 4 ml full medium and centrifuged at 1000 rpm for 5 min. The supernatant was discarded and the pellet was dissolved in 4 ml full medium. Cell suspension in fresh medium was transferred to cell culture flasks and 6 ml full medium was added to complete the volume to 10 ml.

### **2.2.3 Cell counting by Trypan Blue cell exclusion method**

To count the cells, they were harvested as described above and centrifuged for 5 min at 1000 rpm. The cell pellet was washed with 5 ml PBS and centrifuged for 5 min at 1000 rpm. Then, the supernatant was removed and the pellet was resuspended in full medium. 90 µl cell suspension was mixed with 10 µl 0.5% trypan blue solution. 10 µL of stained cell mixture was transferred to a Neubauer hemacytometer (Brightline, Hausser Scientific, USA). Then, the stained cells were counted by using a phase contrast microscope (Olympus, USA). The Neubauer hemacytometer has 16 large squares, each of which consist of 16 smaller squares with a volume of 0.00025 mm<sup>3</sup>.

Cell number/ml was determined by using the formula given below:

Cell number/ml = Average cell count per square x Dilution factor x 4 x 10<sup>6</sup>

## **2.3 Gene Expression Analysis**

### **2.3.1 Isolation of Total RNA**

Total RNA was isolated by TRIzol reagent (Thermo Fisher Scientific, USA) according to manufacturer's instructions. Briefly, the cells were harvested as described above and centrifuged for 5 min at 1000 rpm. Then, the supernatant was removed, the cell pellet was homogenized in 1 ml TRIzol reagent by pipetting and transferred to sterile Eppendorf tubes. Then, 200  $\mu$ l chloroform was added and the mixture was centrifuged for 15 min at 12000 g to facilitate phase formation. After centrifugation, three phases appear in the tubes; the aqueous phase which contains RNA, the DNA interphase and the pink organic phase which contains protein. RNA-containing aqueous phase was carefully taken into sterile Eppendorf tubes and mixed with 500  $\mu$ l ice-cold isopropanol. The mixture was centrifuged at for 15 min at 12000 g to precipitate RNA. After centrifugation, RNA pellet was washed with 1 ml 75% ethanol and centrifuged at for 5 min at 12000 g. Then, the RNA pellet was air-dried and dissolved in nuclease-free water. The integrity of RNA samples was monitored by running the samples on 2% agarose gel (w/v) at 90V for 1h. Concentrations of the isolated RNA samples were determined by using BioDrop spectrophotometer (BioDrop, UK). The RNA samples with A260/A280 and A260/230 values between 1.8-2.2 were used for further experiments.

### **2.3.2 DNase Treatment and cDNA Synthesis**

DNase treatment was carried out to eliminate possible DNA contamination. In brief, 1  $\mu$ g total RNA was mixed with 1  $\mu$ l DNase buffer, 1  $\mu$ l DNase and nuclease-free water (Thermo Fisher Scientific, USA). The mixture was

incubated for 30 min at 37°C. Then, 1 µl EDTA was added into the tubes and incubated for 10 min at 65°C to stop the reaction. 1 µl random hexamer primer and 0.5 µl nuclease-free water was added to DNase treated samples and incubated at 65°C for 5 min. Then, 4 µl reaction buffer, 2 µl ready-to-use dNTP mix, 0.5 µl RiboLock RNase inhibitor and 1 µl RevertAid Reverse Transcriptase was added. The reaction mixture was incubated at 25°C for 10 min, 42°C for 1h and 72°C for 10 min to synthesize cDNA. cDNA samples were stored at -20°C.

### **2.3.3 Quantitative Real Time Polymerase Chain Reaction (qRT-PCR)**

To analyze gene expression, qRT-PCR was used. For PDCD10 expression, Light Cycler® 480 Probes Master mix and RealTime Ready Assay containing primers (Roche Diagnostics, Switzerland) was used. β-actin was used as reference. The ingredients and reaction conditions were given in Table 2.1.

**Table 2.1.** PCR ingredients and conditions for *PDCD10* expression

<b>Ingredient</b>	<b>Concentration</b>	<b>Volume</b>	<b>Final concentration</b>
LightCycler® 480 Probes Master Mix	2X	10 µl	1X
Real Time Ready Assay	20X	1 µl	8 pmol primers 4 pmol UPL probe
Template		5 µl	
PCR grade water		4 µl	
<b>Total</b>		20 µl	

Pre-incubation	95°C	10 s	1 cycle
Amplification	95°C	10 s	45 cycles
	60°C	30 s	
	72°C	1 s	
Cooling	40°C	30 s	1 cycle

The expressions of apoptosis-related *BCL2*, *BAX*, *SURVIVIN* and *PUMA* genes were performed by using SsoAdvanced Universal SYBR Green Supermix (Bio-Rad Laboratories, USA). *β-actin* was used as reference. The primer sequences were given in Table 2.2 and the ingredients and reaction conditions were given in Table 2.3.

**Table 2.2.** Primer sequences

<b>Gene</b>	<b>Primer Type</b>	<b>Sequence</b>	<b>Amplicon size</b>
<i>BCL2</i>	Forward	5'CCCGCGACTCCTGATTCATT3'	166 bp
	Reverse	5'AGTCTACTTCCTCTGTGATGTTGT3'	
<i>BAX</i>	Forward	5'TCTGACGGCAACTTCAACTG3'	188 bp
	Reverse	5'TTGAGGAGTCTCACCCAACC3'	
<i>SURVIVIN</i>	Forward	5'AGCCAGATGACGACCCCATAGAGG3'	60 bp
	Reverse	5'AAAGGAAAGCGCAACCGGACGA3'	
<i>PUMA</i>	Forward	5'GACGACCTCAACGCACAGTA3'	109 bp
	Reverse	5'GTAAGGGCAGGAGTCCCAT3'	
<i>β-actin</i>	Forward	5'CCAACCGCGAGAAGATGA3'	97 bp
	Reverse	5'CCAGAGGCGTACAGGGATAG3'	

**Table 2.3.** PCR ingredients and conditions for expressions of apoptosis-related genes

<b>Ingredient</b>	<b>Concentration</b>	<b>Volume</b>	<b>Final Concentration</b>
SsoAdvanced Universal SYBR Green Supermix	2X	5 µl	1X
Forward primer	5 µM	1 µl	0.25 µM
Reverse primer	5 µM	1 µl	0.25 µM
Template		3 µl	
<b>Total</b>		10 µl	

Initial denaturation	95°C	5 min	1 cycle
Denaturation	95°C	30 s	45 cycles
Annealing	59°C	30 s	
Extension	72°C	30 s	
Final elongation	72°C	10 min	1 cycle
Melting	55 – 99 °C		1 cycle

### 2.3.4 Quantification of qRT-PCR

Data were quantified by using  $DDC_t$  ( $2^{\Delta\Delta Ct}$ ) method (Livak & Schmittgen, 2001). Fold changes in expression were calculated by the formula of  $2^{-\Delta\Delta Ct}$  where  $\Delta\Delta Ct$  is calculated by the formula below:

$$\Delta\Delta Ct = ((Ct_{Target}) - (Ct_{Reference})_{Treated}) - ((Ct_{Target}) - (Ct_{Reference})_{Untreated})$$

## **2.4 siRNA Mediated Silencing**

To knockdown *PDCD10* expression in parental MCF7, doxorubicin-resistant HeLa and imatinib-resistant K562 cells, *PDCD10*-specific siRNA (siPDCD10; Qiagen, Germany) was used.

### **2.4.1 *PDCD10* Knockdown in 6-Well Plates**

$3 \times 10^5$  MCF7, HeLa/DOX and K562 cells/well were seeded in 6-well plates. siControl (control siRNA that does not target any sequence in human transcriptome) and siPDCD10 (5 nM for MCF7 and HeLa/DOX cells, and 50 nM for K562/IMA cells) were diluted in serum-free medium and mixed with 9  $\mu$ l HiPerFect transfection reagent (Qiagen, Germany) according to the manufacturer's instructions. The mixture was briefly vortexed and incubated for 15 min at room temperature for transfection complex formation. Then, 100  $\mu$ l transfection complex was added dropwise to cells and incubated at 37°C for 24, 48 and 72h. After the incubation period is completed, total RNA was isolated as described before and *PDCD10* knockdown was validated by qRT-PCR.

### **2.4.2 *PDCD10* Knockdown in 96 Well Plates**

$5 \times 10^3$  MCF7 or HeLa/DOX cells/well, and  $3 \times 10^4$  K562/IMA cells/well were seeded in sterile 96-well plates. siControl and siPDCD10 (5 nM for MCF7 and HeLa/DOX cells, and 50 nM for K562/IMA cells) were diluted in serum-free medium and 0.5  $\mu$ l HiPerFect transfection reagent (Qiagen, Germany) was added to the mix according to the manufacturer's instructions. The mixture was vortexed briefly and incubated for 15 min at room temperature

for the transfection complex formation. Then, 10  $\mu$ l transfection complex mixture was added dropwise to cells and incubated at 37°C for 48h.

## 2.5 Overexpression of PDCD10

In order to overexpress PDCD10 in different cancer cells, PDCD10 should be cloned into an expression vector. For that purpose, *PDCD10* open reading frame containing pPHAGE C-TAP vector (plasmid ID: HsCD00450681) was purchased from Harvard PlasmID Database (Harvard University, USA).

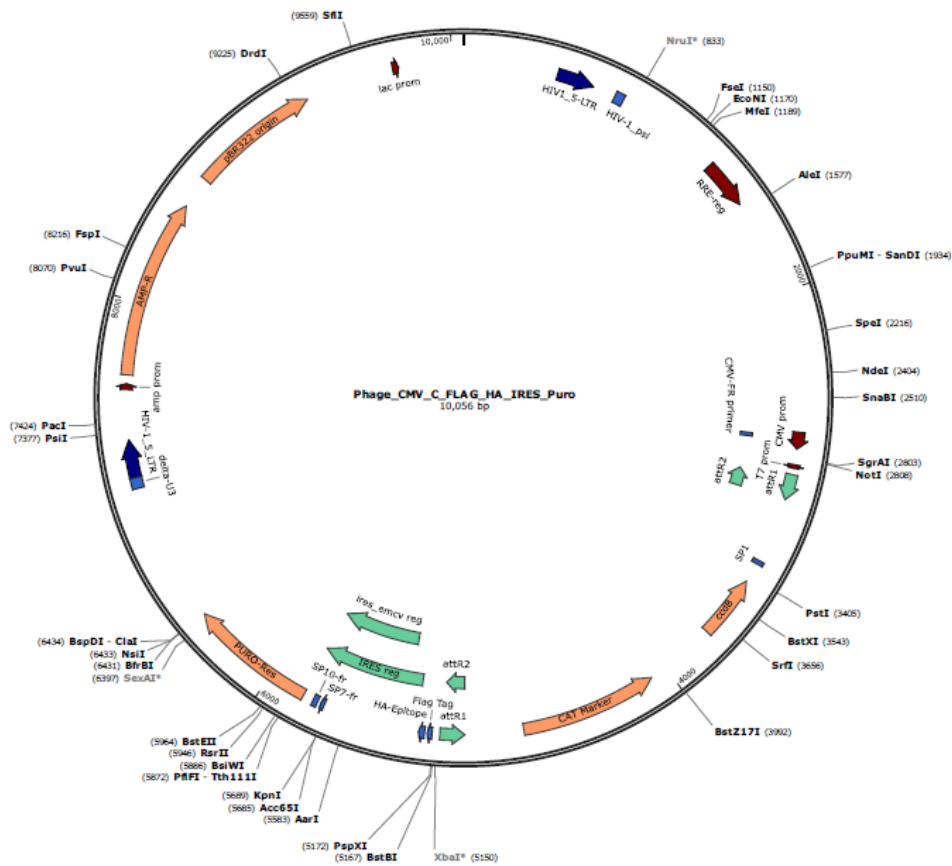


**Figure 2.1.** PHAGE cTAP vector backbone

*PDCD10* open reading frame containing pPHAGE C-TAP vector should be amplified by transforming *E. coli* cells with the vector. However, *E. coli* cells were not naturally competent so that they should be made competent to facilitate horizontal gene transfer.

### **2.5.1 Competent *E. coli* preparation**

TOP10 *E. coli* cells were streaked on LB agar and grown overnight at 37°C. After selection of a single colony, it was inoculated in 10 ml LB media and grown overnight at 37°C. 5 ml of TOP10 *E. coli* culture was transferred into 100 ml LB media and grown at 37°C while shaking at 250 rpm until OD<sub>600</sub>=0.4 is achieved. Cells were taken on ice for 20 min and centrifuged for 10 min at 3000 g at 4°C. After discarding the supernatant, the pellet was dissolved in 30 ml of cold 0.1 M CaCl<sub>2</sub> solution and incubated on ice for 30 min. After that, the cells were centrifuged for 10 min at 3000 g at 4°C. The supernatant was removed and the cell pellet was gently dissolved in 10 ml cold 0.1M CaCl<sub>2</sub> in 15% glycerol solution. Competent *E. coli* cells were either used for transformation or stored at -80°C.

### **2.5.2 Transformation**

After competent *E. coli* cells were obtained, 50 µl competent TOP10 *E. coli* cells were mixed with 10 µl pPHAGE C-TAP vector and incubated in ice for 1h. Then, heat shock was applied at 42 °C for 45 min to enable pore formation on bacterial membrane. After heat shock, the *E. coli* cells were immediately taken in ice for 2 min. Then, 750 µl LB was added and the cells were allowed to grow at 37 °C for 1h by shaking at 200 rpm.

### **2.5.3 Plasmid isolation**

The amplified vector was isolated by using Zyppy Plasmid Miniprep Kit (Zymo Research, USA) according to the manufacturer's instructions. Briefly, 600  $\mu$ l transformed *E. coli* cells were lysed in 100  $\mu$ l 7X lysis buffer for 2 min. The lysed cells appeared in dark blue color. Then, 350  $\mu$ l cold neutralization buffer was added onto the lysed cells and mixed well until the color became yellow. The mixture was centrifuged at 14000 g for 2 min to eliminate cell debris. The supernatant was taken into Zymo-Spin IIN column and the column was placed into a collection tube. Then, the supernatant was centrifuged at 14000 g for 1 min to bind the plasmids on the filter. 200  $\mu$ l Endo-Wash buffer was added to the column and centrifuged at 14000 g for 1 min. Then, 400  $\mu$ l Zyppy Wash buffer was added and the column was centrifuged at 14000 g for 30 sec. To eliminate the remnants of any buffers on the filter, the column was centrifuged at 14000 g for 30 sec without any solutions. After that, the column was transferred into a 1.5 ml sterile Eppendorf tube, 30  $\mu$ l Zyppy Elution buffer was directly applied on to the filter and incubated at room temperature for 2 min. The column was centrifuged at 14000 g for 1 min to elute plasmid DNA. The concentration of the plasmid was measured by using BioDrop spectrophotometer (BioDrop, UK).

### **2.5.4 Insert preparation**

After plasmid was isolated, PDCD10 encoding region with a FLAG epitope at N terminus was cloned into pcDNA3.1(-) vector. To that end, PDCD10 encoding region of the pPHAGE C-TAP vector should be amplified by PCR by using a specific primer set. PCR ingredients and reaction conditions were given in Table 2.4.

**Table 2.4.** PCR ingredients and conditions for insert amplification

<b>Ingredient</b>	<b>Concentration</b>	<b>Volume</b>	<b>Final Concentration</b>
Taq buffer	10X	5 µl	1X
MgCl <sub>2</sub>		4 µl	
dNTP mix	10 mM each	1.25 µl	0.25 mM each
Forward primer	5 µM	5 µl	0.5 µM
Reverse primer	5 µM	5 µl	0.5 µM
Taq polymerase		0.5 µl	
Template	50 ng/µl	1 µl	
PCR grade water		28.25 µl	
<b>Total</b>		50 µl	

Pre-incubation	94°C	5 min	1 cycle
Denaturation	94°C	30 s	35 cycles
Annealing	52°C	30 s	
Elongation	72°C	1 min	
Final elongation	72°C	10 min	1 cycle

Sense Primer:

5' CGCAT **CTCGAG** **CCATGG** AA **GACTACAAAGACGATGACGACAAG** **GATATC** ATGAGGATGACAATGGAAGAG 3'

**XhoI** **NcoI**

**Flag Tag**

**EcoRV**

Antisense Primer:

5' CGCAT **GGATCC** **TTTATA** AGCCACAGTTTGAAGGICTG 3'

**BamHI** **polyA**

**Figure 2.2.** Primer sequences used in insert preparation

PCR products were run on 1% agarose gel at 90V for 1h to check correct amplification.

### **2.5.5 Gel Extraction**

Amplified inserts were extracted from agarose gel by using Zymoclean Gel DNA Recovery Kit (Zymo Research, USA). Firstly, DNA was excised from the gel with a sterile blade and taken into a sterile 1.5 ml Eppendorf tube. Then, 3 volumes of ADB Buffer was added and the gel slice was incubated at 55°C for 10 min until the gel was completely dissolved. Melted agarose solution was transferred to a Zymo-Spin column and the column was placed into a collection tube. The column was centrifuged at 12000 g for 2 min and flow-through was discarded. 200 µl DNA Wash buffer was added and the column was centrifuged at 12000 g for 1 min. After wash step was repeated, 10 µl DNA elution buffer was added directly to the filter and incubated at room temperature for 1 min. To elute DNA, the column was transferred into a sterile 1.5 ml Eppendorf tube and centrifuged at 12000 g for 1 min.

### **2.5.6 Double digestion**

To clone the insert into pcDNA3.1(-) vector, both the vector and the insert were digested with suitable restriction enzymes to create sticky ends.

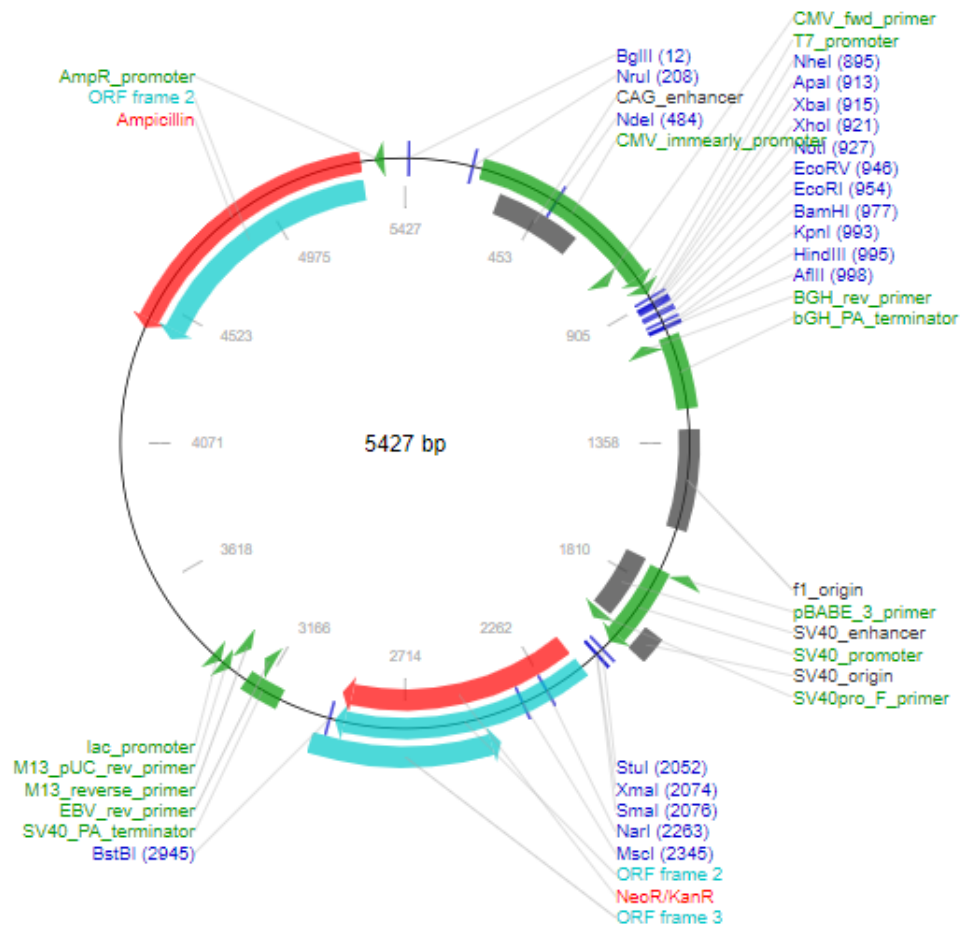


**Figure 2.3** Map of pcDNA3.1(-) vector

For that purpose, *XhoI* and *BamHI* (Thermo Fisher Scientific, USA) restriction enzymes were chosen in order not to cut the insert or the vector while creating sticky ends. The ingredients and amounts of digestion reaction were shown in Table 2.5.

**Table 2.5.** Ingredients of digestion reaction

Insert	10 $\mu$ l	pcDNA3.1(-) vector	25 $\mu$ l
Tango Buffer	10 $\mu$ l	Tango Buffer	10 $\mu$ l
<i>Bam</i> HI	4 $\mu$ l	<i>Bam</i> HI	4 $\mu$ l
<i>Xho</i> I	2 $\mu$ l	<i>Xho</i> I	2 $\mu$ l
Nuclease free water	24 $\mu$ l	Nuclease free water	9 $\mu$ l
<b>Total</b>	50 $\mu$ l	<b>Total</b>	50 $\mu$ l

The digestion mixtures were incubated at 37°C for 4h. After the incubation period, the digested insert and vector were run on 1% agarose gel at 90V for 1h. Then, both the digested insert and the vector were extracted from agarose gel as described before.

### 2.5.7 DNA Clean Up

To obtain the DNA insert and the vector at a sufficient quality for cloning, the extracted DNA elutes were cleaned and concentrated by using DNA Clean & Concentrator 5 kit (Zymo Research, USA). For that purpose, 100  $\mu$ l PCR product was mixed with 500  $\mu$ l DNA Binding buffer by vortexing. The mixture was transferred to Zymo-Spin Column placed in a collection tube. The mixture was centrifuged at 12000 g for 1 min and the flow-through was discarded. 200  $\mu$ l DNA Wash buffer was added and the column was centrifuged at 12000 g for 30 sec. After repeating the wash step, 6  $\mu$ l DNA elution buffer was added directly to the column matrix and incubated at room temperature for 1 min. The column was transferred to a sterile 1.5 ml Eppendorf tube and centrifuged at 12000 g for 1 min to elute DNA. The

concentration of the eluted insert was measured by using BioDrop spectrophotometer (BioDrop, UK).

### 2.5.8 Ligation

To ligate the insert and the vector with sticky ends, T4 DNA Ligase (Thermo Fisher Scientific, USA) was used. Briefly, 50 ng vector was mixed with the insert at a ratio 1:9. The ingredients and amounts of ligation reaction were given below:

**Table 2.6.** Ingredients of ligation reaction

<b>Ingradients</b>	<b>Volume</b>
T4 DNA Ligase buffer	1 $\mu$ l
Vector	1 $\mu$ l
Insert	5 $\mu$ l
T4 DNA Ligase	1.5 $\mu$ l
Nuclease free water	1.5 $\mu$ l
<b>Total</b>	10 $\mu$ l

The mixture was incubated at 25°C for 2h to ligate the sticky ends and form a circular plasmid. The ligated plasmid (pcDNA\_PDCD10) was transformed into competent *E. coli* cells as described before and streaked on ampicillin-containing agar plates.

### 2.5.9 Colony PCR

The insertion of the FLAG\_PDCD10 coding sequence into the pcDNA3.1(-) vector was confirmed by colony PCR. The PCR ingredients and conditions were shown in Table 2.7.

**Table 2.7** Ingredients and conditions of colony PCR

Ingredients	Concentration	Volume	Final concentration
Taq buffer	10X	2.5 $\mu$ l	1X
MgCl <sub>2</sub>		2 $\mu$ l	
dNTP mix	10 mM each	0.5 $\mu$ l	
Forward primer	25 $\mu$ M	0.5 $\mu$ l	
Reverse primer	25 $\mu$ M	0.5 $\mu$ l	
Taq polymerase		0.2 $\mu$ l	
Template		2.5 $\mu$ l	
PCR grade water		16.3 $\mu$ l	
<b>Total</b>		25 $\mu$ l	

Pre-incubation	94°C	5 min	1 cycle
Denaturation	94°C	30 s	35 cycles
Annealing	52°C	30 s	
Elongation	72°C	1 min	
Final elongation	72°C	10 min	1 cycle

PCR products were run on 2% (w/v) agarose gel at 90V for 1h. The colonies showing correct band was taken into LB and grown at 37°C with shaking at 200 rpm. The *FLAG\_PDCD10* coding sequence containing plasmids

(pcDNA\_PDCD10) were isolated by Zyppy Plasmid Isolation kit (Zymo Research, USA) as described before.

## **2.5.10 Transfection of cells with overexpression vector**

### **2.5.10.1 Transfection in 6 Well Plates**

$3 \times 10^5$  MCF7/DOX, HeLa, and K562/IMA cells were seeded in 6-well plates. 1.5  $\mu$ g of the pcDNA\_PDCD10 vector was diluted in 200  $\mu$ l serum-free medium and mixed with 3  $\mu$ l TurboFect transfection reagent (Thermo Fisher Scientific, USA). The mixture was allowed to incubate at room temperature for 30 min for the formation of transfection complexes. Then, 200  $\mu$ l transfection complex was added dropwise to the cells.

### **2.5.10.2 Transfection in 96 Well Plates**

$5 \times 10^3$  MCF7/DOX, HeLa and K562/IMA cells were seeded in 6-well plates. 72.5 ng of pcDNA\_PDCD10 vector was diluted in 22.5  $\mu$ l serum-free medium and mixed with 0.15  $\mu$ l TurboFect transfection reagent (Thermo Fisher Scientific, USA). The mixture was allowed to incubate at room temperature for 30 min for formation of transfection complexes. After adding 77.5  $\mu$ l full medium into the mixture, 100  $\mu$ l transfection complex was added dropwise to the cells.

### **2.5.11 Total Protein Isolation and Determination of Protein Concentration**

Total protein was isolated from EV and pcDNA\_PDCD10 transfected MCF7/DOX cell lines by using RIPA Lysis and Extraction Buffer (Thermo Fisher Scientific, USA) according to the manufacturer's instructions. In short, the cells were harvested as described and lysed in 1 ml of cold RIPA buffer containing 100X Halt Protease and Phosphatase Inhibitor cocktails (Thermo Fisher Scientific, USA) for 30 min on ice by vortexing in regular intervals. Then, lysed samples were centrifuged for 30 at 14000 g to pellet cell debris. Protein containing supernatant was taken to a sterile Eppendorf tube.

### **2.5.12 Sodium dodecyl sulfate-Polyacrylamid Gel Electrophoresis (SDS-PAGE)**

To separate 29 kDa PDCD10 and 41 kDa  $\beta$ -actin proteins, isolated protein samples were firstly run on sodium dodecyl sulfate-polyacrylamid gels in Mini-PROTEAN Tetra Cell gel system (Bio-Rad Laboratories, USA). For that purpose, 8% separating gel mixture was prepared and loaded between the glass sandwich system. The surface of the mixture was covered with isopropanol to prevent inhibition of gel polymerization and provide a smooth gel surface. After polymerization, 5% stacking gel mixture was prepared and loaded on separating gel. Comb was placed and the gel mixture was allowed to polymerize. The ingredients and concentrations of separating and stacking gels were given in Table 2.8.

**Table 2.8.** Ingredients and amounts of stacking and separating gels

<b>Ingredient</b>	<b>5% stacking gel</b>	<b>8% separating gel</b>
30% acrylamide-bisacrylamide solution (37:5:1)	850 $\mu$ l	2.7 ml
1M Tris buffer (pH 6.8)	625 $\mu$ l	----
1.5M Tris buffer (pH 8.8)	----	2.5 ml
10% APS	50 $\mu$ l	100 $\mu$ l
10% SDS	50 $\mu$ l	100 $\mu$ l
TEMED	5 $\mu$ l	5 $\mu$ l
dH <sub>2</sub> O	3.4 ml	4.6 ml
<b>Total</b>	5 ml	10 ml

30  $\mu$ g of protein solution was mixed with 4X loading buffer which contains  $\beta$ -mercaptoethanol and incubated for 5 min at 95°C to completely denature proteins. The denatured protein samples were vortexed briefly, loaded on previously casted polyacrylamide gel with pre-stained protein marker (Thermo Fisher Scientific, USA) and run at 100V in stacking and 150V in separating gel.

### 2.5.13 Wet Transfer

After gel running, the gel, pre-cut nitrocellulose membrane and filter papers, which will be used in wet transfer process, were incubated in cold transfer buffer for 15 min. Then, the first set of pre-wetted filter papers, gel, nitrocellulose membrane and another set of filter papers were carefully placed on the sandwich such that gel would face the cathode and membrane would face to anode. The sandwich was placed in the gel tank with an ice box. After

that, the tank was filled with cold transfer buffer and transfer was carried out at 25V at 4°C for 1h.

#### **2.5.14 Membrane Blocking**

Before blotting, membrane should be blocked to eliminate antibody binding to non-specific antigens. To that end, the membrane was blocked by incubating in 5% BSA (w/v) in 0.1% TBST buffer (1X TBS buffer containing 0.1% v/v Tween20) for 1h at room temperature by gently shaking on a shaker.

#### **2.5.15 Western Blotting and Imaging**

To visualize FLAG\_PDCD10 fusion protein, anti-FLAG antibody (Sigma-Aldrich, USA) was used.  $\beta$ -actin was used as loading control and anti- $\beta$ -actin antibody was obtained from Abcam, USA. Both primary antibodies had mouse origins.

After blocking, the membrane was incubated in anti-FLAG or anti- $\beta$ -actin antibody diluted in 5% BSA in 0.1% TBST (1:1000) at 4°C overnight. Then, the membrane was washed with 0.1% TBST six times for 5 min and incubated in horseradish peroxidase (HRP) tagged secondary goat anti-mouse antibody (Abcam, USA) diluted in 5% BSA in 0.1% TBST (1:2000) for 1h at room temperature. The blotted membrane was washed with 0.1% TBST six times for 5 min. After washing, the membrane was incubated in ECL Western Blotting Substrate (Thermo Fisher Scientific, USA) prepared by mixing detection reagents at a 1:1 ratio for 1 min. Excess ECL substrate was drained and images were taken by exposing the blot to UV light with ChemiDoc Imaging System (Bio-Rad Laboratories, USA).

## 2.6 Cell Viability Assay

Viability of MCF7, HeLa and K562 cells as well as their drug-resistant sublines was assessed after genetically altering *PDCD10* expression by XTT cell proliferation assay (Biological Industries, Israel). Briefly,  $5 \times 10^3$  cells/well was seeded in 96-well plates for overnight attachment except for column #1 which serves as “medium control group” for background absorbance detection. Then, the cells transfected with either *siControl/siPDCD10* or *EV/pcDNA\_PDCD10* for 48h. After that, transfected cells were treated with serial dilutions of corresponding anti-cancer agent for 48h. The cells in column #2 were not treated with any anti-cancer agent and used as “cell control group”. For doxorubicin-treated cells, “DOX control group” was prepared by serial dilutions of doxorubicin in full medium without cells since doxorubicin itself gave absorbance at the measurement wavelength. Later, XTT reagent and activator agent was mixed with a ratio of 49:1 and added onto cells. After 4h incubation at 37°C, the absorbance was measured at 500 nm. The viability non-drug treated cells was accepted as 100% growth and the viability of treated cells was determined with respect to the control group. Cellular viability vs Drug concentration graph was plotted and inhibitory concentration 50 ( $IC_{50}$ ) was calculated for each subline and treatment. Relative resistance index (R) for each subline and treatment was determined with the formula below:

$$R = \frac{IC_{50} \text{ of treated group}}{IC_{50} \text{ of control group}}$$

## 2.7 Intracellular Drug Accumulation Assay

To measure intracellular drug accumulation with respect to alterations in PDCD10 expression, the fluorescent nature of doxorubicin (excitation at 488 nm and emission at 590 nm) was used (de Lange et al, 1996). For that purpose, MCF7 and HeLa cells as well as their doxorubicin-resistant sublines were seeded in black 96-well plates with a final concentration of  $5 \times 10^3$  cells/well. After transfection with either *siPDCD10* or pcDNA\_PDCD10 depending on endogenous *PDCD10* expression, the cells were treated with 10  $\mu$ M doxorubicin for 4h. Then, medium was discarded and the cells were washed twice with PBS to eliminate free doxorubicin. Intracellular drug accumulation was measured by using SpectraMax iD3 Multi-Mode Microplate Reader (Molecular Devices, USA).

## 2.8 Apoptosis Assay

$5 \times 10^5$  MCF7 cells/well were seeded in 6-well plates and transfected with either 5 nM of *siPDCD10* or *siControl* for 48 and 72h. Only transfection reagent treated cells (vehicle only) was used as negative control and 50  $\mu$ M etoposide treated cells were used as positive control. Then, floating dead cells and alive cells (still attached on the plate surface) collected into the same 15 ml Falcon tube. After centrifugation at 250 g for 5 min, supernatant was discarded and pellet containing both dead and live cells was resuspended in 400  $\mu$ L PBS buffer. AnnexinV-PI staining was performed by using Annexin-V-FLUOS Staining Kit (Roche, Switzerland) according to the manufacturer's instructions. Briefly, 100  $\mu$ L incubation buffer was added onto 400  $\mu$ L cell suspension. Then, 2  $\mu$ L of AnnexinV and/or PI was added into each sample. Fluorescence signal of FITC-conjugated AnnexinV was measured in FL1

channel and fluorescence of PI was measured in FL3 channel by using Accuri Flow Cytometer (BD Biosciences, USA).

## **2.9 Caspase 3/7 Activity Assay**

Caspase 3/7 activity with respect to changing *PDCD10* expression was determined by Apo-ONE® Homogeneous Caspase 3/7 Assay (Promega, USA). For that purpose,  $5 \times 10^3$  MCF7 cells/well were seeded in black 96-well plates for overnight attachment. Then, MCF7 cells were transfected with either *siControl* or *siPDCD10* for 48h and treated with different concentrations of etoposide for 24h. Apo-ONE® Caspase Reagent was prepared according to the manufacturer's instructions by mixing caspase substrate with reaction buffer (1:100) and added to each well with 1:1 ratio. Only medium and caspase reagent containing wells were used as blank. Fluorescent signal was measured at 521 nm by using SpectraMax iD3 Multi-Mode Microplate Reader (Molecular Devices, USA).

## **2.10 Wound Healing Assay**

To determine whether PDCD10 expression affects migratory activity of drug-sensitive and -resistant cells,  $3 \times 10^5$  cells/well were seeded in 6-well plates on sterile coverslips. Then, cells were transfected with either *siControl/siPDCD10* or EV/pcDNA\_PDCD10 for 48h. After that, a scratch was made on coverslips by using a sterile yellow pipette tip. Images of the cells were taken in regular intervals with Olympus CKX41 microscope. Image analysis was done by using ImageJ image processing program.

## **2.11 Statistical Analysis**

All experiments were performed as three independent experimental set, each of which containing triplicates. Data were represented as mean  $\pm$  SEM and analyzed with t-test or one-way ANOVA test followed by post-hoc Tukey's test. Results were accepted as significant when  $p < 0.05$ .

## CHAPTER 3

### RESULTS AND DISCUSSION

Programmed cell death (PDCD) family is a novel protein family that involves in the regulation of cell survival and cell death. Up to now, 12 proteins which belong to PDCD family have been identified.

Gene Name	Gene Symbol	Description	Gene Ontology	MCF-7/ 30DOC	MCF-7/ 120DOC	MCF-7/ 1000DOX
213581_at	PDCD2	programmed cell death 2	BP: cell death; MF: apoptosis regulator	NS	-3.40	NS
212593_s_at, 202730_s_at	PDCD4	programmed cell death 4 (neoplastic transformation inhibitor)	BP cell death; MF: apoptosis regulator	3.23	-2.55	-2.78
205512_s_at	PDCD8	programmed cell death 8 (apoptosis-inducing factor)	BP: cell growth and maintenance, cell death; MF: binding, catalytic activity, apoptosis regulator	NS	-2.13	-2.01
210907_s_at	PDCD10	programmed cell death 10	BP: cell growth and maintenance, cell death; MF: binding, catalytic activity, apoptosis regulator	NS	-133.33	-113.90

Gene Name	Gene Symbol	Description	Ontology	Fold change	
				MCF-7/Vinc	MCF-7/Pac
213581_at	PDCD2	programmed cell death 2	BP death, MF apoptosis regulator	-2.232	-2.801
205512_s_at	PDCD8	programmed cell death 8 (apoptosis-inducing factor)	BP Growth-M, MF binding	NS	-2.463
212594_at	PDCD4	programmed cell death 4 (neoplastic transformation inhibitor)	BP death, MF apoptosis regulator	NS	-4.405
1569110_x_at	PDCD6	programmed cell death 6	BP death, MF apoptosis regulator, MF transcription regulatory	-62.50	-34.13
210907_s_at	PDCD10	programmed cell death 10	BP death, MF transporter activity, MF apoptosis regulator activity	-118.62	-130.38

**Figure 3.1** Microarray-based expression levels of *PDCD* family genes in drug-resistant MCF7 sublines compared to parental MCF7 cells (Kars, 2008; İşeri, 2009).

Previous microarray based studies in our laboratory showed that PDCD10 was significantly downregulated in docetaxel-, doxorubicin-, vincristine- and paclitaxel-resistant MCF7 cells (Figure 3.1).

### 3.1 Isolation of Total RNA from Parental and Drug-Resistant Cancer Cell Lines

Total RNAs isolated from parental and drug-resistant MCF7, HeLa and K562 cell lines were analyzed on 2% agarose gel before cDNA synthesis to check their structural integrity and purity (Figure 3.2). Since ribosomal RNA population makes up more than 80% of total RNA species in the cell, they can be easily visualized on agarose gel. The sharp and distinct ribosomal RNA (28S and 18S) bands are an indication of intact RNA samples for gene expression analysis. Moreover, the concentration and purity of isolated RNA samples were checked by BioDrop Spectrophotometer (BioDrop, UK). The isolated RNA samples with A260/A280 (nucleic acid/protein) values between 1.8-2.2 were considered suitable for further experimentation.

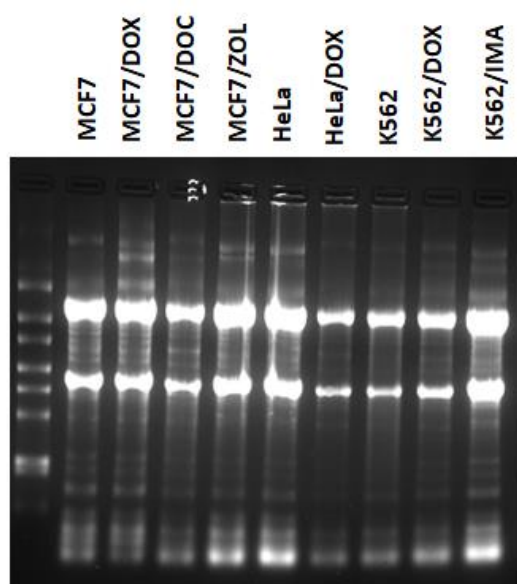


**Figure 3.2** Total RNAs isolated from parental and drug-resistant MCF7, HeLa and K562 cells. Total RNA was isolated by using TRIzol reagent (Thermo Fisher Scientific, USA) and visualized on 2% agarose gel.

### 3.2 Screening of parental and drug-resistant MCF7, HeLa and K562 cancer cells for *PDCD10* expression

Parental MCF7, HeLa and K562 cells and their drug-resistant sublines were examined for *PDCD10* expression by qRT-PCR.

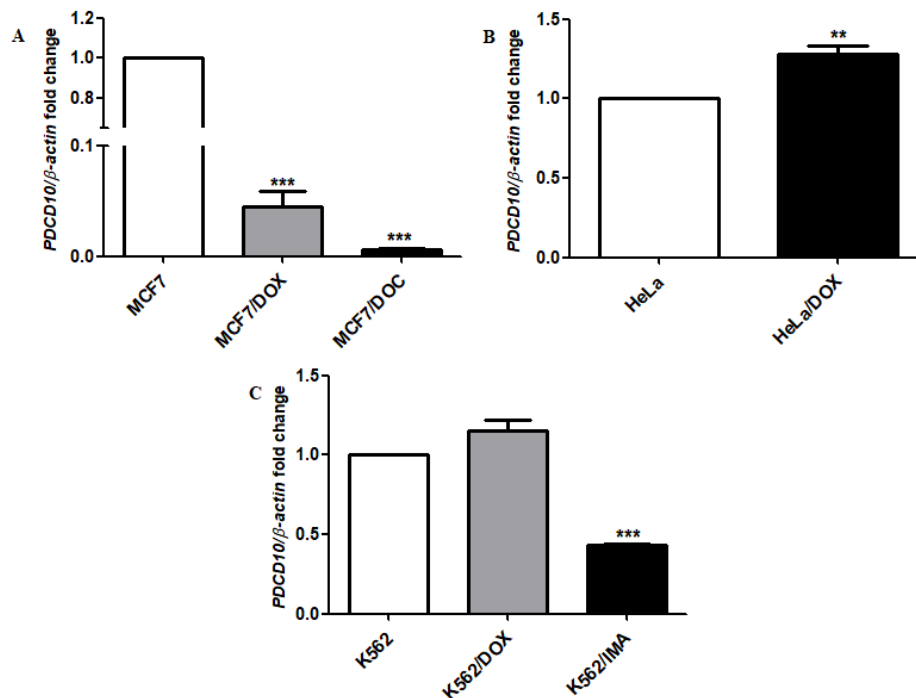


**Figure 3.3** Expression of *PDCD10* in parental and drug-resistant A) MCF7, B) HeLa and C) K562 cells. *PDCD10* expression was determined by using LightCycler 480 Probes Master Mix and Real Time Ready Assay primers (Roche Diagnostics, Switzerland).  $\beta$ -actin was used as internal control. Fold changes were calculated by  $2^{-\Delta\Delta C_t}$  method compared to drug-sensitive parental cell lines and analyzed by one-way ANOVA test followed by post-hoc Tukey's test. (n=3; \*\* = p<0.01; \*\*\* = p<0.001).

Gene expression analyses showed that *PDCD10* expression was significantly downregulated in MCF7/DOC and MCF7/DOX cells compared to parental MCF7 cell line. Similarly, K562/IMA cells displayed 2-fold downregulation in *PDCD10* expression with respect to parental K562 cells; however, K562/DOX cells did not exhibit any significant alterations in *PDCD10* expression. On the other hand, *PDCD10* expression was upregulated when HeLa cells gained resistance to doxorubicin (Figure 3.3). The results indicated that *PDCD10* expression between drug-sensitive and resistant cell lines differ depending on cell type and the selective anti-cancer drug.

This differential expression could be a result of the presence/absence of different transcription factors and activator/repressor complexes at the promoter site as well as different microRNA profile of each cell type. miRDB (MicroRNA Target Prediction and Functional Study Database) finds 64 possible microRNA matches (of 36 are experimentally validated) that target *PDCD10* in different cell types. Accordingly, Zhang et al showed that miR-425-5p overexpression in colon cancer cells significantly downregulated *PDCD10* (Zhang et al, 2016). Similarly, Fu et al reported that miR-103 inhibited proliferation of prostate cancer cells by targeting *PDCD10* (Fu et al, 2016). In addition, RNA-binding proteins could prevent degradation of *PDCD10* mRNA by preventing the interaction between mRNA molecule and miRNAs. Poria et.al showed that PDCD4, a member of PDCD protein family, contains AU-rich sequences on its mRNA. HuR (Human antigen R), an RNA-binding protein, competitively binds to these regions and inhibits the binding of miR-21 to mRNA in MCF7 cells (Poria et al, 2016). Sequence analysis showed that other PDCD family proteins including PDCD10 also possess AU-rich sequences in their mature mRNA. The presence or absence of these RNA-binding proteins can facilitate or prevent the degradation of *PDCD10* mRNA, ultimately leading to a differential expression pattern for *PDCD10* gene.

### 3.3 Effect of *PDCD10* Expression on Drug Resistance

To check the effects of *PDCD10* expression on drug resistance, firstly parental MCF7 cells were transfected with *PDCD10*-specific siRNA for 24, 48 and 72h. The downregulation in *PDCD10* expression was confirmed by qRT-PCR. As seen in Figure 3.4, approximately 85% downregulation in *PDCD10* expression was achieved after 48h transfection and the *PDCD10* level remained downregulated at 72h (Figure 3.4).

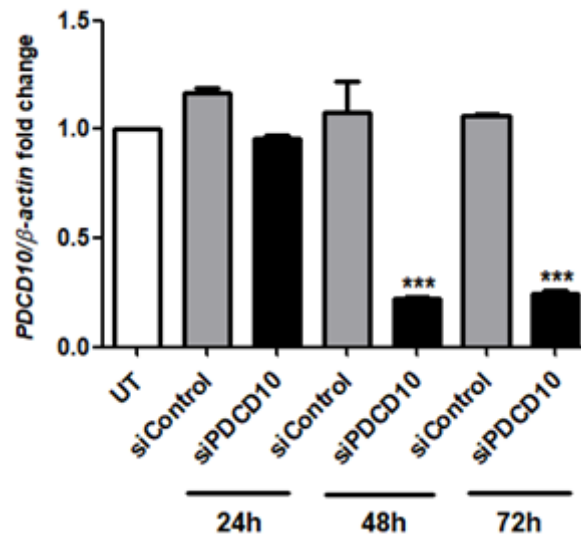


**Figure 3.4** Expression of *PDCD10* in parental MCF7 cells after siRNA-mediated *PDCD10* knockdown. MCF7 cells were transfected with either 5 nM control (*siControl*) or *PDCD10*-specific (*siPDCD10*) siRNA for 24, 48 and 72h. *PDCD10* expression was determined by using LightCycler 480 Probes Master Mix and Real Time Ready Assay primers (Roche Diagnostics, Switzerland).  $\beta$ -actin was used as internal control. Fold changes were calculated by  $2^{-\Delta\Delta C_t}$  method compared to untransfected (UT) cells and analyzed by one-way ANOVA test followed by post-hoc Tukey's test. (n=3; \*\*\* = p<0.001).

XTT cell proliferation assay was carried out to investigate the effect of *PDCD10* expression on docetaxel and doxorubicin resistance in MCF7 cells. For that purpose, MCF7 cells were transfected with either *PDCD10*-specific siRNA or control for 48h and treated with different concentrations of docetaxel or doxorubicin for another 48h. Cell viability analysis showed that MCF7 cells were more viable after transfection with *PDCD10*-specific siRNA compared to untransfected (UT) and control siRNA-transfected cells when they were treated with docetaxel or doxorubicin (Figure 3.5-3.6).

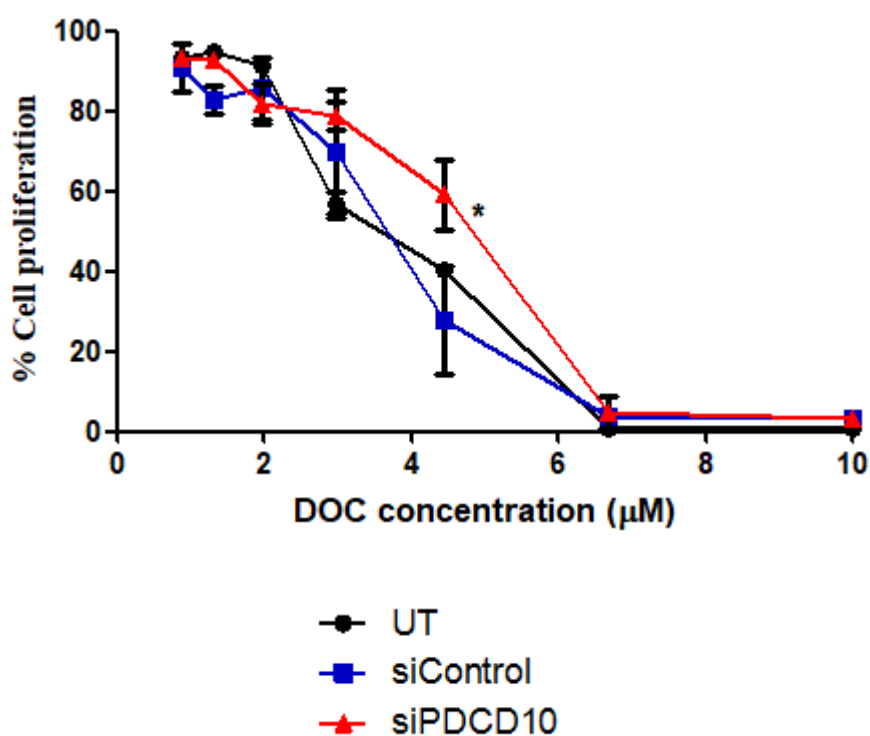


**Figure 3.5** The viability of parental MCF7 cells in increasing concentrations of docetaxel (DOC) after *PDCD10* knockdown. MCF7 cells were transfected with either 5 nM control (*siControl*) or *PDCD10*-specific (*siPDCD10*) siRNA for 48h and treated with increasing concentrations of DOC. Cell viability was measured by using XTT cell proliferation assay (Biological Industries, Israel). (n=3; \* = p<0.05).

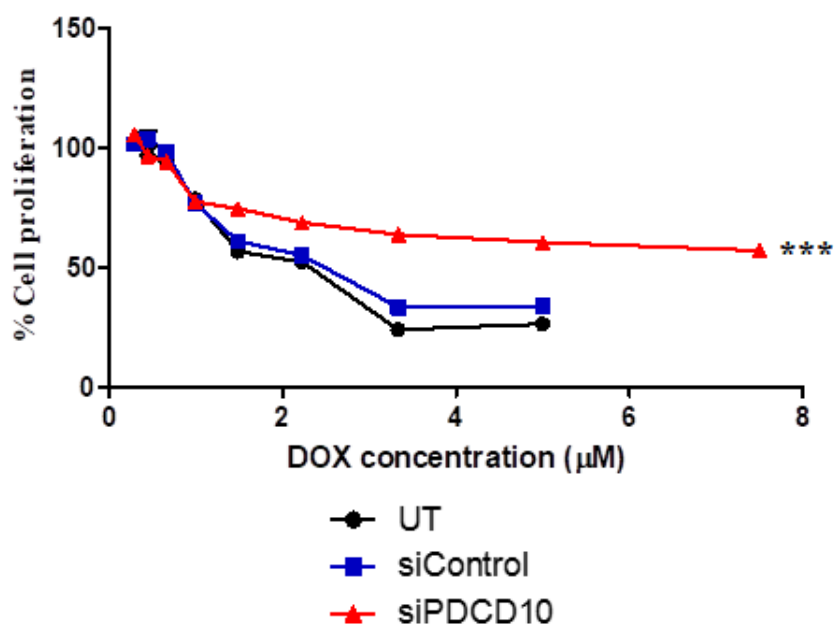


**Figure 3.6** The viability of parental MCF7 cells in increasing concentrations of doxorubicin (DOX) after *PDCD10* knockdown. MCF7 cells were transfected with either 5 nM control (*siControl*) or *PDCD10*-specific (*siPDCD10*) siRNA for 48h and treated with increasing concentrations of DOX. Cell viability was measured by using XTT cell proliferation assay (Biological Industries, Israel).  $IC_{50}$  value of doxorubicin was calculated for each treatment and analyzed by one-way ANOVA test followed by post-hoc Tukey's test (n=3; \*\*\* =  $p < 0.001$ ).

As shown in Table 3.1,  $IC_{50}$  value of docetaxel increased from  $3.24 \pm 0.06 \mu\text{M}$  to  $3.71 \pm 0.05 \mu\text{M}$  and  $IC_{50}$  value of doxorubicin increased from  $2.07 \pm 0.04 \mu\text{M}$  to  $9.03 \pm 0.35 \mu\text{M}$  after *PDCD10* silencing, resulted in 1.2-fold resistance to docetaxel and approximately 4.5-fold resistance to doxorubicin compared to untransfected (UT) group, respectively. Control siRNA did not have any effect on  $IC_{50}$  value of either anti-cancer agent, indicating that the increase in  $IC_{50}$  value can be attributed to *PDCD10* silencing. The results showed that *PDCD10* downregulation in MCF7 cells can drive the cells become drug-resistant.

**Table 3.1** IC<sub>50</sub> values and resistance indices of *PDCD10*-silenced and *PDCD10*-overexpressed cells

Cell Line	Treatment	Drug	IC <sub>50</sub> ± SEM (μM)	Resistance index‡
MCF7	UT	DOX	2.07±0.04	
	siControl		2.77±0.50	1.34
	siPDCD10		>7.5 (9.03±0.35)***‡	4.36
	UT	DOC	3.24±0.06	
	siControl		3.12±0.11	0.96
	siPDCD10		3.71±0.05*	1.19
MCF7/DOX	UT	DOX	183.45±4.84	
	EV		193.29±10.19	1.05
	pcDNA_PDCD10		124.99±3.00**	0.65
HeLa	UT	DOX	19.47±0.14	
	EV		23.56±0.42	1.21
	pcDNA_PDCD10		40.21±3.05**	2.07
HeLa/DOX	UT	DOX	202.01±4.57	
	siControl		214.15±3.89	1.06
	siPDCD10		166.09±7.06*	0.82

n=3; \* = p<0.05; \*\* = p<0.01 and \*\*\* = p<0.001.

‡ Data is out of experimental range and determined by extrapolation of the graph formula

‡ Resistances indices were calculated for each treatment compared to untransfected (UT) control group of corresponding cell line.

The downregulation of *PDCD10* in MCF7 cells promoted doxorubicin resistance approximately 4.5-fold while it increased docetaxel resistance only 1.2-fold. The difference between the effect of *PDCD10* on doxorubicin and docetaxel resistance in MCF7 cells could be explained by the different action mechanisms of the aforementioned anti-cancer agents. Doxorubicin, an

anthracycline antibiotic, intercalates with DNA and inhibits DNA replication and transcription. Moreover, its interference with the activity of topoisomerase II results in double breaks in DNA. On the other hand, docetaxel is a microtubule poison that causes hyper-stabilization of microtubules preventing depolymerization of tubulin subunits. This difference between the action mechanisms of the anti-cancer agents results in two different completely altered genomic profile in doxorubicin- and docetaxel-resistant MCF7 cells (İşeri, 2009).

In a similar manner, *PDCD10* was overexpressed in MCF7/DOX cells to check whether the overexpression of *PDCD10* would re-sensitize the doxorubicin-resistant cells to the anti-cancer agent. For that purpose, MCF7/DOX cells were transfected with an overexpression vector containing *PDCD10* coding sequence tagged with *FLAG* coding sequence at the N-terminus (pcDNA\_PDCD10). According to Figure 3.7, *PDCD10* expression was upregulated more than 10-fold in MCF7/DOX cells after transfection with the pcDNA\_PDCD10 vector compared to empty vector (EV)-transfected cells (Figure 3.7).

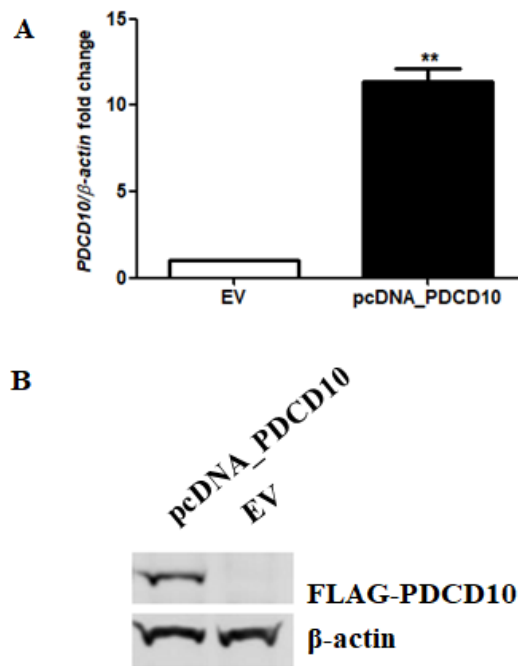


**Figure 3.7** Expression of *PDCD10* in MCF7/DOX cells after *PDCD10* overexpression. A) *PDCD10* expression was determined by using LightCycler 480 Probes Master Mix and Real Time Ready Assay primers (Roche Diagnostics, Switzerland).  $\beta$ -actin was used as internal control. Fold changes were calculated by  $2^{-\Delta\Delta C_t}$  method compared to empty vector (EV)-transfected cells and analyzed by one-way ANOVA test followed by post-hoc Tukey's test. B) MCF7/DOX cells were transfected with FLAG-*PDCD10*-expressing vector (pcDNA\_PDCD10). Total protein was isolated by using RIPA lysis and extraction buffer (Thermo Fisher Scientific, USA), run on 8% SDS-polyacrylamide gel and transferred to nitrocellulose membrane blocked with 5% BSA in 0.1% TBST. FLAG-*PDCD10* expression was detected by anti-FLAG antibody (Santa Cruz Biotechnology, USA; 1:1000 dilution in 5% BSA in 0.1% TBST) (n=3; \*\* = p<0.01).

XTT cell proliferation assay showed that *PDCD10*-overexpressed MCF7 cells showed less cellular viability at high doxorubicin concentrations compared to untransfected (UT) and empty vector (EV)-transfected groups (Figure 3.8).

IC<sub>50</sub> of doxorubicin decreased to 124.99±3.00 μM from 183.45±4.84 μM, sensitizing MCF7/DOX cells by 45% (Table 3.1).

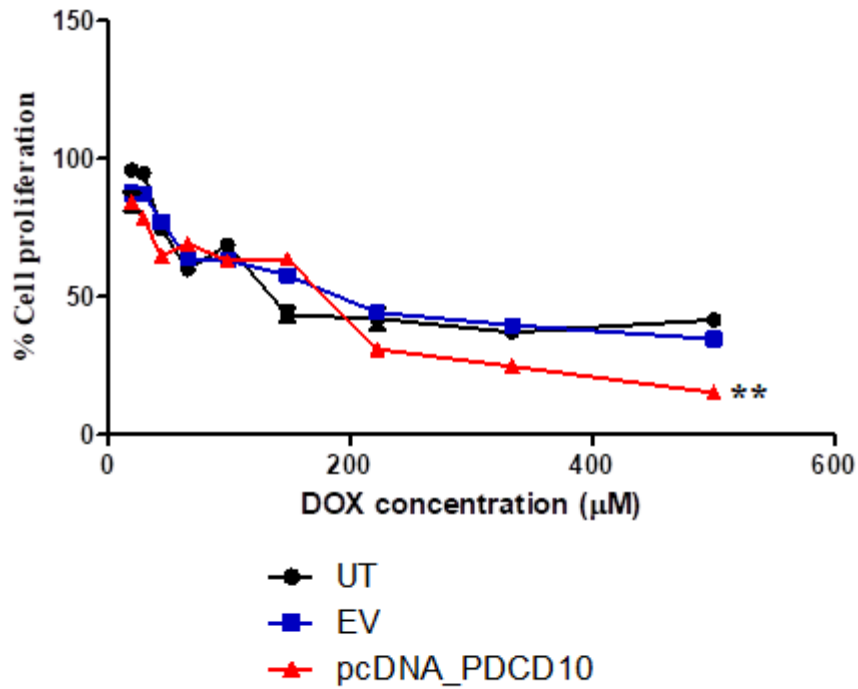


**Figure 3.8** The viability of MCF7/DOX cells in increasing concentrations of doxorubicin (DOX) after *PDCD10* overexpression. MCF7/DOX cells were transfected with either empty vector (EV) or *PDCD10*-overexpressing vector (pcDNA\_PDCD10) and treated with increasing concentrations of DOX. Cell viability was measured by using XTT cell proliferation assay (Biological Industries, Israel). IC<sub>50</sub> value of doxorubicin was calculated for each treatment and analyzed by one-way ANOVA test followed by post-hoc Tukey's test (n=3; \*\* = p<0.01).

Unlike MCF7 and its drug-resistant sublines, parental HeLa cells had higher *PDCD10* expression than its doxorubicin-resistant counterpart (Figure 3.3B). To check whether *PDCD10* overexpression in HeLa cells could cause

elevation in drug-resistant status, parental HeLa cells were transfected with pcDNA\_PDCD10 vector. Figure 3.9 shows that transfection with pcDNA\_PDCD10 vector resulted in approximately 50-fold increase in *PDCD10* expression in HeLa cells (Figure 3.8).

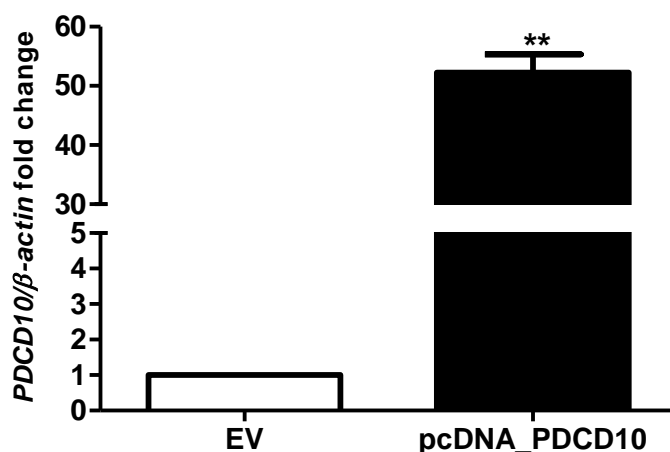


**Figure 3.9** Expression of *PDCD10* in HeLa cells after *PDCD10* overexpression. *PDCD10* expression was determined by using LightCycler 480 Probes Master Mix and Real Time Ready Assay primers (Roche Diagnostics, Switzerland).  $\beta$ -actin was used as internal control. Fold changes were calculated by  $2^{-\Delta\Delta C_t}$  method compared to empty vector (EV)-transfected cells and analyzed by one-way ANOVA test followed by post-hoc Tukey's test. (n=3; \*\* = p<0.01)

The overexpression of *PDCD10* in HeLa cells led to a higher cellular viability in increasing concentrations of doxorubicin compared to untransfected (UT) and empty vector (EV)-transfected groups (Figure 3.10). IC<sub>50</sub> of doxorubicin elevated from 19.47±0.14  $\mu$ M to 40.21±3.05  $\mu$ M, causing 2-fold increase in doxorubicin resistance in HeLa cells (Table 3.1).

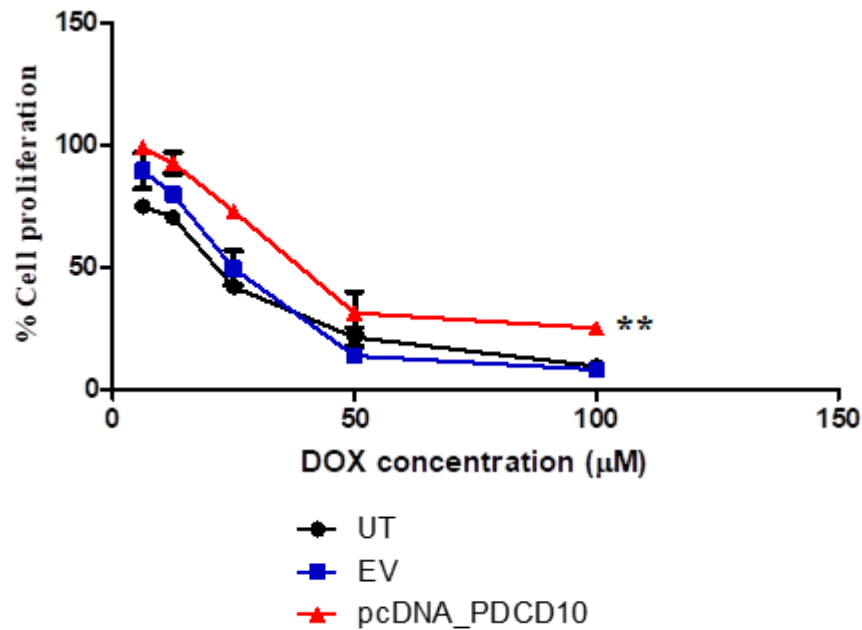


**Figure 3.10** The viability of HeLa cells in increasing concentrations of doxorubicin (DOX) after *PDCD10* overexpression. HeLa cells were transfected with either empty vector (EV) or *PDCD10*-overexpressing vector (pcDNA\_PDCD10) and treated with increasing concentrations of DOX. Cell viability was measured by using XTT cell proliferation assay (Biological Industries, Israel). IC<sub>50</sub> value of doxorubicin was calculated for each treatment and analyzed by one-way ANOVA test followed by post-hoc Tukey's test (n=3; \*\* = p<0.01).

Similarly, HeLa/DOX cells were transfected with *PDCD10*-specific siRNA to detect the effects of *PDCD10* downregulation on doxorubicin resistance. *PDCD10* expression was downregulated by 80% in HeLa/DOX cells after *siPDCD10* transfection for 48h (Figure 3.11).

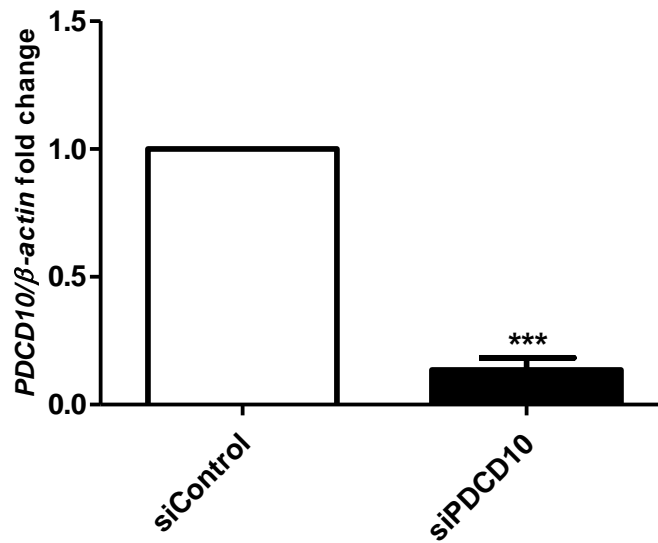


**Figure 3.11** Expression of *PDCD10* in HeLa/DOX cells after siRNA-mediated *PDCD10* knockdown. HeLa/DOX cells were transfected with either 5 nM control (*siControl*) or *PDCD10*-specific (*siPDCD10*) siRNA for 48h. *PDCD10* expression was determined by using LightCycler 480 Probes Master Mix and Real Time Ready Assay primers (Roche Diagnostics, Switzerland).  $\beta$ -actin was used as internal control. Fold changes were calculated by  $2^{-\Delta\Delta C_t}$  method compared to *siControl*-transfected cells and analyzed by one-way ANOVA test followed by post-hoc Tukey's test. (n=3; \*\*\* = p<0.001).

*PDCD10*-silenced HeLa/DOX cells displayed a downregulation in cellular viability compared to untransfected (UT) and control siRNA-transfected groups (Figure 3.12). Table 3.1 shows that  $IC_{50}$  of doxorubicin decreased from  $202.01 \pm 4.57 \mu\text{M}$  to  $166.09 \pm 7.06 \mu\text{M}$ , causing a 20% reversal in doxorubicin resistance (Table 3.1).

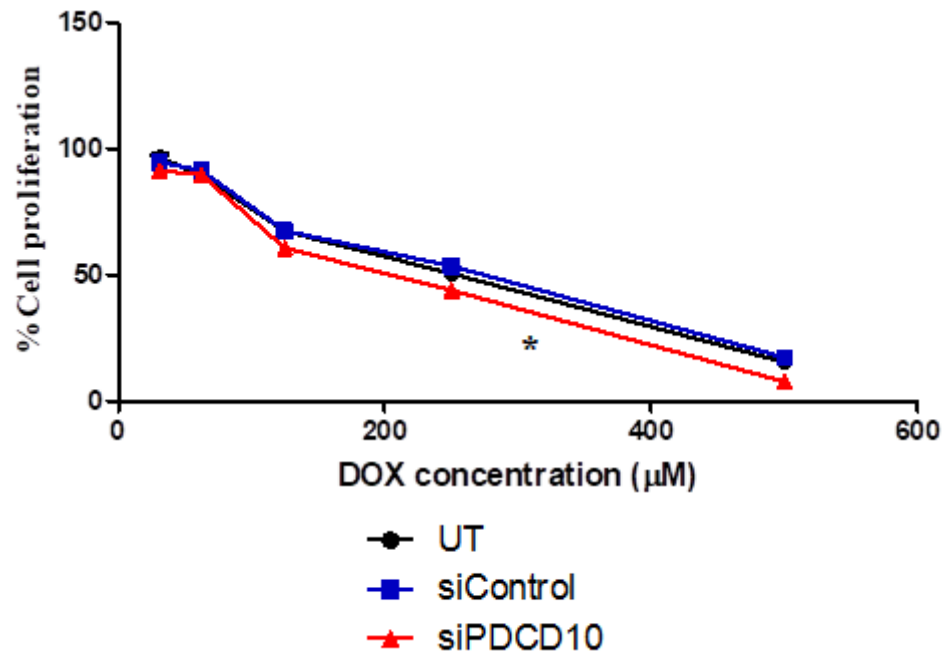


**Figure 3.12** The viability of HeLa/DOX cells in increasing concentrations of doxorubicin (DOX) after siRNA-mediated *PDCD10* knockdown. HeLa/DOX cells were transfected with 5 nM control (*siControl*) or *PDCD10*-specific (*siPDCD10*) siRNA for 48h and treated with increasing concentrations of DOX. Cell viability was measured by using XTT cell proliferation assay (Biological Industries, Israel). IC<sub>50</sub> value of doxorubicin was calculated for each treatment and analyzed by one-way ANOVA test followed by post-hoc Tukey's test (n=3; \* = p<0.05).

### 3.4 The Effect of *PDCD10* Expression on Intracellular Drug Accumulation

Drug resistance can be acquired through several cellular mechanisms, one of which is the decreased drug accumulation inside the cell caused by decreased drug influx and/or increased drug efflux by ABC transporters. Earlier studies revealed that the decreased influx of anti-cancer agents to the cells caused development of drug resistance in different leukemia cells (Ramu et al, 1989;

Pisco et al, 2014). Similarly, several studies reported that the upregulation in the expression of ABC transporters (P-glycoprotein/MDR1, MRP1-12 and BCRP) confers resistance to various anti-cancer agents in different cancer cells. (Keppler et al, 1996; Ambudkar et al, 2005; Kars et al, 2007; Kars et al, 2011; Keppler, 2011; İşeri et al, 2012; Housman et al 2014).

The changes in *PDCD10* expression resulted in altered drug resistance, either driving drug-sensitive cells to become more drug-resistant or resensitizing drug-resistant cells to the corresponding anti-cancer agent. However, how the changes in *PDCD10* expression caused altered drug resistance has not been established yet. Therefore, intracellular drug accumulation was observed in MCF7 and HeLa cells as well as their doxorubicin-resistant sublines after *PDCD10* expression was altered to examine the effect of *PDCD10* expression changes on intracellular drug accumulation. Intracellular drug accumulation was determined by using the fluorescent nature of doxorubicin (excitation at 480 nm and emission at 560-590 nm; de Lange et al, 1996) with SpectraMax iD3 Multi-mode Microplate Reader (Molecular Devices, USA).

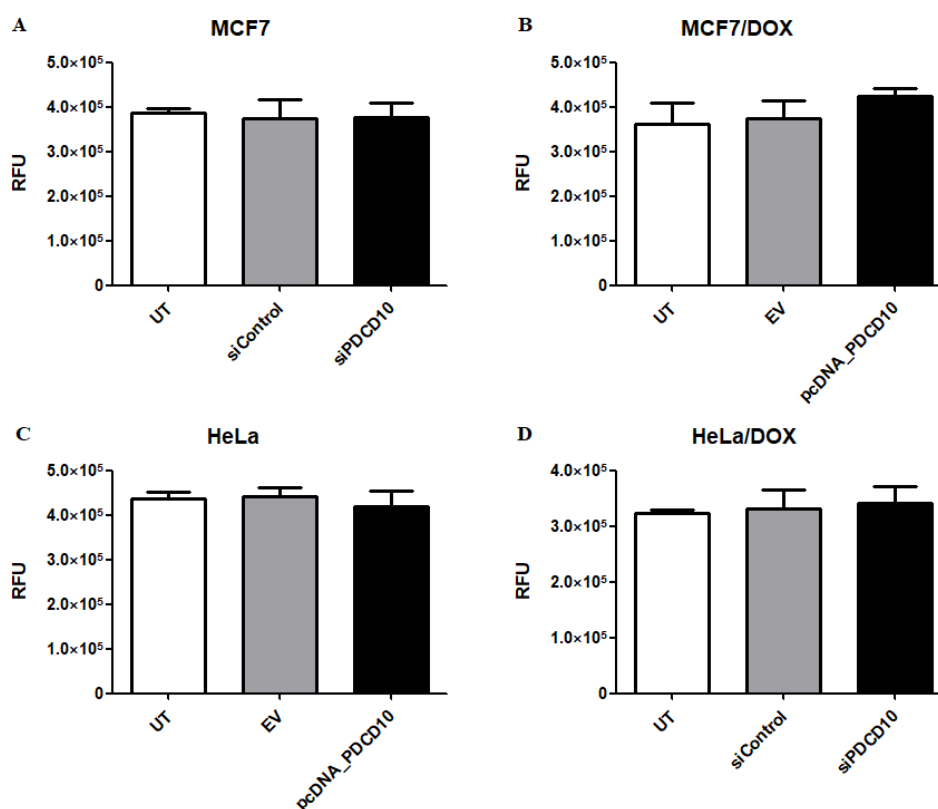


**Figure 3.13** Intracellular doxorubicin accumulation in a) parental MCF7 cells after *PDCD10* knockdown, b) MCF7/DOX cells after *PDCD10* overexpression, c) HeLa cells after *PDCD10* overexpression and d) HeLa/DOX cells after *PDCD10* knockdown. The cells were transfected with either *siControl*/*siPDCD10* or *EV*/*pcDNA\_PDCD10* and treated with doxorubicin. Fluorescent signal of doxorubicin was measured at 590 nm after excitation at 488 nm by using SpectraMax iD3 Multi-mode Microplate Reader (Molecular Devices, USA; n=3).

Figure 3.13 shows that the alterations in *PDCD10* expression did not result in any detectable change in intracellular doxorubicin accumulation in any parental or drug-resistant cell lines after was altered (Figure 3.12;  $p < 0.05$ ). Earlier studies showed that downregulation in the expression or the activity of different ABC transporters resulted in increased drug accumulation inside the

cells, thereby leading to a significant chemosensitization in drug-resistant cancer cells (Lehne, 2000; Zhou et al, 2006; Zhang et al, 2012). Previously, Dönmez et al showed that the siRNA-mediated *MDR1*-silencing caused a remarkable doxorubicin accumulation in MCF7/DOX cells and reversed doxorubicin resistance by 70% (Dönmez et al, 2011). However, the changes in *PDCD10* expression did not affect the intracellular drug accumulation in MCF7 and HeLa cells as well as their doxorubicin-resistant sublines. The results indicated that *PDCD10* may not regulate drug resistance by altering drug accumulation inside the cells and could exert its effects through the modulation of other cellular pathways.

### **3.5 The Effect of *PDCD10* Expression on Apoptosis and Caspase Activity**

Apoptosis is a well-regulated form of programmed cell death mechanism. During apoptotic process, the cells go through several morphological and biochemical changes. Apoptotic cells display a smooth and spherical shape which is a result of cytoskeletal reorganization. In apoptotic cells, microfilaments are fragmented and formed thick bundles at the cell periphery. This reorganization of cytoskeletal elements results in a decrease in cell volume, thus cell shrinkage. Moreover, cytoskeleton rearrangement leads to the formation of plasma protrusions through a process called blebbing (Saraste and Pulkli, 2000; Abbro and Dini, 2003). Consequently, ER and Golgi apparatus swells and gets fragmented. Permeabilization of lysosomal membrane results in the release of enzymatic content of lysosome into cytoplasm. Lysosomes contain several enzymes, especially proteases which cleaves different apoptosis-related proteins such as Bcl-2 family members. This fragmentation of cellular organelles combined with blebbing leads to the formation of densely packed apoptotic bodies. Similarly, mitochondrial membrane is also permeabilized, causing the release of cytochrome c and other mitochondrial content into cytosol. The apoptosis-inducing factor (AIF)

is one of the proteins released from mitochondria. Active AIF translocates into the nucleus and triggers chromatin condensation and DNA degradation (Bottone et al, 2013). Chromatin condensation (pyknosis) begins at nuclear membrane as a result of the cleavage of lamins by caspases. Firstly, degraded lamins form a ring-like shape at nuclear membrane, and then DNA and nucleus is fragmented with an intact cell membrane through a process called karyorrhexis (Ziegler and Groscurth, 2004; Elmore, 2007).

Apoptosis is not associated with inflammation due to the fact that cellular content is not released from dying cells. On the contrary, apoptotic cells are recognized and phagocytosed by macrophages and parenchymal cells, and degraded in phagolysosomes (Saraste and Pulkki, 2000; Fink and Cookson, 2005; Elmore, 2007). The recognition of apoptotic cells by phagocytes is facilitated by the exposure of phosphatidylserine residues on the plasma membrane. The asymmetric nature of lipid bilayer restricts membrane lipids to specific locations such that phosphatidylcholine and sphingomyelin are located on the outer leaflet whereas aminophospholipids such as phosphatidylserine (PS), phosphatidylinositol and phosphatidylethanolamine reside strictly in the inner leaflet (Bratton et al, 1997; Fadok et al, 1998; van Genderen et al, 2008; Marino and Kroemer, 2013). The membrane asymmetry is regulated by several ATP- and  $\text{Ca}^{2+}$ -dependent enzymes called flippase, floppase, scramblase and aminophospholipid translocase. During apoptosis, phosphatidylserine residues are externalized due to the inhibition of aminophospholipid translocase (Fadok et al, 1998; Marino and Kroemer, 2013). Annexin V, a 35 kDa  $\text{Ca}^{2+}$ -binding protein, binds the exposed phosphatidylserine residues with a high affinity and establishes a membrane-bound two-dimensional crystal structure (Ziegler and Groscurth, 2004; van Genderen et al, 2008). This specific interaction between Annexin V and exposed PS molecules is benefited by monitoring of apoptotic process by conjugating Annexin V with fluorophores.

To investigate the effect of *PDCD10* expression on apoptotic behavior, parental MCF7 cells were transfected with either *siControl* or *siPDCD10* for 48h and treated with an apoptosis inducer, etoposide. The changes in apoptosis were monitored by Annexin V-FITC and propidium iodide (PI) staining. PI is an intercalating agent that gives a fluorescent signal when bound to DNA. Since PI is cell-impermeable, it cannot diffuse into live cells which have intact plasma membrane. However, disruption of cell membrane during apoptosis provides PI a free passage to nucleus where it can bind to DNA. The green fluorescent signal coming from FITC-tagged Annexin V was measured in FL1 channel while the purple fluorescent signal from PI was measured in FL3 channel by using BD Accuri C6 flow cytometer (Accuri, BD, USA). Early apoptotic cells gives fluorescent signal only in FL1 channel while late apoptotic cells with disrupted cellular membrane can be stained with both Annexin V-FITC and PI so that fluorescent signal was detected in both FL1 and FL3 channels.

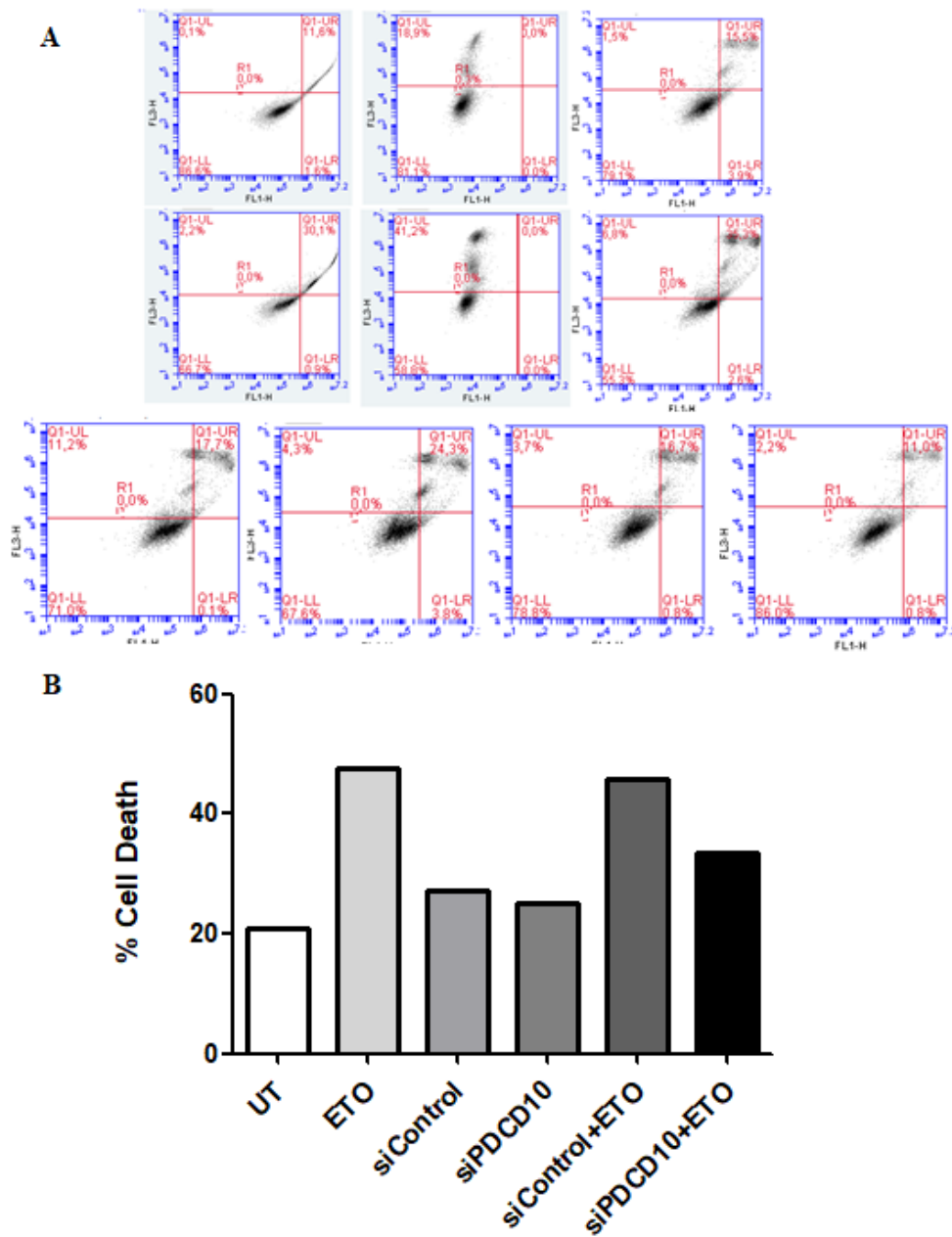


**Figure 3.14** Apoptotic activity in *PDCD10*-silenced MCF7 cells. MCF7 cells were transfected with either 5 nM control (*siControl*) or *PDCD10*-specific (*siPDCD10*) siRNA for 48h and treated with etoposide to induce apoptosis. Both dead and live cells were collected in HEPES buffer and stained with FITC-AnnexinV and PI. Bar graph shows the collective signal obtained from both FL-1 and FL-3 channels.

As seen in Figure 3.14, etoposide (ETO) treatment killed approximately 50% of the MCF7 population. Neither *siControl* nor *siPDCD10* transfection alone caused any increase in apoptotic activity in parental MCF7 cells compared to untransfected (UT) control group. However, etoposide treatment resulted in an increase in apoptosis in *siControl*-transfected MCF7 cells. On the other hand, *PDCD10*-silenced MCF7 cells displayed less apoptotic activity after etoposide treatment. The results indicated that *PDCD10* knockdown in MCF7 cells did not only drive MCF7 cells to be more resistant to doxorubicin and docetaxel but also caused in development of resistance to etoposide-induced apoptosis.

Caspase activity is an essential step in programmed cell death and the activation/inactivation of effector caspases (caspase 3 and caspase 7) is needed to stimulate/inhibit apoptosis (Shi, 2004; Denault and Salvesen, 2008; Li and Yuan, 2008). Friedrich et al reported that caspase 3 overexpression resulted in higher sensitivity to paclitaxel-, etoposide- and epirubicin-induced apoptosis in MCF7 cells (Friedrich et al, 2001). Similarly, Yang et al showed that overexpression of caspase 3 in MCF7 cells caused chemosensitization to etoposide- and doxorubicin-induced apoptosis (Yang et al, 2001). In addition, Fulda et al showed that re-expression of another effector caspase, caspase 8, in Ewing tumor cells, which are intrinsically resistant to TRAIL and TNF $\alpha$ -induced apoptosis, led to elevated apoptotic signaling, thus higher cell death (Fulda et al, 2001).

Earlier studies showed that MCF7 cells do not have caspase 3 expression (Liang et al, 2001; McGee et al, 2002). Although several studies indicated that caspase 3 and caspase 7 have different roles in intrinsic apoptotic pathway (Walsh et al, 2008; Brentnall et al, 2013), the presence of caspase 7

is sufficient to promote cell death in MCF7 cells (Liang et al, 2001; McGee et al, 2002).

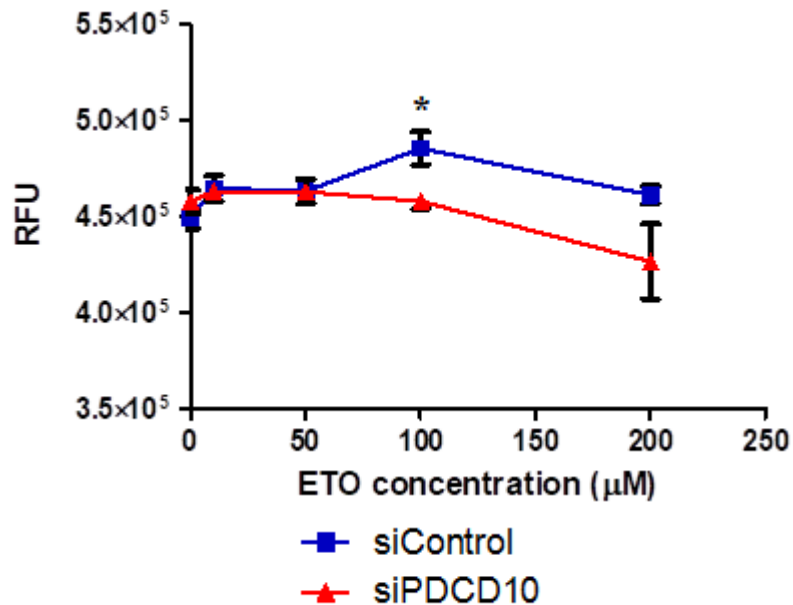


**Figure 3.15** Caspase 3/7 activity in *PDCD10*-silenced MCF7 cells. MCF7 cells were transfected with either control (*siControl*) or *PDCD10*-specific (*siPDCD10*) siRNA for 48h, treated with different concentrations of etoposide for 24h and with non-fluorescent caspase for 4h. Fluorescent signal was measured at 511 nm after excitation of fluorescent caspase product at 499 nm by SpectraMax iD3 Multi-mode Microplate Reader (Molecular Devices, USA) (n=3; \* = p<0.05).

Figure 3.15 shows the caspase activity in MCF7 cells after transfection with either control or *PDCD10*-specific siRNA for 48h. Relative fluorescence unit (RFU) represents caspase activity since the caspase activity assay relies on the fact that active caspase 3/7 can cleave the non-fluorescent caspase substrate into fluorescent Rhodamine 110 molecule. Higher fluorescent signal is a representation of higher caspase 3/7 activity. *PDCD10*-silenced MCF7

cells displayed lower caspase 7 activity, compared to control siRNA transfected group (Figure 3.15). The results of caspase 3/7 activity assay further indicated that *PDCD10* knockdown caused an elevation in resistance to etoposide-induced apoptosis. The resistance to apoptosis in *PDCD10*-silenced MCF7 cells suggested that PDCD10 can regulate drug resistance by modulating apoptotic signaling in MCF7 cell line.

### **3.6 The Effect of *PDCD10* Expression on Apoptosis-related Genes**

Apoptosis is a complex process regulated by several pathways involving various proteins. Kroemer classified apoptotic process into three phases as initiation, effector and degradation. The regulation of effector phase is controlled by the members of BCL-2 protein family and inhibitors of apoptosis (IAP) proteins which are important modulators of apoptosis in cancer cells (Kroemer, 1997).

Bcl-2 (B-cell lymphoma 2) family proteins are vital for apoptotic regulation. As major regulators of apoptotic machinery, Bcl-2 and its related proteins are conserved in *C. elegans* and mammals (Willis et al, 2003). The Bcl-2 family proteins are categorized three subgroups depending on their Bcl-2 homology (BH) domains (BH1-4) which are the key determinants of the interaction of Bcl-2 family members with other proteins (Kroemer, 1997; Gross et al, 1999; Willis et al, 2003; Akl et al, 2014; Czabotar et al, 2014). Pro-apoptotic BH3-only proteins (the Bcl-2 members that only contains BH3 domain) receive and transfer the signal that triggers apoptosis. The anti-apoptotic (pro-survival) proteins having all four BH domains function to prevent apoptosis whereas multi-domain (BH1-3) pro-apoptotic effectors act to promote apoptotic cell death (Brunelle and L'Etai, 2009; Czabotar et al, 2014). The ratio between pro-apoptotic and anti-apoptotic Bcl-2 family proteins is

important for the determination of cell fate (Kroemer, 1997; Gross et al, 1999; Willis et al, 2003).

Bcl-2, the major member of Bcl-2 protein family, is encoded by the *BCL2* gene in humans. The pro-apoptotic Bcl-2 family proteins as well as Bcl-2 itself stimulate apoptosis whereas the anti-apoptotic ones inhibit apoptotic signaling. As reviewed by many groups, Bcl-2 acts as “pro-survival guardian” and enhances cellular proliferation by inhibiting apoptosis triggered by different stimuli. Although high levels of *BCL-2* alone do not cause cancer, *BCL-2* is found to be upregulated in different malignancies (Kroemer, 1997; Tsujimoto, 1998; Akl et al, 2014; Czabotar et al, 2014). Cancer cells require high Bcl-2 activity for survival since Bcl-2 has been shown to block apoptosis by inhibiting the activation and oligomerization of pro-apoptotic Bcl-2 family proteins, mainly Bax and Bak (Brunell and Letai, 2009). Overexpression of *BCL-2* is also associated with decreased phosphatidylserine exposure, decreased lipid peroxidation and ROS production, low levels of caspase activation and cytochrome c release (Kroemer, 1997), increased tumorigenesis, inhibition of autophagy via interaction with Beclin-1 and resistance to apoptosis (Czabotar et al, 2014). The function of Bcl-2 is regulated by phosphorylation. The phosphorylation of Ser or Thr residues of Bcl-2 was shown to be associated with decreased or enhanced protein stability and pro-survival activity as well as abrupt mitosis (Czabotar et al, 2014). Moreover, proteolytic cleavage of Bcl-2 by active caspases results in the inactivation of the protein, thus low pro-survival activity (Kroemer, 1997; Tsujimoto, 1998)

Bax, also known as bcl-2-like protein 4, is encoded by the human *BAX* gene. Several studies reported that the integration of Bax in the outer mitochondrial membrane was essential for apoptosis (Khaled et al, 1999; Lalier et al, 2007;

Westphal et al, 2011). Bax is predominantly localized in cytosol but a small portion of Bax population can be found loosely attached to the mitochondrial membrane in healthy cells. After the cells receive apoptotic signals, Bax undergoes a conformational change from soluble monomeric form to oligomers that can be integrated into the mitochondrial membrane. This insertion is mediated by the hydrophobic residues on C-terminus (Khaled et al, 1999; Lalier et al, 2007; Westphal et al, 2011). Khaled et al reported that the deletion of C-terminus or point mutations in Ser/Thr residues at C-terminal domain completely blocked apoptotic process (Khaled et al, 1999). The insertion of Bax into the outer mitochondrial membrane causes loss of membrane potential and the release of cytochrome c into the cytoplasm. Therefore, increased *BAX* expression is often associated with elevated apoptosis. Finucane et al showed that ectopic Bax expression triggered apoptosis through early cytochrome c release into the cytoplasm and activation of caspases which resulted in increased proteolysis (Finucane et al, 1999). The loss of function in Bax was also associated with drug resistance by inhibiting the release of cytochrome c into the cytosol (Chandrika et al, 2010) and/or preventing p53-dependent apoptosis (McCurrach et al, 1997). Bax/Bak double deficient murine embryonic fibroblasts were reported to be resistant to various apoptotic signals (Dagi et al, 1998, Degenhardt et al, 2002). Bax-deficient colorectal cancer cells were shown to be partially resistant to apoptosis induced by 5-fluorouracil and completely insensitive to the apoptotic response caused by non-steroidal anti-inflammatory drugs (Zhang et al, 2000).

The p53 upregulated modulator of apoptosis (PUMA), also called as Bcl-2-binding component 3 (BBC3), is another pro-apoptotic member of the Bcl-2 protein family. The expression of *PUMA* gene is induced by p53, a major tumor suppressor protein (Yu et al, 2001; Nakano and Vousden, 2001). PUMA contains only BH3 domain and similar to other BH3-only members of

Bcl-2 family, it transduces various apoptotic signals including growth factor starvation, deregulated expression of oncogenes and redox imbalance to mitochondrial membrane (Yu and Zhang, 2008). PUMA can directly activate pro-apoptotic Bcl-2 proteins, Bax and/or Bak on mitochondrial membrane or acts on pro-survival Bcl-2 members such as Bcl-2 itself by inhibiting their interaction with Bax and Bak (Yu and Zhang, 2008; Bean et al, 2013). *PUMA* expression alone was shown to be sufficient for the induction of apoptosis in *BID*<sup>-/-</sup> and *BIM*<sup>-/-</sup> cells which were lacking other BH3-only proteins (Jabbour et al, 2009). Expression of *PUMA* and following activation of Bax and Bak result in permeabilization of mitochondrial membrane, cytochrome c release and caspase activation, thus rapid apoptosis (Yu et al, 2001; Nakano and Vousden, 2001). Additionally, it was reported that PUMA was also involved in p53-independent apoptosis stimulated by a wide range of signals, and is regulated by other transcription factors. Exposure to PI3K-AKT inhibitors resulted in translocation of several transcription factors, mainly FOXO, to nucleus where they can directly initiate *PUMA* expression. In a HER2-inactivated mouse breast cancer model, *PUMA* expression was found to be upregulated, indicating that *PUMA* expression could be controlled by several signaling cascades apart from p53 (Bean et al, 2013). Elevated PUMA levels were associated with increased sensitivity to chemo- and radiotherapy (yu and Zhang, 2008).

Survivin, also named as baculoviral inhibitor of apoptosis repeat-containing 5 (BIRC5), is encoded by the *BIRC5* (*SURVIVIN*) gene. Survivin belongs to the inhibitor of apoptosis (IAP) protein family. As all IAP members, Survivin contains a 70 amino acid-long Baculovirus IAP repeats at its N-terminus. The presence of these repeats is vital for anti-apoptotic function. Survivin is mostly localized in cytosol; however, a small portion can be found in nucleus. Moreover, Khan et al reported that an extracellular pool of Survivin was detected in membrane-bound vesicles which were secreted by various tumor

cells (Khan et al, 2015). Survivin is abundantly expressed during embryonal development; however, its expression cannot be detected in terminally differentiated cells. Most cancer cells exhibit upregulated Survivin expression. On the other hand, the expression of Survivin in stem cells indicates a possible involvement in stem cell generation (Garg et al, 2016). The main function of Survivin protein is to downregulate apoptosis that is induced by Fas, anti-apoptotic Bcl-2 family proteins (mostly Bax), p53, caspase 3/7 and several chemotherapeutic agents and to regulate cell cycle (Tamm et al, 1998; Singh et al, 2014). Beside its well-established roles in the regulation of cell proliferation and cell death, Survivin was shown to regulate mitotic spindle checkpoint and promote aggressiveness, metastasis and angiogenesis (Mita et al, 2008; Park et al, 2011; Garg et al, 2016). As reviewed by Singh et al, Survivin expression was downregulated by Beclin-1 knock-down, a major regulator of autophagy, indicating that Survivin could be an intermediary between apoptotic cell death and autophagy (Singh et al, 2014). Survivin is also essential in the development of drug resistance. Overexpression of Survivin confers resistance to various anticancer agents including microtubule-stabilizers and DNA-alkylating agents (Jiang et al, 2009). Komino et al reported that Survivin was co-expressed with ABC transporter proteins in drug-resistant multiple myeloma cells (Komino et al, 2011). Wu et al reported that silencing of Survivin reversed drug resistance in AML cells (Wu et al, 2008). Similarly, inhibition of Survivin expression in combination with conventional chemotherapy resulted in complete remission in xenograft model of primary ALL as well as drug-resistant ALL cells (Park et al, 2011).

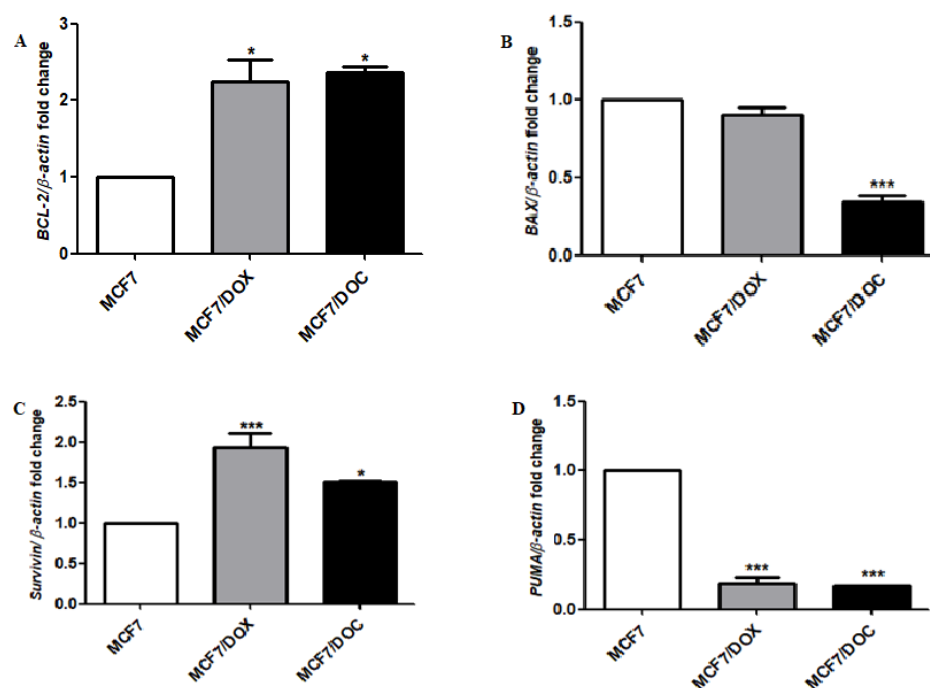
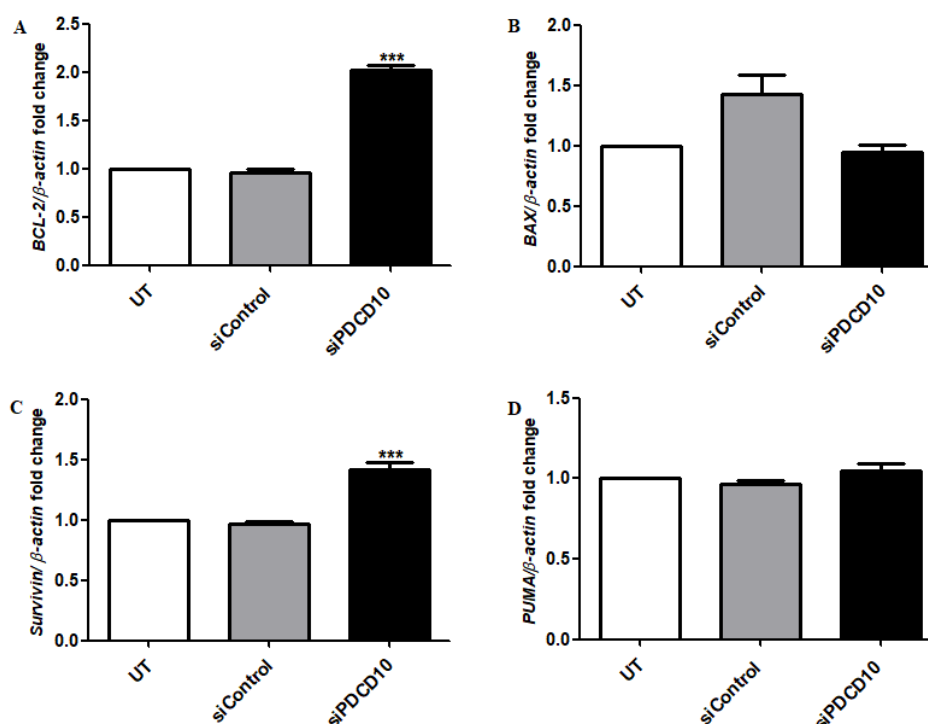


**Figure 3.16** Expressions of a) *BCL-2*, b) *BAX*, c) *SURVIVIN* and d) *PUMA* genes in parental and drug-resistant MCF7 cells. Expressions of apoptosis-related genes were determined by using SsoAdvanced Universal SYBR Green Supermix (Bio-Rad Laboratories, USA).  $\beta$ -actin was used as internal control. Fold changes were calculated by  $2^{-\Delta\Delta C_t}$  method compared to drug-sensitive parental cells and analyzed by one-way ANOVA test followed by post-hoc Tukey's test. (n=3; \* = p<0.05, \*\* = p<0.01; \*\*\* = p<0.001).

As seen in Figure 3.16, anti-apoptotic *BCL-2* expression was upregulated more than 2-fold in both doxorubicin- and docetaxel-resistant MCF7 cells. The pro-apoptotic *BAX* expression decreased more than 2-fold in docetaxel-resistant MCF7 cells; however, no significant change was detected in doxorubicin-resistant MCF7 cells compared to parental MCF7 cell line. Similar to *BCL-2*, in both drug-resistant MCF7 sublines, anti-apoptotic *SURVIVIN* was significantly upregulated (2-fold in MCF7/DOX cells and 1.5-fold in MCF7/DOC cells). On the other hand, pro-apoptotic *PUMA* was remarkably downregulated in both MCF7/DOX and MCF7/DOC cells (Figure

3.16). The results indicated that the upregulation of anti-apoptotic *BCL-2* and *SURVIVIN* genes and the downregulation of pro-apoptotic *BAX* and *PUMA* genes provide drug-resistant cells a survival advantage in anti-cancer agent containing environment by preventing pro-apoptotic signaling inside the cell.

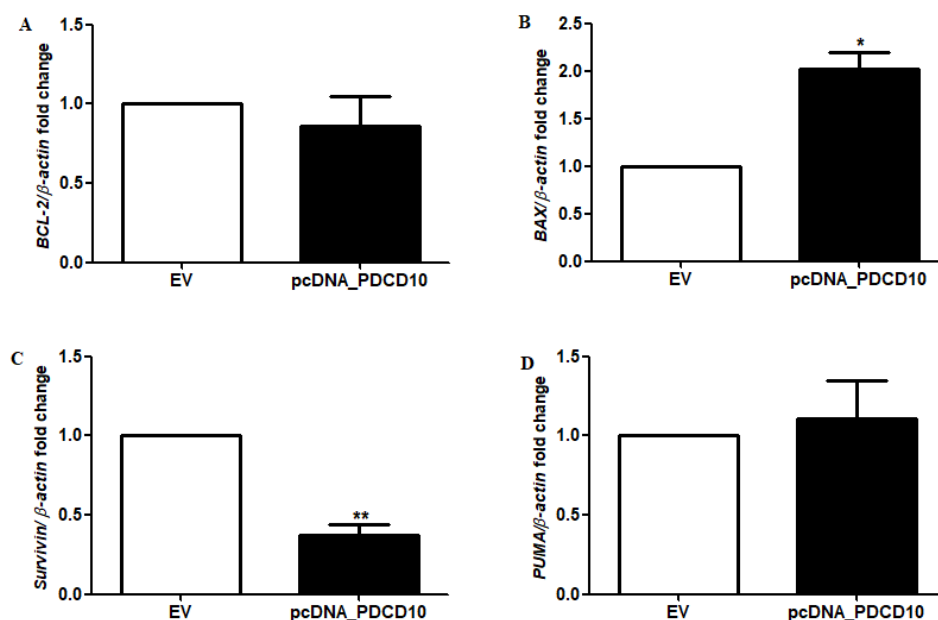
After 48h transfection with *siPDCD10*, MCF7 cells displayed 2-fold upregulation in *BCL-2* expression. Similarly, *SURVIVIN* expression increased 1.5-fold in *PDCD10*-silenced MCF7 cells. However, expression levels of pro-apoptotic *BAX* and *PUMA* genes did not show any significant change after *PDCD10* knockdown (Figure 3.17). The upregulation in anti-apoptotic gene expression levels without any alterations in pro-apoptotic genes resulted in a shift towards pro-survival signaling in MCF7 cells after *PDCD10* silencing. Coupled with resistance to apoptosis and lower caspase activity in *PDCD10*-silenced MCF7 cells, these results suggested that downregulation of *PDCD10* promotes drug resistance by stimulating anti-apoptotic signaling.



**Figure 3.17** Expressions of a) *BCL-2*, b) *BAX*, c) *SURVIVIN* and d) *PUMA* genes in *PDCD10*-silenced MCF7 cells. Expressions of apoptosis-related genes were determined by using SsoAdvanced Universal SYBR Green Supermix (Bio-Rad Laboratories, USA).  $\beta$ -actin was used as internal control. Fold changes were calculated by  $2^{-\Delta\Delta Ct}$  method compared to untransfected (UT) parental cells and analyzed by one-way ANOVA test followed by post-hoc Tukey's test. (n=3; \*\*\* = p<0.001).

*PDCD10*-overexpressed MCF7/DOX cells did not exhibit any significant change in *BCL-2* expression; however, *BAX* expression was significantly upregulated. It was shown that the decrease in *BCL-2/BAX* ratio is an indication of induced apoptosis. Similarly, *SURVIVIN* expression was downregulated more than 2-fold in *PDCD10*-overexpressed MCF7/DOX cells, indicating the inhibition of apoptosis in these cells. On the other hand, pro-apoptotic *PUMA* expression did not show any significant change after *PDCD10* was overexpressed in MCF7/DOX cells (Figure 3.18). The results

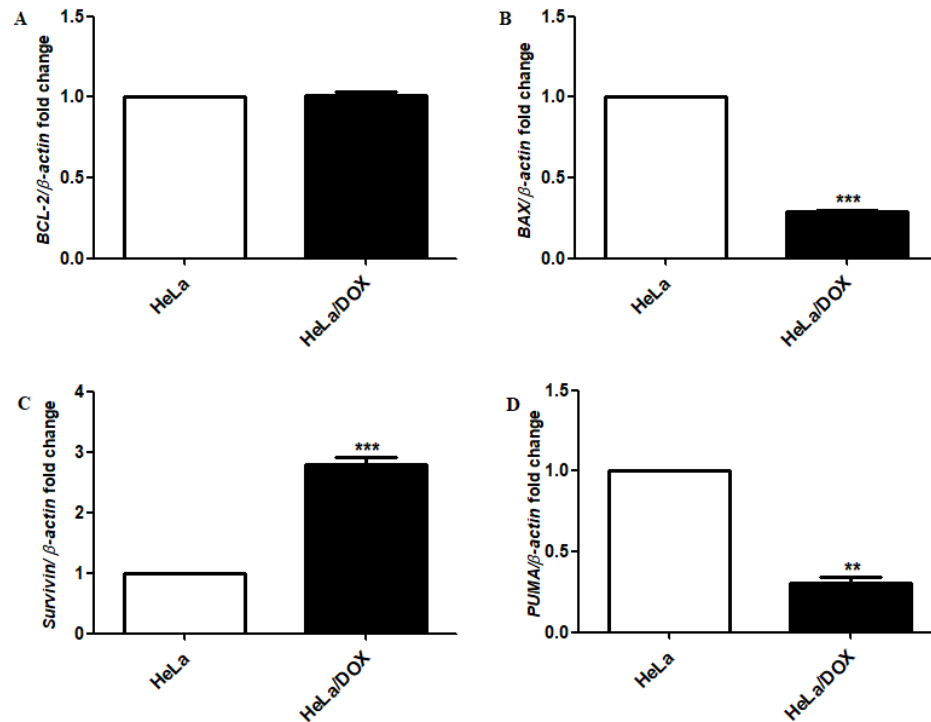
indicated that the reversal in the chemoresistance in MCF7/DOX cells is the stimulation of pro-apoptotic signaling after overexpression of *PDCD10*.



**Figure 3.18** Expressions of a) *BCL-2*, b) *BAX*, c) *SURVIVIN* and d) *PUMA* genes in *PDCD10*-overexpressed MCF7/DOX cells. Expressions of apoptosis-related genes were determined by using SsoAdvanced Universal SYBR Green Supermix (Bio-Rad Laboratories, USA).  $\beta$ -actin was used as internal control. Fold changes were calculated by  $2^{-\Delta\Delta C_t}$  method compared to empty vector (EV)-transfected cells and analyzed by one-way ANOVA test followed by post-hoc Tukey's test. (n=3; \* = p<0.05 and \*\* = p<0.01).

Similar to drug-resistant MCF7 cells, doxorubicin-resistant HeLa cells displayed a general upregulation in anti-apoptotic gene expression while the expressions of pro-apoptotic genes were downregulated. Although *BCL-2* expression did not show any significant change in HeLa/DOX cells compared to parental HeLa cell line, the downregulation in *BAX* expression could inhibit pro-apoptotic signaling in HeLa/DOX cells. Almost 3-fold

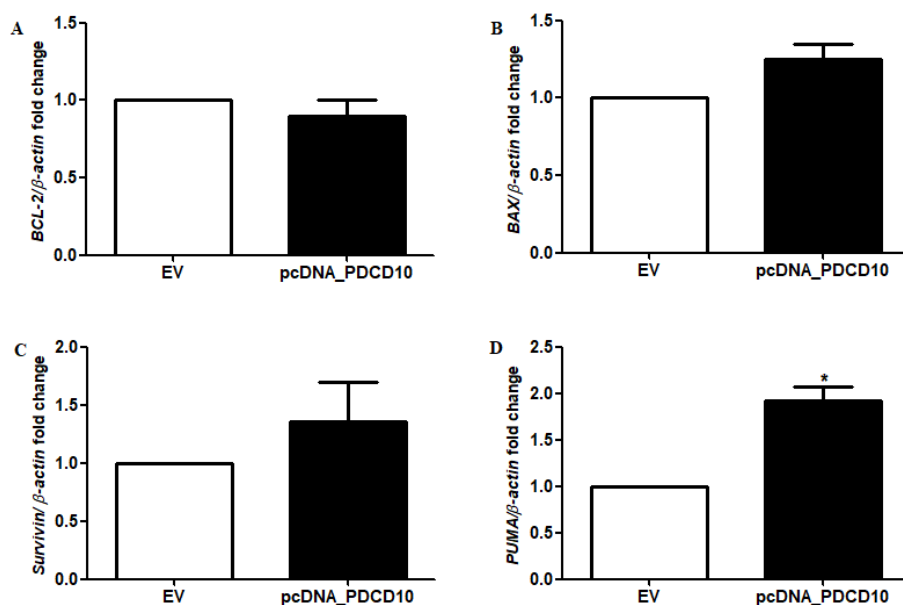
upregulation in *SURVIVIN* and more than 2-fold downregulation in *PUMA* genes also contributed to the inhibition of induction of apoptosis in HeLa/DOX cells (Figure 3.19).



**Figure 3.19** Expressions of a) *BCL-2*, b) *BAX*, c) *SURVIVIN* and d) *PUMA* genes in parental and drug-resistant HeLa cells. Expressions of apoptosis-related genes were determined by using SsoAdvanced Universal SYBR Green Supermix (Bio-Rad Laboratories, USA).  $\beta$ -actin was used as internal control. Fold changes were calculated by  $2^{-\Delta\Delta C_t}$  method compared to drug-sensitive parental cells and analyzed by one-way ANOVA test followed by post-hoc Tukey's test. (n=3; \*\* = p<0.01 and \*\*\* = p<0.001).

The overexpression of *PDCD10* did not alter the expression levels of *BCL-2*, *BAX* and *SURVIVIN*. Surprisingly, *PUMA* expression was upregulated approximately 2-fold after *PDCD10* overexpression in HeLa cells (Figure 3.20). Although it is significantly upregulated, the increase in *PUMA*

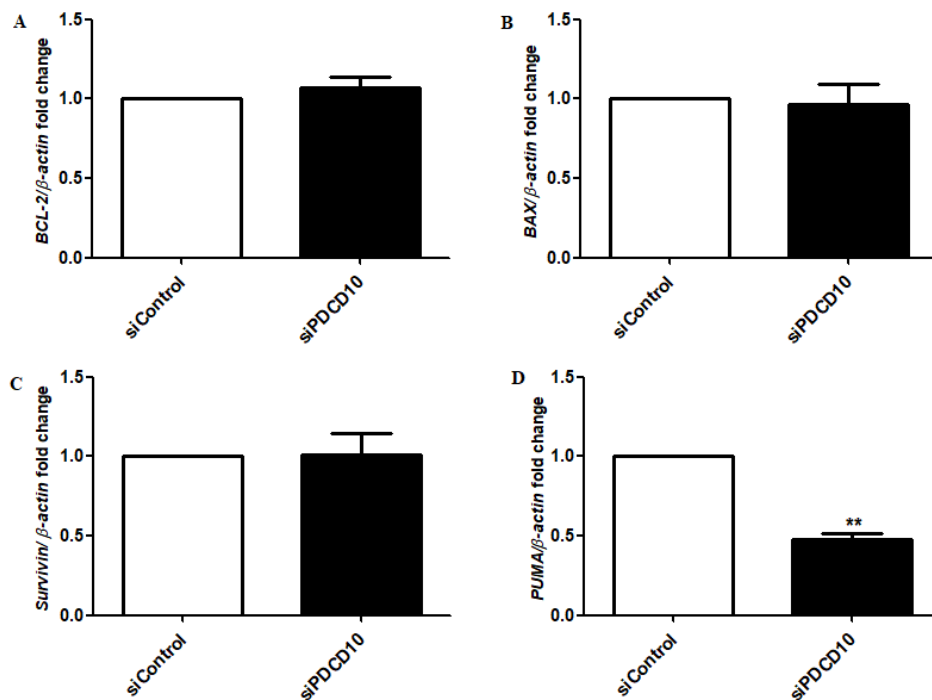
expression alone may not lead HeLa cells to apoptosis. Moreover, the elevation in drug resistance in *PDCD10*-overexpressed HeLa cells may not be a result of the modulation of caspase-dependent apoptotic signaling in which BCL-2 and IAP protein family members have essential roles.



**Figure 3.20** Expressions of a) *BCL-2*, b) *BAX*, c) *SURVIVIN* and d) *PUMA* genes in *PDCD10*-overexpressed HeLa cells. Expressions of apoptosis-related genes were determined by using SsoAdvanced Universal SYBR Green Supermix (Bio-Rad Laboratories, USA).  $\beta$ -actin was used as internal control. Fold changes were calculated by  $2^{-\Delta\Delta Ct}$  method compared to empty vector (EV)-transfected cells and analyzed by one-way ANOVA test followed by post-hoc Tukey's test. (n=3; \* = p<0.05).

Similar to *PDCD10*-overexpressed HeLa cells, *PDCD10*-silenced HeLa/DOX cells did not show significant alterations in the expression levels of *BCL-2*, *BAX* and *SURVIVIN*. However, a significant downregulation was detected in *PUMA* expression (Figure 3.21). Although HeLa/DOX cells were found to be

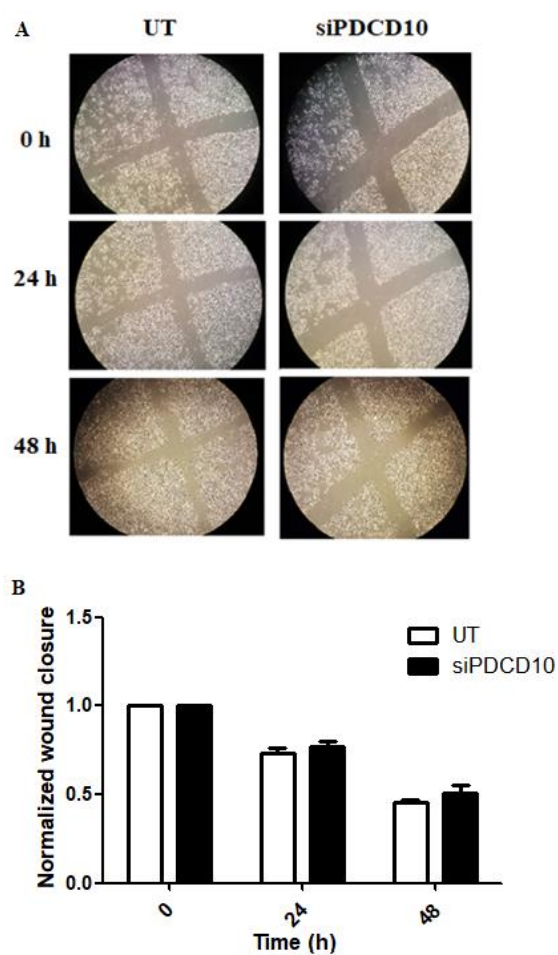
resensitized to doxorubicin after silencing of *PDCD10*, the expression of pro-apoptotic *PUMA* was 2-fold downregulated in *PDCD10*-silenced HeLa/DOX cells. Even though the alterations in *PUMA* expression could be compensated by the changes in expression levels of other apoptosis-related proteins, further studies are needed to elucidate the relationship of *PUMA* with *PDCD10*-mediated drug resistance.



**Figure 3.21** Expressions of a) *BCL-2*, b) *BAX*, c) *SURVIVIN* and d) *PUMA* genes in *PDCD10*-silenced HeLa/DOX cells. Expressions of apoptosis-related genes were determined by using SsoAdvanced Universal SYBR Green Supermix (Bio-Rad Laboratories, USA).  $\beta$ -actin was used as internal control. Fold changes were calculated by  $2^{-\Delta\Delta C_t}$  method compared to control siRNA (*siControl*)-transfected cells and analyzed by one-way ANOVA test followed by post-hoc Tukey's test. (n=3; \* = p<0.05).

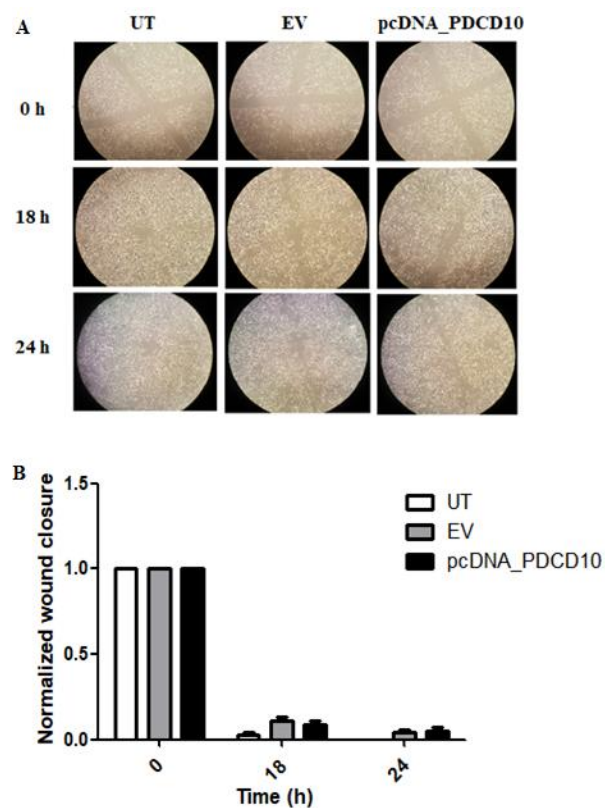
### 3.7 The Effect of *PDCD10* Expression on Migration

Several studies reported that drug-resistant cells exhibit enhanced migratory activity and invasion and metastasis properties compared to drug-susceptible cells. The modified extracellular matrix components and the activation of epithelial-mesenchymal transition provide drug-resistant cells an enhanced migratory activity (İşeri et al, 2010; İşeri et al, 2011; Jeon et al, 2016).



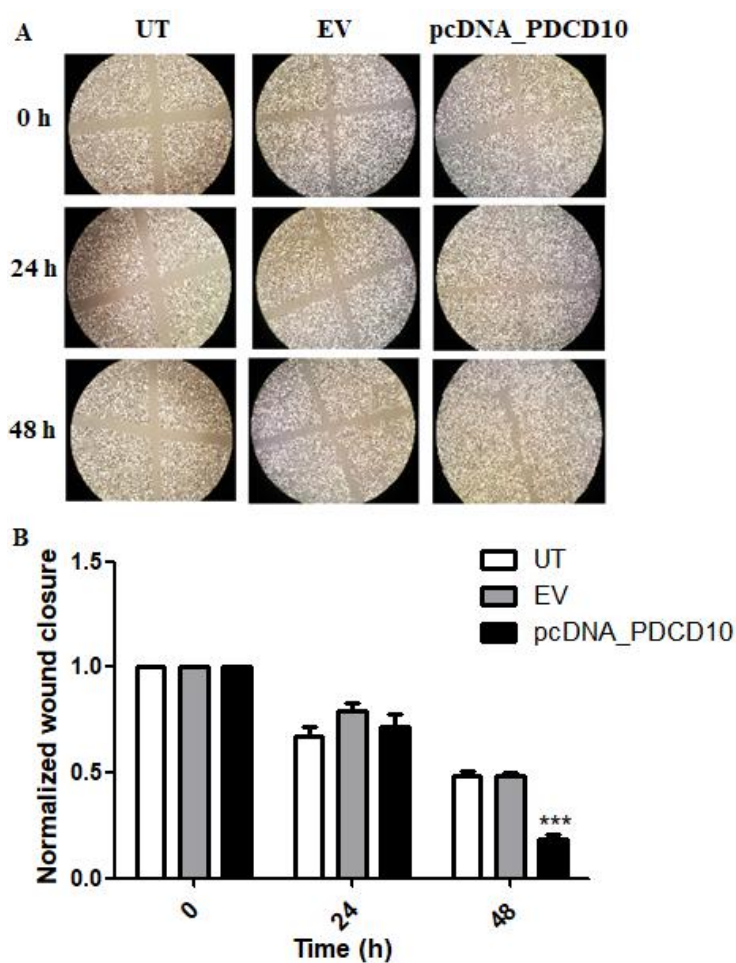
**Figure 3.22** Migratory activity of *PDCD10*-silenced MCF7 cells at different time intervals. MCF7 cells were transfected with 5 nM *PDCD10*-specific siRNA (*siPDCD10*) for 48h and the wound was generated. The wound closure was determined compared to untransfected (UT) control group (n=3).

Figure 3.22 shows that *PDCD10*-silenced MCF7 cells did not show any significant change in migratory activity. The knockdown of *PDCD10* caused increased resistance to both docetaxel and doxorubicin as well as altered the expression pattern of apoptosis-related genes such that it resembled that of drug-resistant cells. However, the downregulation in *PDCD10* in MCF7 cells did not cause elevated migratory activity which is a characteristic that is attributed to drug-resistant cells.



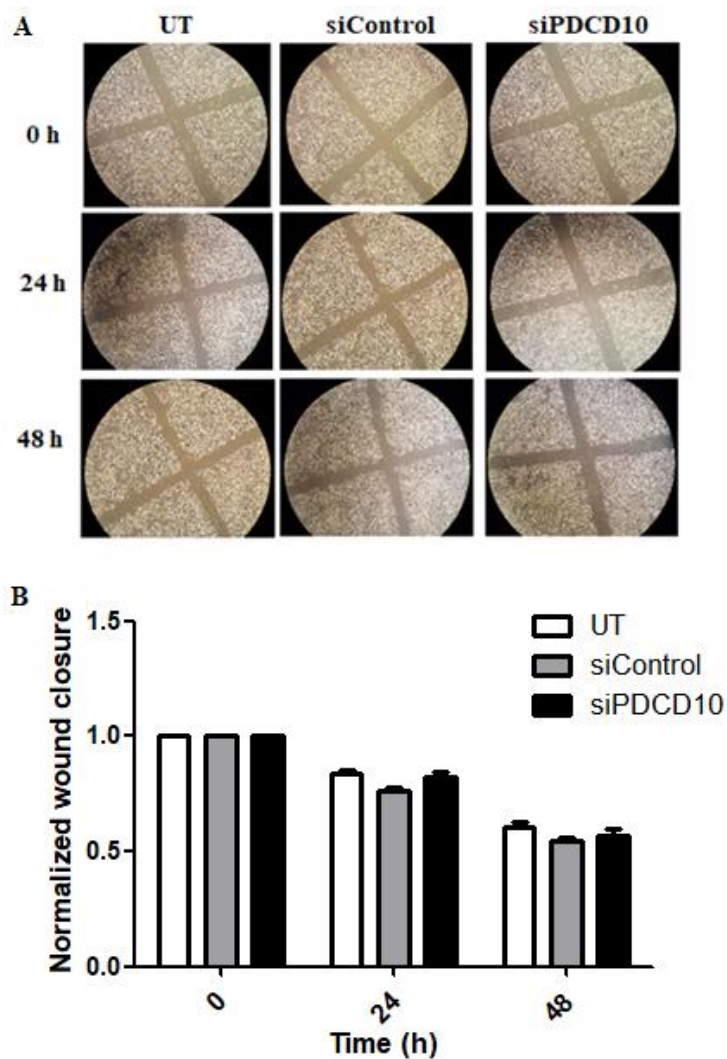
**Figure 3.23** Migratory activity of *PDCD10*-overexpressed MCF7/DOX cells at different time intervals. MCF7/DOX cells were transfected with either empty vector (EV) or pcDNA\_PDCD10 and the wound was generated. The wound closure was determined compared to untransfected (UT) control group (n=3).

As seen in Figure 3.23, the wound area was almost completely closed in 24h in untransfected (UT), empty vector (EV) and pcDNA\_PDCD10 transfected MCF7/DOX cells. The migratory activity of *PDCD10*-overexpressed MCF7/DOX cells did not show any significant change compared to control groups, indicating that PDCD10 did not affect migration of doxorubicin-resistant MCF7 cells although overexpression of *PDCD10* resulted in re-sensitization of these cells to doxorubicin.



**Figure 3.24** Migratory activity of *PDCD10*-overexpressed HeLa cells at different time intervals HeLa cells were transfected with either empty vector (EV) or pcDNA\_PDCD10 and the wound was generated. The wound closure was determined compared to untransfected (UT) control group (n=3; \*\*\*=p<0.001).

*PDCD10*-overexpressed HeLa cells closed the scratch area faster than untransfected (UT) and empty vector (EV)-transfected control groups, indicating that *PDCD10* overexpression did not only increase drug resistance in HeLa cells but also resulted in enhanced migratory activity (Figure 3.24).



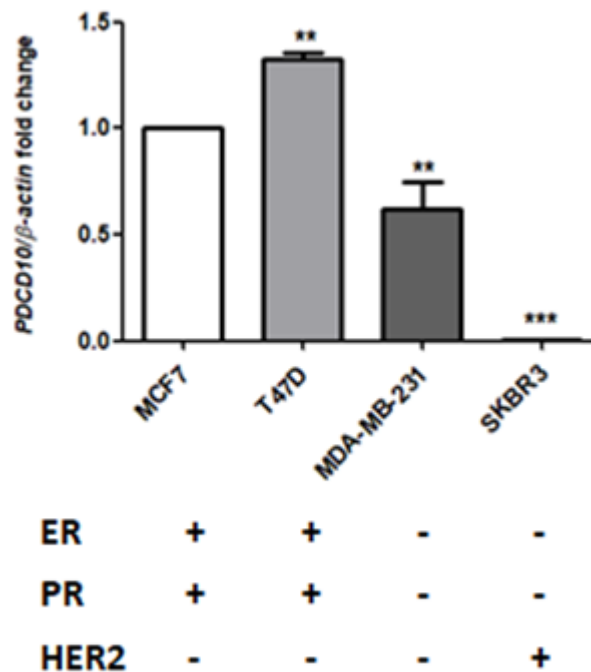
**Figure 3.25** Migratory activity of *PDCD10*-silenced HeLa/DOX cells at different time intervals. HeLa/DOX cells were transfected with 5 nM control (*siControl*) or *PDCD10*-specific (*siPDCD10*) siRNA for 48h and the wound was generated. The wound closure was determined compared to untransfected (UT) control group (n=3).

Figure 3.25 shows that the migratory activity of *PDCD10*-silenced HeLa/DOX did not change significantly compared to control groups. Similar to MCF7/DOX cells, the alteration in *PDCD10* expression did not affect the migratory activity of doxorubicin-resistant HeLa cells despite the increased chemosensitivity to the anti-cancer agent.

There are contradictory reports regarding the effect of *PDCD10* on cellular motility and migration. Schleider et al showed that *PDCD10* expression inhibited the migration and tube formation in endothelial cells (Schleider et al, 2011). On the other hand, You et al reported that the loss of *PDCD10* decreased the migratory and hyper-angiogenic activity in the same endothelial cell line (You et al, 2013). Louvi et al revealed that loss of *PDCD10* caused the inhibition of neuronal migration in mice, leading to vital malformations in neuronal development (Louvi et al, 2014). This differential effect of *PDCD10* on cellular migration and metastatic behavior could be related to the different downstream pathways that *PDCD10* modulates in different cell types. These downstream pathways and involving proteins should be examined in detail to figure out the association of *PDCD10* with cellular migration.

### **3.8 *PDCD10* Expression in Breast Cancer Cells**

Breast cancer cells can be classified depending on the presence of estrogen receptor (ER), progesterone receptor (PR) and human epithelial growth factor receptor (HER2) in four different subgroups, namely Luminal A, Luminal B, HER2-positive and triple negative. All Luminal A and Luminal B cells express ER and PR while HER2-positive cells do not express any receptor other than HER2. On the other hand, triple negative cells do not have either ER, PR or HER2 expression (Holliday and Speirs, 2011).



**Figure 3.26** *PDCD10* expression in T47D, MDA-MB-231 and SKBR3 breast cancer cells compared to MCF7 cell line. *PDCD10* expression was determined by using LightCycler 480 Probes Master Mix and Real Time Ready Assay primers (Roche Diagnostics, Switzerland).  $\beta$ -actin was used as internal control. Fold changes were calculated by  $2^{-\Delta\Delta C_t}$  method compared to MCF7 cells and analyzed by one-way ANOVA test followed by post-hoc Tukey's test. (n=3; \*\* = p<0.01 and \*\*\* = p<0.001).

Figure 3.26 shows that *PDCD10* expression differs depending on the cell type. T47D cells, which were ER(+)/PR(+), had higher *PDCD10* expression compared to MCF7 cell line, which also expressed ER and PR, whereas triple-negative MDA-MB-231 and HER2(+) SKBR3 cells displayed lower levels of *PDCD10* expression. The differential expression could be a result of several cellular conditions as well as receptor status of these breast cancer cells. The lower *PDCD10* expression in ER-negative MDA-MB-231 and

SKBR3 cells could be an indication of possible estrogen-dependent activation of *PDCD10* transcription. Previously, İşeri et al showed that MCF7/DOX cells underwent epithelial-mesenchymal transition (EMT) and lost estrogen receptor expression during EMT (İşeri et al, 2011). The significant downregulation in *PDCD10* expression in MCF7/DOX cells (Figure 3.3) could further indicate the relationship between estrogen-ER signaling with *PDCD10* expression. Moreover, Chen et al reported that *PDCD10* expression was regulated by a 851 bp-long bidirectional promoter which had a c-Myc binding sequence (Chen et al, 2007). The activation of c-Myc by estrogen (Murphy et al, 1987; Dubik and Shiu, 1992; Wang et al 2011) could indirectly activate *PDCD10* transcription in ER-positive cell lines.

## CHAPTER 4

### CONCLUSIONS

PDCD10 is a novel apoptotic regulator which involves in the modulation of cell survival and cell death under different cellular conditions. However, the function of PDCD10 in drug resistance has not been established yet. The main objective of this study was to determine the role of PDCD10 in various drug-resistant cancer cells.

This study revealed that *PDCD10* expression was cell- and anti-cancer agent-specific. *PDCD10* expression was significantly downregulated in doxorubicin- and docetaxel-resistant MCF7 cells and upregulated in doxorubicin-resistant HeLa cells. On the other hand, doxorubicin-resistant K562 cells did not show any significant change in *PDCD10* expression.

The downregulation of *PDCD10* in parental MCF7 cells resulted in the increased docetaxel and doxorubicin resistance. On the other hand, the overexpression of *PDCD10* resensitized doxorubicin-resistant MCF7 cells to the anti-cancer agent. The elevated drug resistance status was achieved in parental HeLa cells by overexpression of *PDCD10* whereas the downregulation of HeLa/DOX cells led to re-sensitization to doxorubicin.

The alterations in *PDCD10* expression did not affect intracellular drug accumulation in any cell line, indicating that the change in drug resistance status was not a result of altered drug accumulation in the cell.

In *PDCD10*-silenced MCF7 cells, apoptosis was found to be inhibited and caspase 7 activity was lower compared to control groups. The drug resistance modulated by *PDCD10* was found to be associated with the apoptotic regulation.

Even though the expression patterns were different, drug-resistant cancer cells displayed significant upregulation in the expressions of anti-apoptotic genes and downregulations in those of pro-apoptotic ones. The up- and down-regulations in the expressions of the apoptosis-related genes seemed to provide a survival advantage to drug-resistant cancer cells in anti-cancer drug containing environment and drive them to be resistant to apoptosis.

*PDCD10*-silenced MCF7 cells displayed upregulation in anti-apoptotic gene expression with downregulation in the expressions of pro-apoptotic genes, resembling the expression pattern of drug-resistant cells. This alteration in gene expression pattern helped *PDCD10*-silenced MCF7 cells to develop drug-resistant phenotype. On the other hand, *PDCD10*-overexpressed MCF7/DOX cells, which were found to be resensitized to doxorubicin, exhibited downregulation in the expressions of anti-apoptotic genes and upregulations in pro-apoptotic ones.

Surprisingly, *PDCD10*-overexpressed HeLa and *PDCD10*-silenced HeLa/DOX cells did not show any significant alterations in the expressions of apoptosis-related genes, except for *PUMA*. Interestingly, pro-apoptotic

*PUMA* expression was found to be upregulated in *PDCD10*-overexpressed HeLa and downregulated in *PDCD10*-silenced HeLa/DOX cells. Although the change in *PUMA* expression may not be sufficient to stimulate or inhibit apoptotic signaling, further studies are required to determine the relationship between *PUMA* expression and *PDCD10*-mediated drug resistance in HeLa cells.

The alterations in *PDCD10* expression did not alter the migratory activity in MCF7, MCF7/DOX and HeLa/DOX cells. However, *PDCD10*-overexpressed HeLa cells displayed enhanced migratory activity, indicating that the effect of *PDCD10* on motility and migration is cell-specific.

This study revealed that cell-specific *PDCD10* expression regulated drug resistance by modulation of apoptosis in different ways. In drug-resistant MCF7 cells, *PDCD10* downregulation was shown to promote drug resistance whereas upregulation of *PDCD10* was found to be one of the drug resistance mechanisms in HeLa cells. Similarly, the effect of *PDCD10* on the expressions of apoptosis-related genes and cellular motility varied depending on the cell type. Differential *PDCD10* expression and *PDCD10*-related pathways should be further examined in detail for a better understanding in *PDCD10*-mediated drug resistance.



## CHAPTER 5

### FUTURE PROSPECTIVES

With this study, it was revealed that *PDCD10* had dual functions in the development of drug-resistant phenotype, either promoting or inhibiting drug resistance in different cell types. The results of this study as well as earlier reports indicated that *PDCD10* exerts its effects on drug resistance and apoptosis via the modulation of other proteins, possibly through the regulation of several serine-threonine kinases. To figure out the proteins involving in *PDCD10*-mediated drug resistance, the activity of serine-threonine kinases known to interact with *PDCD10* will be examined in different drug-resistant cells.

This study showed that *PDCD10* expression was significantly higher in ER-positive breast cancer cells, MCF7 and T47D, compared to ER-negative MDA-MB-231 and SKBR3 cell lines. The potential estrogen-dependent activation of *PDCD10* transcription will be examined in ER-positive and ER-negative cells following estrogen stimulation and estrogen withdrawal. Moreover, the presence of c-Myc binding site on *PDCD10* promoter suggested that estrogen could indirectly increase *PDCD10* expression through c-Myc which is known to be induced by estrogen. To that end, a c-Myc knockout of ER-positive cells will be generated to examine whether the estrogen-dependent activation of *PDCD10* expression is indeed associated with c-Myc.



## REFERENCES

Abbro, L., Dini, L. (2003). Common morphological features of apoptotic cell blebs. *Ital. J. Zool.*, 70, 297-299.

Aguirre, A. J., Brennan, C., Bailey, G., Sinha, R., Feng, B., et al. (2004). High resolution characterization of the pancreatic adenocarcinoma genome, *Proc. Natl. Acad. Sci. USA*, 101, 9067-9072.

Ahmed, R., Rahman, N. (2006). ATM and breast cancer susceptibility. *Oncogene*, 25, 5906-5911.

Akl, H., Vervloessem, T., Kiviluoto, S., Bittremieux, M., Parys, J. B., et al. (2014). A dual role for the anti-apoptotic Bcl-2 protein in cancer: mitochondria versus endoplasmic reticulum. *Biochim Biophys Acta.*, 1843(10), 2240-2252.

Ambudkar, S. V., Sauna, Z. E., Gottesman, M. M., Szakacs, G. (2005). A novel way to spread drug resistance in tumor cells: functional intercellular transfer of P-glycoprotein (ABCB1). *Trends Pharmacol Sci*, 26(8), 385–387.

American Cancer Society. (2017). *Cancer Facts & Figures 2017*. Atlanta: American Cancer Society; 2017.

Anvekar, R. A., Asciolla, J. J., Missert, D. J., Chipuk, J. E. (2011). Born to be alive: a role for the BCL-2 family in melanoma tumor cell survival, apoptosis, and treatment. *Front Oncol.*, 1(34).

Apostolou, P., Papatirou, I. (2017). Current perspectives on CHEK2 mutations in breast cancer. *Breast Cancer*, 9, 331-335.

Baran, Y., Salas, A., Senkal, C. E., Gunduz, U., Bielawski, J., et al. (2007). Alterations of Ceramide/Sphingosine 1-Phosphate rheostat involved in the regulation of resistance to imatinib-induced apoptosis in K562 human chronic myeloid leukemia cells. *J Biol Chem.*, 282(15), 10922-10934.

Bean, G. R., Ganesan, Y. T., Dong, Y., Takeda, S., Liu, H., et al. (2013). PUMA and BIM Are Required for Oncogene Inactivation–Induced Apoptosis. *Sci. Signal.*, 6(268), ra20. doi: 10.1126/scisignal.2003483.

Bertram, J. S. (2000). The molecular biology of cancer. *Molecular Aspects of Medicine*, 21(6),167-223.

Boland, C. R., Goel, A. (2005). Somatic evolution of cancer cells. *Seminars in cancer biology*, 15(6), 436-50.

Bottone, M. G., Santin, G., Aredia, F., Bernocchi, G., Pellicciari, C., Scovassi, A. I. (2013). Morphological features of organelles during apoptosis: an overview. *Cells*, 2, 294-305.

Bratton, D. L., Fadok, V. A., Richter, D. A., Kailey, J. M., Guthrie, L. A., Henson, P. M. (1997). Appearance of phosphatidylserine on apoptotic cells requires calcium-mediated nonspecific flip-flop and is enhanced by loss of the aminophospholipid translocase. *The Journal of Biological Chemistry*, 272(42), 26159–26165.

Brentnall, M., Rodriguez-Menocal, L., De Guevera R. L., Cepero, E., Biose L. H. (2013). Caspase-9, caspase-3 and caspase-7 have distinct roles during intrinsic apoptosis. *BMC Cell Biol.*, 14, 32. doi:10.1186/1471-2121-14-32.

Brunelle, J. K., Letai, A. (2009). Control of mitochondrial apoptosis by the Bcl-2 family. *J Cell Sci.*, 15, 122(Pt.4), 437-441.

Chandrika, B. B., Maney, S. K., Lekshmi, S. U. Joseph, J., Seervi, M., Praveen, K. S., Santhoshkumar, T. R. (2010). Bax deficiency mediated drug resistance can be reversed by endoplasmic reticulum stress induced death signaling. *Biochemical Pharmacology*, 79(11), 1589-1599.

Chen, J. X., Fan, J. P., Yin, G. K., Sun, A. H., Liao, J. C., et al. (2001). Study of differentially expressed genes in laryngeal squamous cell carcinoma by cDNA microarray. *Chin. Acad. J. Sec. Mil. Med. Univ.*, 22, 519–522.

Chen, P. Y., Chang, W. S., Chou, R. H., Lai, Y. K., Lin, S. C., et al. (2007). Two non-homologous brain diseases-related genes, SERPINI1 and PDCD10, are tightly linked by an asymmetric bidirectional promoter in an evolutionarily conserved manner. *BMC Mol Biol.*, 8, 2.

Czabotar, P. E., Lessene, G., Strasser, A., Adams, J. M. (2014). Control of apoptosis by the BCL-2 protein family: implications for physiology and therapy. *Nat Rev Mol Cell Biol.*, 15(1), 49-63.

Dan, I. Ong, S. E., Watanabe, N. M., Blagoev, B., Nielsen, M. M., et al. (2002). Cloning of MASK, a novel member of the mammalian germinal center kinase III subfamily, with apoptosis inducing properties. *J. Biol. Chem.*, 277, 5929-5939.

Danisz, K., Blasiak, J. (2013). Role of anti-apoptotic pathways activated by BCR/ABL in the resistance of chronic myeloid leukemia cells to tyrosine kinase inhibitors. *Acta Biochim Pol.*, 60(4), 503-514.

Degenhardt, K., Chen, G., Lindsten, T., White, E. (2002). BAX and BAK mediate p53-independent suppression of tumorigenesis. *Cancer Cell*, 2, 193-203.

Dönmez, Y., Gündüz, U. (2011). Reversal of multidrug resistance by small interfering RNA (siRNA) in doxorubicin-resistant MCF-7 breast cancer cells. *Biomed Pharmacother*, 65(2), 85-89.

Drummond, M. W., Holyoake, T. L. (2001). Tyrosine kinase inhibitors in the treatment of chronic myeloid leukaemia: so far so good? *Blood Rev.*, 15(2), 85-95.

Dubik, D., Shiu, R. P. (1992). Mechanism of estrogen activation of c-myc oncogene expression. *Oncogene*, 7(8), 1587-1594.

Ejendal, K. F. K., Hrycyna, C. A. (2002). Multidrug resistance and cancer: the role of the human ABC transporter ABCG2. *Current Protein & Peptide Science*, 3(5), 503-511.

Elmore, S. (2007). Apoptosis: a review of programmed cell death. *Toxicol Pathol.*, 35(4), 495–516.

Fadok, V. A., Bratton, D. L., Frasch, S. C., Warner, M. L., Henson, P. M. (1998). The role of phosphatidylserine in recognition of apoptotic cells by phagocytes. *Cell Death and Differentiation*, 5, 551-562.

Fink, S. L., Cookson, B. T: (2005). Apoptosis, pyroptosis, and necrosis: mechanistic description of dead and dying eukaryotic cells. *Infect Immun.*, 73(4), 1907-1916.

Finucane, D. M., Bossy-Wetzler, E., Waterhouse, N. J., Cotteri, T. G., Green, D. R. (1999). Bax-induced caspase activation and apoptosis via cytochrome c release from mitochondria is inhibitable by Bcl-xL. *The Journal Of Biological Chemistry*, 274(4), 2225–2233.

Foulkes, W. D. (2003). Germline BRCA1 mutations and a basal epithelial phenotype in breast cancer. *Cancer Spectrum Knowledge Environment*, 95(19), 1482-1485.

Friedrich, K., Wieder, T., Von Haefen, C., Radetzki, S., Jänicke, R., et al (2001). Overexpression of caspase-3 restores sensitivity for drug-induced apoptosis in breast cancer cell lines with acquired drug resistance. *Oncogene*, 20(22), 2749-2760.

Fu, X., Zhang, W., Su, Y., Lu, L., Wang, D., Wang, H. (2016). MicroRNA-103 suppresses tumor cell proliferation by targeting PDCD10 in prostate cancer. *Prostate*, 76(6), 543-551.

Fulda, S., Küfer, M. U., Meyer, E., van Valen, F., Dockhorn-Dworniczak, B., Debatin, K. M. (2001). Sensitization for death receptor- or drug-induced apoptosis by re-expression of caspase-8 through demethylation or gene transfer. *Oncogene*, 20, 5865–5877.

Garg, H., Suri, P., Gupta, J. C., Talwar, G. P., Dubey, S. (2016). Survivin: a unique target for tumor therapy. *Cancer Cell Int*, 16:49. doi: 10.1186/s12935-016-0326-1.

van Genderen, H. O., Kenis, H., Hofstra, L., Narula, J., Reutelingsperger, C. P. M. (2008). Extracellular annexin A5: functions of phosphatidylserine-binding and two-dimensional crystallization. *Biochim Biophys Acta.*, 1783(6), 953-63.

Glück, S. (2005). Adjuvant chemotherapy for early breast cancer : optimal use of epirubicin, *The Oncologist*, 10, 780-791.

Gottesman, M. M., Fojo, T., Bates, Susan E. (2002). Multidrug resistance in cancer: role of ATP-dependent transporters. *Nature Reviews Cancer*, 2(1), 48-58.

Gross, A., McDonnell, J. M., Korsmeyer, S.J. (1999). BCL-2 family members and the mitochondria in apoptosis. *Genes and Development*, 13, 1899-1911.

Hanahan, D., Weinberg, R. A., Francisco, S. (2000). The Hallmarks of Cancer Review. *Cell*, 100, 57-70.

Hanahan, D., & Weinberg, R. A. (2011). Hallmarks of cancer: the next generation. *Cell*, 144(5), 646-74.

Holliday, D. L., Speirs, V. (2011). Choosing the right cell line for breast cancer research. *Breast Cancer Research*, 13, 215. doi.org/10.1186/bcr2889.

Holohan, C., Schaeybroeck, S. V., Longley, D. B., Johnston, P. G. (2013). Cancer drug resistance: an evolving paradigm, *Nature Reviews Cancer*, 13(10), 714-726.

Housman, G., Byler, S., Heerboth, S., Lapinska, K., Longacre, M., Snyder, N., Sarkar, S. (2014). Drug resistance in cancer: an overview. *Cancers*, 6, 1769-1792.

Huerta, S., Harris, D. M., Jazirehi, A., Bonavida, B., Elashoff, D., et al. (2003). Gene expression profile of metastatic colon cancer cells resistant to cisplatin-induced apoptosis, *Int. J. Oncol.*, 22, 663-670.

İşeri Ö.D. (2009). Investigation of docetaxel and doxorubicin resistance in MCF-7 breast carcinoma cell line, PhD Thesis, Middle East Technical University.

İşeri, Ö. D., Kars, M. D., Arpacı, F., Gündüz, U. (2010). Gene expression analysis of drug-resistant MCF-7 cells: implications for relation to extracellular matrix proteins. *Cancer Chemother Pharmacol*, 65(3), 447-455.

İşeri, Ö. D., Kars, M.D, Arpacı, F., Atalay, C., Pak, I., Gündüz, U. (2011). Drug resistant MCF-7 cells exhibit epithelial-mesenchymal transition gene expression pattern. *Biomed Pharmacother.*, 65(1), 40-45.

Jabbour, A. M., Heraud, J. E., Daunt, C. P., Kaufmann, T., Sandow, J., et al. (2009). Puma indirectly activates Bax to cause apoptosis in the absence of Bid or Bim. *Cell Death and Differentiation*, 16, 555–563.

Jahagirdar, B. N., Miller, J. S., Shet, A., Verfaillie C. M. (2001). Novel therapies for chronic myelogenous leukemia. *Experimental Hematology*, 29, 543-556.

Jeon, J. H., Kim, D. K., Shin, Y., Kim, H. Y., Song, B., et al. (2016). Migration and invasion of drug-resistant lung adenocarcinoma cells are dependent on mitochondrial activity. *Exp Mol Med.*, 48(12), e277. doi:10.1038/emm.2016.129

Jiang, G., Ren, B., Xu, L., Song, S., Zhu, C., Ye, F. (2009). Survivin may enhance DNA double-strand break repair capability by up-regulating Ku70 in human KB cells. *Anticancer Res.*, 29(1), 223-228.

Kantarjian, H. M., Cortes, J., La Rosee, P., Hochhaus, A. (2010). Optimizing therapy for patients with chronic myelogenous leukemia in chronic phase. *Cancer*, 116(6), 1419-1430.

Kars, M. D., İşeri, Ö. D., Gündüz, U. (2007). In vitro evaluation of zoledronic acid resistance developed in MCF-7 cells. *Anticancer Res.*, 27(6B), 4031-4037

.

Kars, M.D. (2008). Molecular mechanisms of vincristine and paclitaxel resistance in MCF-7 cell line, PhD Thesis, Middle East Technical University.

Kars, M. D., İseri, O. D., Gunduz, U. (2011). A microarray based expression profiling of paclitaxel and vincristine resistant MCF-7 cells. *Eur J Pharmacol.*, 25, 657(1-3), 4-9.

Keppler, D., Leier, I., Jedlitschky, G., Mayer, R., Büchler, M. (1996). The function of the multidrug resistance proteins (MRP and cMRP) in drug conjugate transport and hepatobiliary excretion. *Adv Enzyme Regul.*, 36, 17-29.

Kepler, D. (2011). Multidrug resistance proteins (MRPs, ABCs): importance for pathophysiology and drug therapy. *Handb Exp Pharmacol.*, 201, 299-323.

Keen, A., Lennan, E. (2011). Women's Cancers. 1st Ed. West Sussex: John Wiley & Sons, Inc. p110.

Kerr, J. F., Winterford, C. M., Harmon, B. V. (1994). Apoptosis. Its significance in cancer and cancer therapy. *Cancer*, 73(8), 2013-2026.

Khaled, A. R., Kim, K., Hofmeister, R., Muegge, K., Durum, S. K. (1999). Withdrawal of IL-7 induces Bax translocation from cytosol to mitochondria through a rise in intracellular pH. *Proc. Natl. Acad. Sci. USA*, 96, 14476–14481.

Khan, S., Bennit, H. F., Wall, N. R. (2015). The emerging role of exosomes in Survivin secretion. *Histol Histopathol.*, 30(1), 43–50.

King, M. C., Marks, J.H., Mandell, J. B., The New York Breast Cancer Study Group. (2003). Breast and ovarian cancer risks due to inherited mutations of BRCA1 and BRCA2. *Science*, 302(5645), 643-646.

Komina, O., Nosske, E., Maurer, M., Wesierska-Gadek, J. (2011). Roscovitine, a small molecule CDK inhibitor induces apoptosis in multidrug-resistant human multiple myeloma cells. *J Exp Ther Oncol.*, 9(1), 27-35.

Krishna, R., Mayer, L. D. (2000). Multidrug resistance (MDR) in cancer: mechanisms, reversal using modulators of MDR and the role of MDR modulators in influencing the pharmacokinetics of anti-cancer drugs. *European Journal of Pharmaceutical Sciences*, 11(4), 265-83.

Kroemer, G. (1997). The proto-oncogene Bcl-2 and its role in regulating apoptosis. *Nat Med.*, 3(6), 614-620.

Krystal, G. W. (2001). Mechanisms of resistance to imatinib (STI571) and prospects for combination with conventional chemotherapeutic agents. *Drug Resist Updat.*, 4(1), 16-21.

Lalier, L., Cartron, P. F., Juin, P., Nedelkina, S., Manon, S., Bechinger, B., Vallette, F. M. (2007). Bax activation and mitochondrial insertion during apoptosis. *Apoptosis*, 12(5), 887-96.

de Lange, J. H., Schipper, N. W., Schuurhuis, G. J., ten Kate, T. K., van Heijningen, T. H., et al. (1992). Quantification by laser scan microscopy of intracellular doxorubicin distribution. *Cytometry.*, 13(6), 571-576.

Lehne, G. (2000). P-glycoprotein as a drug target in the treatment of multidrug resistant cancer. *Curr Drug Targets*, 1(1), 85-99.

Lin, J. L., Chen, H. C, Fang, H. I, Robinson, D., Kung, H. J, Shih, H. M. (2001). MST4, a new Ste20-related kinase that mediates cell growth and transformation via modulating ERK pathway. *Oncogene*, 20, 6559-6569.

Livak, K. J., Schmittgen, T. D. (2001). Analysis of relative gene expression data using real-time quantitative PCR and the 2(-Delta Delta C(T)) method. *Methods*, 25(4), 402-408.

Longley, D. B., Johnston, P. G. (2005). Molecular mechanisms of drug resistance. *The Journal of Pathology*, 205(2), 275-292.

Louvi, A., Nishimura, S., Gunel, M. (2014). Ccm3, a gene associated with cerebral cavernous malformations, is required for neuronal migration. *Development*, 141(6), 1404-1415.

Ma, X., Zhao, H., Shan, J., Long, F., Chen, Y. et al. (2007). PDCD10 interacts with Ste20-related kinase MST4 to promote cell growth and transformation via modulation of the ERK pathway. *Mol. Bio. Cell*, 18, 1965-1978.

Maricic, M. (2006). The use of zoledronic acid in Paget's disease. *Current Osteoporosis Reports*, 4(1), 40-44.

Marino, G., Kroemer, G. (2013). Mechanisms of apoptotic phosphatidylserine exposure. *Cell Research*, 23, 1247-1248.

McCurrach, M. E., Connor, T. M. F., Knudson, C. M., Korsmeyer, S. C., Lowe, S. W. (1997). bax-deficiency promotes drug resistance and oncogenic transformation by attenuating p53-dependent apoptosis. *Proc. Natl. Acad. Sci. USA*, 94, 2345-2349.

Mita, A. C., Mita, M. M., Nawrocki, S. T., Giles, F. J. (2008). Survivin: key regulator of mitosis and apoptosis and novel target for cancer therapeutics. *Clin Cancer Res.*, 14(16), 5000-5005.

Murphy, L. J., Murphy, L. C., Friesen, H. G. (1987). Estrogen induction of N-myc and c-myc proto-oncogene expression in the rat uterus. *Endocrinology*, 120(5), 1882-1888.

Nakano, K., Vousden, K. H. (2001). PUMA, a novel proapoptotic gene, is induced by p53. *Mol Cell.*, 7(3), 683-694.

National Cervical Cancer Coalition. (2017). Cervical Cancer Overview. North Carolina: National Cervical Cancer Coalition; 2017.

Oltvai, Z. N., Milliman, C. L., Korsmeyer, S. J. (1993). Bcl-2 heterodimerizes in vivo with a conserved homolog, Bax, that accelerates programmed cell death. *Cell*, 74, 609-619.

O'Shaughnessy, J. (2005). Extending survival with chemotherapy in metastatic breast cancer. *The Oncologist*, 10, 3(3), 20-9.

Park, E., Gang, E. J., Hsieh, Y. T., Schaefer, P., Chae, S., et al. (2011). Targeting survivin overcomes drug resistance in acute lymphoblastic leukemia. *Blood*, 118(8), 2191-2199.

Pisco, A. O., Jackson, D. A., Huang, S. (2014). Reduced intracellular drug accumulation in drug-resistant leukemia cells is not only solely due to MDR-

mediated efflux but also to decreased uptake. *Front Oncol.*, 4, 306.  
doi:10.3389/fonc.2014.00306.

Poria, D. K., Guha, A., Nandi, I., Ray, P.S. (2016). RNA-binding protein HuR sequesters microRNA-21 to prevent translation repression of proinflammatory tumor suppressor gene programmed cell death 4. *Oncogene*, 35, 1703-1715.

Radich, J. P. (2007). The biology of CML blast crisis. *Hematology Am Soc Hematol Educ Program*, 384-391.

Ramu, A., Pollard, H. B., Rosario, L. M. (1989). Doxorubicin resistance in p388 leukemia-evidence for reduced drug influx. *Int. J. Cancer*, 44, 539-547.

Rieger, P. (2004). The biology of cancer genetics. *Seminars in Oncology Nursing*, 20(3), 145-154.

Robinson, M., Tian, Y., Delaney, W. E., Greenstein, A. E. (2011). Preexisting drug-resistance mutations reveal unique barriers to resistance for distinct antivirals. *Proceedings of the National Academy of Sciences of the United States of America*, 108(25), 10290-10295.

Salvesen, G. S., Duckett, C. S. (2002). IAP proteins: blocking the road to death's door. *Nat Rev Mol Cell Biol.*, 3(6), 401-410.

Saraste, A., Pulkli, K. (2000). Morphologic and biochemical hallmarks of apoptosis. *Cardiovascular Research*, 45, 528–537.

Schleider, E., Stahl, S., Wüstehube, J., Walter, U., Fischer, A., Felbor, U. (2011). Evidence for anti-angiogenic and pro-survival functions of the cerebral cavernous malformation protein 3. *Neurogenetics*, 12(1), 83-86.

Simon, S. M., Schindler, M. (1994). Cell biological mechanisms of multidrug resistance in tumors, *Proc Natl Acad Sci USA*, 91(9), 3497-3504.

Serova, O. M., Mazoyer, S., Puget, N., Dubois, V., Tonin, P., Shugart, Y. Y., Goldgar, D., et. al. (1997). Mutations in BRCA1 and BRCA2 in breast cancer families: are there more breast cancer-susceptibility genes? *American Journal of Human Genetics*, 60(3), 486-95.

Singh, N., Krishnakumar, S., Kanwar, R. K., Cheung, C. H., Kanwar, J. R. (2014). Clinical aspects for survivin: a crucial molecule for targeting drug-resistant cancers. *Drug Discov Today*, 20(5), 578-587.

Sung, V., Luo, W., Qian, D., Lee, I., Jallal, B., Gishizky, M. (2003). The Ste20 kinase MST4 plays a role in prostate cancer progression. *Cancer Res.*, 63, 3356-3363.

Tamm, I., Wang, Y., Sausville, E., Scudiero, D. A., Vigna, N., Oltersdorf, T., Reed, J. C. (1998). IAP-family protein survivin inhibits caspase activity and apoptosis induced by Fas (CD95), Bax, caspases, and anticancer drugs. *Cancer Res.*, 58(23), 5315-20.

Tomaic, K. (2016). Functional Roles of E6 and E7 Oncoproteins in HPV-Induced Malignancies at Diverse Anatomical Sites. *Cancers*, 8(10), 95.

Trela, E., Glowacki, S., Blasiak, J. (2014). Therapy of chronic myeloid leukemia: twilight of the imatinib era? *ISRN Oncol.*, doi: 10.1155/2014/596483.

Tsujimoto, Y. Role of Bcl-2 family proteins in apoptosis: apoptosomes or mitochondria? *Genes Cells*, 3(11), 697-707.

Tyczynski, J. E., Bray, F., Parkin, D. M. (2002). Breast cancer in Europe. ENCR Cancer Fact Sheets. 2002; 2.

Walsh, J. G., Cullen, S. P., Sheridan, C., Lüthi, A. U., Gerner, C., Martin, S. J. (2008). Executioner caspase-3 and caspase-7 are functionally distinct proteases. *Proc Natl Acad Sci U S A.*, 105(35), 12815-12819.

Wang, Y.G., Liu, H., Zhang, Y., Ma D. (1999). cDNA cloning and expression of an apoptosis-related gene, human TFAR-15 gene. *Science in China C Life Sci.*, 29, 331-336.

Wang, C., Mayer, J. A., Mazumdar, A., Fertuck, K., Kim, H., et al. (2011). Estrogen induces c-myc gene expression via an upstream enhancer activated by the estrogen receptor and the AP-1 transcription factor. *Mol Endocrinol*, 25(9), 1527-1538.

Westphal, D., Dewson, G., Czabotar, P. E., Kluck, R. M. (2011). Molecular biology of Bax and Bak activation and action. *Biochim Biophys Acta.*, 1813(4), 521-531.

Willis, S., Day, C. L., Hinds, M. G., Huang, D. C. (2003). The Bcl-2-regulated apoptotic pathway. *J Cell Sci.*, 116(Pt 20), 4053-4056.

Wu, Y. H., You, Y., Chen, Z. C., Zou, P. (2008). Reversal of drug resistance by silencing Survivin gene expression in acute myeloid leukemia cells. *Acta Biochim Pol.*, 55(4), 673-680.

Wu, Z., Jin, H., and Gu, Y. (2002). Changes of gene expression in atrophic muscle induced by brachial plexus injury in rats. *Chin. J. Traumatol.*, 18, 357-360.

Yagi, O. K., Akiyama, Y., Nomizu, T., Iwama, T., Endo, M., Yuasa, Y. (1998). Proapoptotic gene BAX is frequently mutated in hereditary nonpolyposis colorectal cancers but not in adenomas. *Gastroenterology*, 114, 268-274.

Yang, X., Sladek, H. L., Liu, X., Butler, B. R., Froelich, C. J., Thor, A. D. (2001). Reconstitution of Caspase 3 Sensitizes MCF-7 Breast Cancer Cells to Doxorubicin- and Etoposide-induced Apoptosis. *Cancer Res.*, 61(1), 348-354.

Yim, E. K., Park, J. S. (2005). The Role of HPV E6 and E7 Oncoproteins in HPV-associated Cervical Carcinogenesis. *Cancer Res Treat.*, 37(6), 319-324.

You, C., Sandalcioglu, I. E., Dammann, P., Felbor, U., Sure, U., Zhu, Y. (2013). Loss of CCM3 impairs DLL4-Notch signalling: implication in endothelial angiogenesis and in inherited cerebral cavernous malformations. *J Cell Mol Med.*, 17(3), 407-418.

Yu, J., Zhang, L., Hwang, P. M., Kinzler, K. W., Vogelstein, B. (2001). PUMA Induces the Rapid Apoptosis of Colorectal Cancer Cells. *Molecular Cell* 7(3), 673–682.

Yu, J., Zhang, L. (2008). PUMA, a potent killer with or without p53. *Oncogene*, 27(Suppl 1), S71-83.

Zhang, L., Yu, J., Park, B. H., Kinzler, K. W., Vogelstein, B. (2000). Role of BAX in the Apoptotic Response to Anticancer Agents. *Science*, 290(5493), 989-992.

Zhang, H., Ma, X., Deng, X., Chen, Y., Mo, X., et al. (2012). PDCD10 interacts with STK25 to accelerate cell apoptosis under oxidative stress. *Frontiers in Bioscience*, 17, 2295-2305.

Zhang, H., Wang, J. Cai, K., Jjiang, L., Zhou, D., et al. (2012). Downregulation of gene MDR1 by shRNA to reverse multidrug-resistance of ovarian cancer A2780 cells. *J Cancer Res Ther.*, 8(2), 226-231.

Zhang, Y., Miao, X., Zhu, K., Cui, S., Meng, Q., J., et al (2016). MicroRNA-425-5p regulates chemoresistance in colorectal cancer cells via regulation of Programmed Cell Death 10. *J Cell Mol Med.*, 20(2), 360-369.

Zhou, J., Liu, M., Aneja, R., Chandra, R., Lage, H., Joshi, H. C. (2006). Reversal of P-glycoprotein–Mediated Multidrug Resistance in Cancer Cells by the c-Jun NH2-Terminal Kinase. *Cancer Res.*, 66(1), 445-452.

Ziegler, U., Groscurth, P. (2004). Morphological Features of Cell Death.  
*News Physiol Sci* ,19, 124-128.



## APPENDIX A

### BUFFERS AND SOLUTIONS

#### A.1. Freezing Medium

9ml FBS (Biochrome, Germany)

1ml DMSO (Applichem, Germany)

Mixed and stored at -20°C

#### A.2. Phosphate Buffered Saline (pH 7.2)

1 PBS tablet (Sigma, Germany) was dissolved in 100ml distilled water and autoclaved at 121°C for 20 minutes.

#### A.3. 4X Separating Buffer

91 g Tris base (Bioshop)

2 g SDS (Applichem)

Volume is completed to 500 ml with distilled water, after adjusting pH to 8.8.

#### A.4. 4X Stacking Buffer

30.35 g Tris base (Bioshop)

2 g SDS (Applichem)

After pH was adjusted to 6.8, volume is completed to 500 ml with distilled water.

#### A.5. Running Buffer

100 ml Tris-Glycine buffer (10X)

890 ml distilled water  
10 ml of 10% SDS solution

**A.6. 4X Sample Loading Buffer**

2.0 ml 1M Tris-HCl (pH 6.8)  
0.8 g SDS  
4.0 ml of 100% glycerol  
1.0 ml of 0.5 M EDTA  
8.0 mg bromophenol blue  
2.6 ml distilled H<sub>2</sub>O

The buffer is aliquoted in 96 µl and stored at -20°C at dark. Before experimentation, 4 µl of 17.4 M beta-mercaptoethanol (Amresco) is added to each aliquot and mixed well.

**A.7. 5X Bradford Reagent**

100 mg Coomassie G-250 (Serva)  
47 ml methanol  
100 ml of 85% phosphoric acid (Riedel-de Haen)

Volume is completed to 200 mL with distilled water and stored at 4°C at dark.

**A.8. 10X TBS Buffer**

24.23 g Tris.HCl  
80.06 g NaCl

After pH was adjusted to 7.6, volume was completed to 1000 ml with distilled water. TBS is autoclaved at 121°C for 20 minutes

**A.9. TBST (0.1% Tween 20)**

100 ml of 10X TBS  
900 ml distilled water

1 ml of Tween 20 (Amresco)

#### **A.10. Blocking Buffer**

0.5 g skimmed milk (Amresco) or BSA was dissolved in 10 ml of 0.1% TBST.

#### **A.11. 10X Tris-Glycine Buffer**

30.3 g Tris base

144.1 g Glycine (Bioshop)

After pH was adjusted to 8.3, volume was completed to 1000 ml with distilled water.

#### **A.12. Transfer buffer**

100 ml of 10X Tris-Glycine buffer

5 ml of 10% SDS solution

800 ml Methanol (Sigma)

Volume was completed to 1000 ml with distilled water.

#### **A.13. Stripping buffer**

0.76 g Tris base

2 g SDS

700  $\mu$ l of beta-mercaptoethanol

After pH was adjusted to 6.8, volume was completed to 1000 ml with distilled water.



## APPENDIX B

### PDCD10 PROTEIN DETECTION BY WESTERN BLOT

To detect PDCD10 expression at protein level, anti-PDCD10 pAb (Abcam, USA) was used.

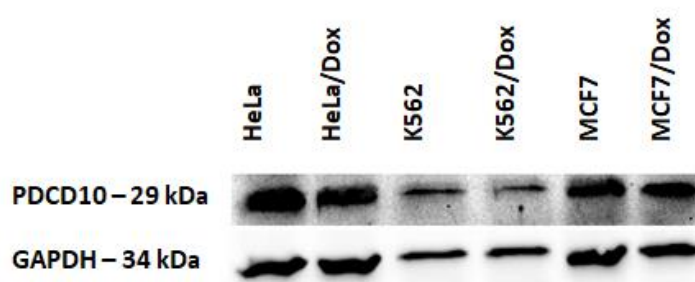


**Figure B.1** PDCD10 expression in doxorubicin-resistant HeLa, K562 and MCF7 cells. Total protein was isolated from each cell line by MPER (Thermo Fisher Scientific, USA). Isolated proteins were run on 12% polyacrylamide gel, the membrane was blocked with 5% BSA and stained with anti-PDCD10 pAb (1:1000 dilution in 5% BSA in 0.1% TBST).

The expression of PDCD10 at protein level was found to be not correlated with the expression of PDCD10 at mRNA level. The blot showed various highly intense non-specific bands.

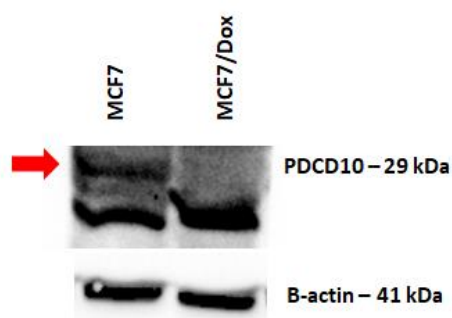


**Figure B.2** PDCD10 expression in parental and doxorubicin-resistant MCF7 cells. Total protein was isolated from each cell line by MPER (Thermo Fisher Scientific, USA). 50  $\mu$ g protein/lane was run on 8% polyacrylamide gel, the membrane was blocked with 5% BSA and stained with anti-PDCD10 pAb (1:1000 dilution in 5% BSA in 0.1% TBST)

An additional band within the desired molecular weight range in MCF7 lane, which was absent in MCF7/DOX lane, was observed when the isolated proteins were run on 8% polyacrylamide gel. To confirm whether this band belonged to PDCD10 or not, PDCD10 was overexpressed in MCF7/Dox by cloning *PDCD10* coding sequence with an N-terminal FLAG-tag into pcDNA3.1(-) expression vector.

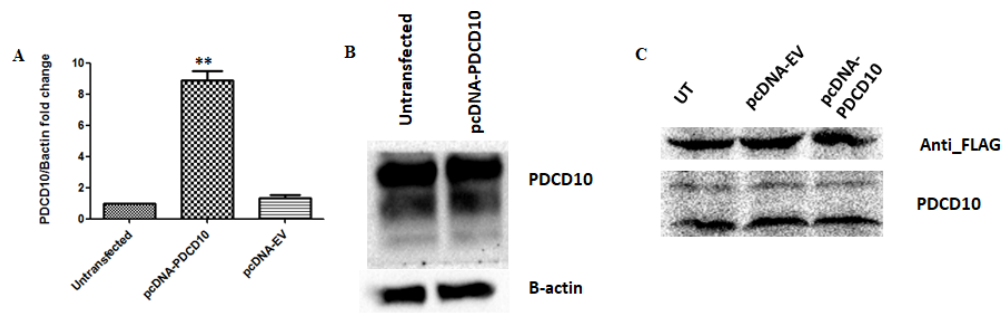


**Figure B.3** Expression of PDCD10 in MCF7/DOX cells after transfection with pcDNA\_PDCD10 overexpression vector. A) *PDCD10* expression at mRNA level, B) PDCD10 expression at protein level detected by anti-PDCD10 antibody and C) PDCD10 expression at protein level detected by anti-FLAG antibody.

Although more than 8-fold upregulation in *PDCD10* expression in pcDNA\_PDCD10- transfected MCF7/DOX cells was observed at mRNA level, PDCD10 protein expression did not show any significant change when stained by anti-PDCD10 antibody. Similarly, anti-FLAG antibody stained untransfected (UT) and empty-vector (EV) transfected MCF7/DOX cells, indicating a possible contamination in antibody source (Figure B.3).

To be able to detect the desired protein band, it was aimed to accumulate the protein by inhibiting its degradation. Since the degradation pathway of PDCD10 has not been known yet, MCF7 and MCF7/DOX cells were treated with both a proteasome inhibitor, MG132, and lysosome inhibitor, Pepstatin A, separately to inhibit either pathway. DMSO was used as control.

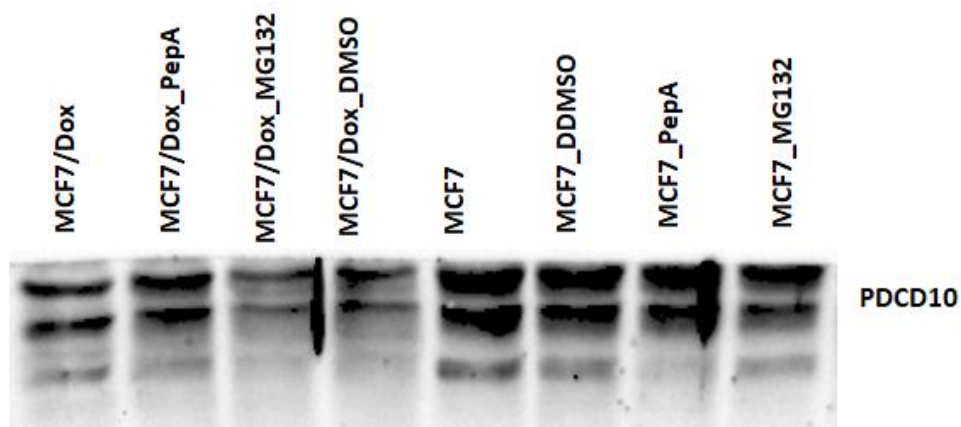


**Figure B.4** PDCD10 expression in Pepstatin A- and MG132-treated MCF7 and MCF7/DOX

As seen in Figure B.4, the expression level of PDCD10 did not show any significant change after treatment with Pepstatin A and MG132 compared to untreated and DMSO-treated control groups (Figure B.4). The effects of lysosomal inhibitor Pepstatin A and proteasome inhibitor MG132 on PDCD10 accumulation could not be detected by using anti-PDCD10 antibody.

Zhang et al reported that endogenous PDCD10 expression was upregulated under oxidative stress (Zhang et al, 2012). Therefore, MCF7/DOX cells were treated with hydrogen peroxide (5 mM and 10 mM) for 24 h to increase endogenous PDCD10 expression.

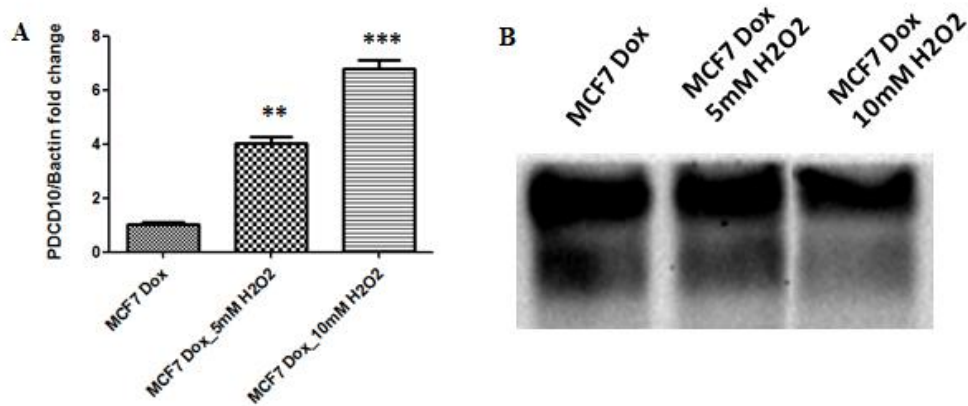


**Figure B.5** PDCD10 expression after treatment with hydrogen peroxide in MCF7/DOX cells. A) *PDCD10* expression at mRNA level and B) PDCD10 expression at protein level.

Hydrogen peroxide treatment caused a gradual increase in PDCD10 expression. 5 mM H<sub>2</sub>O<sub>2</sub>-treated MCF7/DOX cells displayed 4-fold upregulation in PDCD10 expression whereas 7-fold upregulation was observed in 10 mM H<sub>2</sub>O<sub>2</sub>-treated MCF7/DOX cells compared to untreated control group (Figure B.5A). However, this upregulation could not be detected at protein level (Figure B.5B).

To check whether PDCD10 protein could be observed by immunocytochemistry, firstly isolated proteins were run on native polyacrylamide gel.

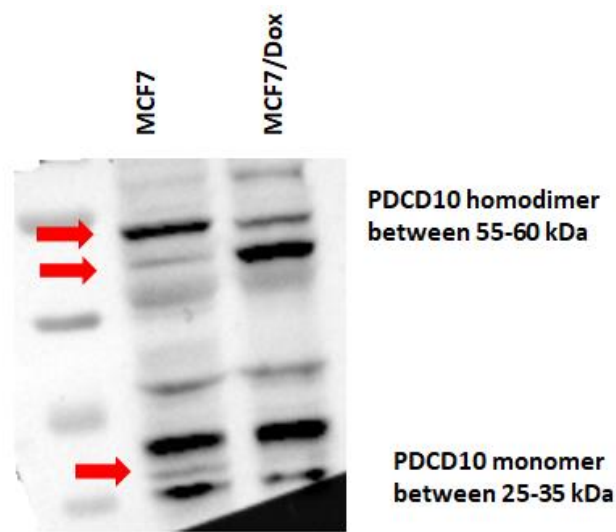


**Figure B.6** PDCD10 expression in parental and doxorubicin-resistant MCF7 cells on native PAGE.

As seen in Figure B.6, different non-specific bands were observed. There was a slight protein band detected between 25 and 35 kDa molecular weight range in MCF7 lane which was absent in MCF7/DOX lane. This slight band was in the desired molecular weight range that corresponded to the monomeric form of PDCD10. On the other hand, between 55 and 60 kDa molecular weight range which corresponded to homodimeric form of PDCD10, MCF7 cells displayed an intense larger protein band and a less intense smaller protein band. In the same molecular weight range, MCF7/DOX cells displayed an intense smaller protein band and less intense larger protein band. The difference between the expressions of these bands may indicate the differential processing or post-translational modifications of PDCD10 although the results were inconclusive due to various non-specific bands.

## APPENDIX C

### RESISTANCE INDICES

**Table C.1** Resistance indices of *PDCD10*-silenced and *PDCD10*-overexpressed cells compared to MCF7 and HeLa cells

Cell Line	Treatment	Drug	IC <sub>50</sub> ± SEM (µM)	Resistance index‡
MCF7	UT	DOX	2.07±0.04	
	siControl		2.77±0.50	1.34
	siPDCD10		>7.5 (9.03±0.35)***‡	4.36
	UT	DOC	3.24±0.06	
	siControl		3.12±0.11	0.96
	siPDCD10		3.71±0.05*	1.19
MCF7/DOX	UT	DOX	183.45±4.84	88.63
	EV		193.29±10.19	93.38
	pcDNA_PDCD10		124.99±3.00**	
HeLa	UT	DOX	19.47±0.14	
	EV		23.56±0.42	1.21
	pcDNA_PDCD10		40.21±3.05**	2.07
HeLa/DOX	UT	DOX	202.01±4.57	10.38
	siControl		214.15±3.89	11.00
	siPDCD10		166.09±7.06*	8.53

n=3; \* = p<0.05; \*\* = p<0.01 and \*\*\* = p<0.001.

‡ Resistances indices were calculated for each treatment compared to IC<sub>50</sub> value of corresponding parental cell line.



## CURRICULUM VITAE

### PERSONAL INFORMATION

Surname, Name : Urfalı Mamatođlu, ađrı

Nationality : Turkish

Date and Place of Birth : 18 October 1987, Samsun

Marital status : Married

Phone : +905333654291

Fax : +903122107976

E-mail : cagriurfali@gmail.com, cagri.urfali@metu.edu.tr

### EDUCATION

Degree	Institution	Year of Graduation
MS	METU, Biology	2012

BS METU, Molecular Biology and 2009

Genetics

High School Samsun Anatolian High 2005

School, Samsun

## WORK EXPERIENCE

Year	Place	Enrollment
2009 February - June	METU Department of Biological Sciences	Project Student
2008 August	Newcastle University, Centre for Life, Institute of Human Genetics, UK	Intern Student

## FOREIGN LANGUAGES

English (Fluent)

German (Beginner)

Dutch (Beginner)

## PUBLICATIONS

### Papers Published in International Journals

1. Urfali-Mamatoglu, C., Kazan, H. H., Gündüz, U. Dual function of PDCD10 in drug resistance. *Biomedicine and*

*Pharmacotherapy*, 101, 129-136.

2. Kazan, H. H., Urfali-Mamatoglu, C., Gunduz, U. Iron metabolism and drug resistance in cancer. *Biometals*, 30(5), 629-641 (2017)
3. Kazan, H. H., Urfali-Mamatoglu, C., Gunduz, U. Resistance to anti-cancer drugs permanently alters electrophoretic mobility of cancer cell lines. *Electrophoresis*, 38(8), 1201-1205 (2017)
4. Urfali-Mamatoglu, C., Kazan, H. H., Gunduz, U. PDCD10 (Programmed cell death 10). *Atlas Genet Cytogenet Oncol Haematol.* in press

## Abstracts Published in International Conferences

1. Urfali-Mamatoglu, C., Kazan, H. H., Gunduz, U. Downregulation of programmed cell death 10 (PDCD10) expression confers doxorubicin resistance in breast cancer cells. Book of Abstracts, page 198, MolBiyKon'17, September 2017, Istanbul, Turkey.
2. Urfali-Mamatoglu, C., Gunduz, U. The role of apoptosis regulator programmed cell death 10 (PDCD10) in multidrug resistance. Book of Abstracts, page 107, Anti-cancer Drug Action and Drug Resistance, June 2015, Florence, Italy.
3. Erdem, M., Yalcin-Azarkan, S., Urfali-Mamatoglu, C., Gunduz, U. Synthesis and characterization of polyethylene glycol coated magnetic nanoparticles and their use for anti-cancer drug delivery. Book of Abstracts, page 126, Anti-cancer Drug Action and Drug Resistance, June 2015, Florence, Italy.
4. Seza, E. G., Yapındı, L., Urfalı-Mamatoğlu, Ç., Gündüz, U. The Effects of Drug-Resistant MCF7 sublines on Cellular Proliferation and Gene Expression Pattern of Drug-Sensitive MCF7 Cells. Book of Abstracts, page 183, 11<sup>th</sup> Symposium on Pharmaceutical Sciences, June 2015, Ankara, Turkey.
5. Akbulut, Ö., İzgi, H., Çakmak, N., Urfalı-Mamatoğlu, Ç., Gündüz, U. Investigation of the Effect of Vimentin on Multidrug

- Resistance in Cancer, Book of Abstracts, page 184, 11<sup>th</sup> Symposium on Pharmaceutical Sciences, June 2015, Ankara, Turkey.
6. Urfalı, Ç., Gündüz, U. Reversal of Multidrug Resistance in Zoledronic Acid Resistant MCF7 Breast Cancer Cell Line. Oral Presentation, Book of Abstracts, page 69, 10<sup>th</sup> International Symposium on Pharmaceutical Sciences, June 2012, Ankara, Turkey.
  7. Urfalı, Ç., Gündüz, U. Reversal of Breast Cancer Resistance Protein Mediated Zoledronic Acid Resistance in MCF7 Cell Line. EMBO Young Scientist Forum, June 2012, Istanbul, Turkey.
  8. Urfalı, Ç., Gündüz, U. Reversal of Multidrug Resistance in Zoledronic Acid Resistant MCF7 Cell Line. In Vivo, 4<sup>th</sup> International Congress of Molecular Medicine, June 2011, Istanbul, Turkey.
  9. Nil, Z., Urfalı, Ç., Şenyılmaz, D., Kars, M. D., İşeri, Ö. D., Gündüz, U. Zoledronik Asite Dirençli MCF-7 Meme Kanseri Hücre Hattında Çapraz Direnç Gelişiminin İncelenmesi, 16<sup>th</sup> National Biochemical Congress, November 2009, Istanbul,

Turkey.

## **AWARDS & HONORS**

1. 2012 - Present : TÜBİTAK 2211 Domestic PhD Scholarship  
Program
2. 2009 – 2012 : TÜBİTAK 2210 Domestic Masters Scholarship  
Program
3. 2005 – 2009 : TÜBİTAK Undergraduate Scholarship  
Program